Wildland-Urban Interface Fire Touristic Infrastructure Protection Solutions

WUITIPS

GA number 101101169

Co-funded by the European Union

WUITIPS – FIRE SAFETY ENGINEERING TECHNICAL NOTE

WP - Task	WP6 – Task 6.4	**Version** (1)	Final
File name		**Dissemination level** (2)	Public
Programmed delivery date	31/01/2025	**Actual delivery date**	05/02/2025

Document coordinator	Elsa Pastor (UPC
Contact	lsa.pastor@upc.edu
Authors	Enrico Ronchi (ULUND), Borja Rengel (EFR), Bruno Guillaume (EFR), Pascale Vacca (UPC), Amira Labhiri (ULUND), Arthur Roahert (ULUND)
Reviewed by	Elsa Pastor (UPC)

Abstract	This technical note gathers the Fire Safety Engineering case studies developed in the WUITIPS project. It contains the following projects: 1. Building vulnerability of SP Case Study - PBD project applied to Punta Milà Camping – l'Escala, Spain. 2. Evacuation modelling of the Punta Milà Camping 3. Building vulnerability of SP Case Studies – PBD project applied to villa "Mas d'Amont" and Campsite "Bois Fleuri" 4. Evacuation modelling of FR Case Studies

(1) *Draft / Final*
(2) *Public / Restricted / Internal*

Disclaimer

WUITIPS is co-funded by the European Union. Views and opinions expressed in this document are however those of the author(s) only and do not necessarily reflect those of the European Union or the European Commission. Neither the European Union nor the granting authority can be held responsible for them.

Wildland-Urban Interface Fire Touristic Infrastructure Protection Solutions

WUITIPS

GA number 101101169

Co-funded by the European Union

Technical Note TN 6.4
Building Vulnerability of SP Case Study

WP - Task	WP6 – Task 6.4	**Version** (1)	Final
File name	WUITIPS-WP6_SP_Case Study	**Dissemination level** (2)	Public
Programmed delivery date	31/01/2025	**Actual delivery date**	05/02/2025

Document coordinator	Pascale Vacca (UPC)
Contact	pascale.vacca@upc.edu
Authors	Matheus Ponte (UPC)
Reviewed by	Elsa Pastor (UPC)

Abstract	In this technical note we provide a vulnerability and protection assessment of the buildings in the SP case study, using a PBD approach.

(1) *Draft / Final*
(2) *Public / Restricted / Internal*

Disclaimer

WUITIPS is co-funded by the European Union. Views and opinions expressed in this document are however those of the author(s) only and do not necessarily reflect those of the European Union or the European Commission. Neither the European Union nor the granting authority can be held responsible for them.

1. Performance-Based Design of a building in Camping Punta Milà

1.1. Characteristics of the building and its surroundings

The camping is located within the Montgrí Natural Park, in the Costa Brava area (Girona, Spain). The analysed building (Figure 1 and Figure 2) is located in the middle of the camping and it includes a restaurant, bar, storage area, and small shop on the ground floor. The first floor presents a flat unit that is not directly connected to the ground level. The building's walls are assembled with concrete, the roof is made of clay tiles and the floor is covered by ceramic tiles.

The building has two semi-confined spaces (SCSs): one is the porch located in front of the restaurant section, where tables and chairs are placed for the clients (Figure 2) and the other is located in front of the supermarket, in which LPG canisters are stored (Figure 3). The porch has a ceiling composed of wood, expanded polystyrene (EPS) insulation, and an oriented strand board (OSB) on the top. The wall that separates this area from the inside of the building includes aluminum shutters with an air leakage height of 2 cm throughout the shutter's base. If the items located in these SCSs are ignited, this could create a great heat build-up that could potentially cause damage to the envelope of the building.

Another vulnerable element of the building is the unprotected (i.e., not protected by shutters) glazing located in the flat (Figure 4).

Inside the camping, there is no smoke detector or fire alarm. According to the self-protection plan of the camping, any fire-related event should be communicated to the person in charge so that necessary action can be taken. ABC fire extinguishers are placed around the camping area.

Figure 1: Left view of the building

Figure 2: Front view of the building

Figure 3: SCS with LPG canister storage rack

Figure 4: Unprotected glazing of the flat

The building's surroundings include camping areas, a swimming pool, bathrooms, a laundry room, and a 25 m³ water tank. Ground vegetation is well-maintained, and the high trees are pruned. Some smaller, non-pruned trees are located near the building, as can be seen in Figure 1. In addition to these trees, which can be potential fuels in case of fire, ornamental vegetation

and artificial fuels (e.g., chairs and tables) are located underneath and in the vicinity of the porch. Additionally, wooden planks and pallets are stored in the vicinity of the windows of the flat, as shown in Figure 5.

Figure 5: Artificial fuels located in front of the windows of the flat

A well-managed fuel break (Figure 6) that follows the regulatory stipulations of a minimum with of 25 m surrounds the camping. The surface vegetation within the fuel break is well maintained and the trees are pruned and spaced apart. This mitigation measure is essential in lowering the possibility that the wildfire front will reach the camping and the analysed building.

Figure 6: Fuel break

1.2. Performance-Based Design Methodology

The Performance-Based Design presented in the following sections follows the SFPE framework (SFPE, 2006). Performance criteria are set for each of the analyzed vulnerable elements of the building and fire scenarios are simulated with the Computational Fluid Dynamics tool FDS (Fire Dynamics Simulator). Results are then compared to the previously set performance criteria, in order to identify whether the analyzed scenario is safe or not.

1.2.1. Goals and objectives of the study

The goal of this study is property protection and its objective is to avoid fire entrance into the building. For that, no window should break, combustible façade elements should not ignite, the integrity of the stored LPG canisters should not be compromised and the loss of containment of these canisters should be prevented.

1.2.2. Performance criteria

By aligning with the goal and objectives, the performance criteria are based on non-life safety measures and include thresholds to avoid failure of the glazing and frame, to avoid LPG canisters' loss of containment, and ignition of the wooden ceiling of the SCS porch. Structural analysis is not performed as the materials are declared to be R90, and the fire scenarios do not expect the fire to burn longer than 90 minutes.

The performance criteria used for each vulnerable element are given in Table 1. Three criteria are used to identify the breakage of the glazing: the temperature difference between the exposed part of the pane and the unexposed part located behind the frame (ΔTcr), the critical surface temperature of the pane (T_{surf}) and the heat load, which is the imposed heat flux throughout the time. When it comes to the frames of the windows located in the flat, one is made out of wood and the other of aluminium. The melting of the frame can make the pane loose and cause it to fall off the window or open spaces in which the flame could enter the room. Therefore, threshold values for melting of aluminium (surface temperature T_{surf}) and for the ignition of wood (surface temperature T_{surf} and incident radiant heat flux $\dot{q}''_{rad}$) are used. When it comes to the LPG canisters, incident radiant heat flux $\dot{q}''_{rad}$ received by the canisters should be below the threshold at which the Pressure Relief Valve (PVI) will open, releasing its contents. For the wooden ceiling, the same criteria as those for the wooden frame are used.

Table 1: Performance criteria

Vulnerable element	Performance criteria	Reference
Glazing	ΔT_{cr} < 83°C T_{surf} < 132°C Heat Load < 1087 kJ/m²	Vacca, 2023
Window frame	Aluminium: T_{surf} < 660°C Wood: T_{surf} < 350°C $\dot{q}''_{rad}$ < 12 kW/m²	Czerwinski, 2020 Drysdale, 2011
LPG canisters	$\dot{q}''_{inc}$ < 22 kW/m²	API, 1996
Wooden ceiling	T_{surf} < 350°C $\dot{q}''_{rad}$ < 12 kW/m²	Drysdale, 2011

1.2.3. Fire scenarios

The fire scenarios are divided into three cases: a fire located in the porch, one located in the vicinity of the LPG canisters, and one in the vicinity of the unprotected windows. All three scenarios are simulated using FDS.

Scenario 1

The first scenario simulates a fire close to the northern façade of the building, where the LPG canisters are stored. The simultaneous combustion of the wooden walls of a garbage deposit, of the garbage within this deposit, and of the bamboo fence on the side of the deposit (shown in Figure 7) is simulated.

Figure 7: Garbage deposit

The entire building is modelled as shown in Figure 8. The combustible elements are represented as red-coloured surfaces. The worst scenario is emulated by adding a wind profile blowing from the North (Tramontane wind), and pushing the flames towards the building. There is a 40% probability of the wind blowing in this direction during summer, with an average velocity of 25 km/h at 10 m height (Weather Spark, 2024).

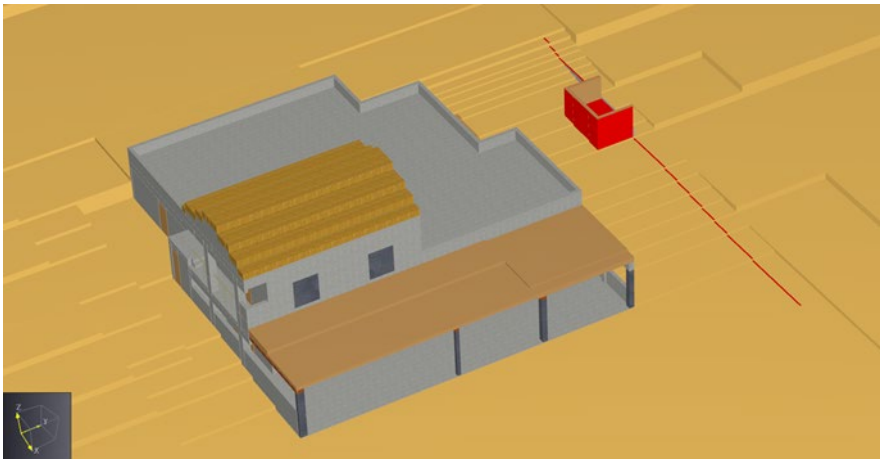

Figure 8: Model of scenario 1

The estimation for the Heat Release Rate (HRR) of the combustion of the walls from the garbage area was approximated by using data from an experiment with four wooden pallets, which resulted in a peak HRR of 2049 kW and a Heat Release Rate Per Unit Area (HRRPUA) of 687 kW/m² (NIST, 2019). The simulated HRR curve is given in Figure 9.

For the combustion of the garbage, the fire data was approximated by using those from experiments with one, two, and three trash bags filled with paper (Babrauskas, 2016). The peak HRR for each is 132kW, 287 kW, and 342 kW, respectively. With a linear correlation of these values and assuming a fuel package of ten trash bags, the total HRR calculated is 1075 kW, and the HRRPUA for a 6 m² garbage deposit area is 179 kW/m². The simulated HRR curve is given in Figure 10.

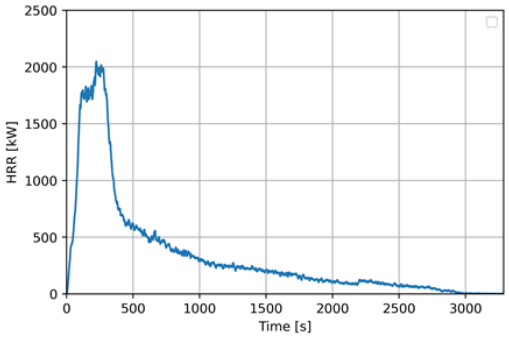

Figure 9: HRR for the wooden walls

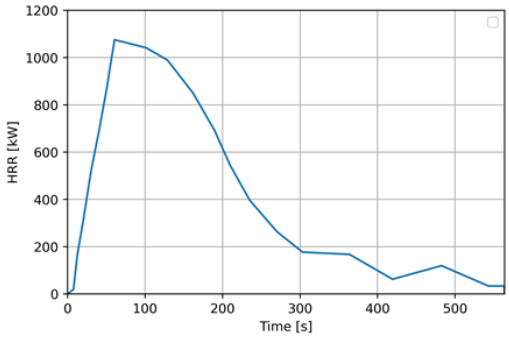

Figure 10: HRR for the garbage

An estimation of the HRR for the bamboo fence is necessary, as no fire test values are available in the literature. This fence is modelled in FDS throughout the entire length of the element (25 m) as Lagrangian particles that undergo a solid-phase thermal decomposition process such as the one of vegetation (McGrattan et al., 2023), with a moisture content of 20%, which is the lowest recorded value in summer (Weather Spark, 2024). Simulating the wooden fence in this way is necessary to generate HRR and burning time data. Four different mesh sizes (20 cm, 10 cm, 5 cm, and 2.5 cm) are analyzed by performing a 300 s simulation in which a burner is active for 30 s. From Figure 11 it is possible to see that there is not much variation in the peak HRR between 5 cm and 2.5 cm mesh sizes. With that, to be more conservative while choosing between 5 cm and 2.5 cm, the selected HRR curve is the one from the mish size of 5 cm. For this case, the peak HRR reaches 8754 kW, resulting in a HRRPUA of 167 kW/m^2.

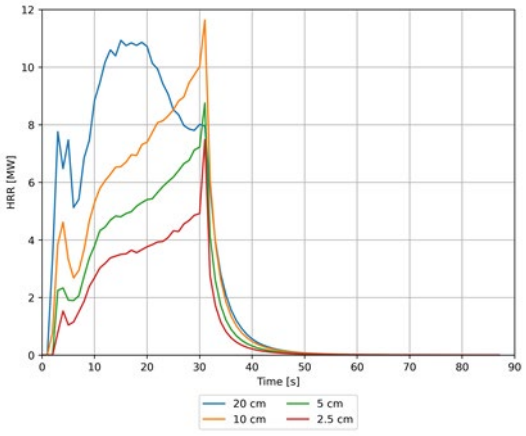

Figure 11: HRR curves for the bamboo fence particles with different mesh sizes

Two different reactions are placed in the simulation: one for the wood and one for the garbage. For the latter, the main considered material is polyethylene, which has a high soot production. For the wood, the reactant material used was pine wood, with the chemical formula $CH_{1.7}O_{0.8}$, soot yield (ys) of 0.015 g/g, and carbon monoxide yield (yCO) of 0.004 g/g. The chemical formula

for the polyethylene reactions is $(C_2H_4)_n$, with y_s of 0.06 g/g, and y_{CO} of 0.024 g/g (Khan et al., 2016). The balanced equations for wood and for polyethylene are the following:

$CH_{1.7}O_{0.83}$ + 0.974348 (O_2 + 3.76 N_2) -> 0.962421 CO_2 + 0.003854286 CO + 0.85 H_2O

+ 0.033725 C + 3.663548 N_2

$(C_2H_4)_n$ + 2.848 (O_2 + 3.76 N_2) -> 1.836 CO_2 + 0.024 CO + 2 H_2O + 0.14 C + 10.70848 N_2

Scenario 2

The second fire scenario corresponds to the combustion of fuels located near the eastern façade, specifically on the porch in front of the restaurant. In summer, tables with plastic chairs are placed on the porch and in its surroundings, as shown in Figure 12.

Figure 12: Restaurant during the summer season

For the simulations, the chairs are grouped into six different fuel packs (FPs), each of them represented by the red rectangles in Figure 13.

Figure 13: Representation of scenario 2

This case is divided into two sub-scenarios, "a" and "b". The first simulates the simultaneous burn of all the plastic chairs in the SCS, and the latter starts the ignition only on one FP, igniting the others depending on specific criteria, specified further on in this document. The objective of this subdivision is to analyze the combustion of different fuel packages and how this change can impact the structure. The wind configuration follows the one of scenario 1. For scenario 2a,

the HRR data comes from test 11 from Sardqvist (1993), in which five polypropylene chairs with steel legs were placed in a row, and the middle one was ignited. The HRR peak is 675 kW (Figure 14) and the chair dimensions are 0.50 x 0.55 m, resulting in a HRRPUA of 490.74 kW/m². For scenario 2b, the HRR comes from a fuel package consisting of six chairs, six cushions, a parasol, and a table (Vacca et al., 2022). This test results in a HRR peak of 2178 kW (Figure 15) and HRRPUA of 1512.5 kW/m². The differentiation in scenarios 2a and 2b, with different fire curves, is based on this fuel package's lack of exact data from experiments. In scenario 2a, the chairs are not entirely made with plastic in the experiment, which contributes to lower HRR values. Scenario 2b consists of more combustible materials besides the plastic chair, which contributes to overestimating the HRR curve. This latter scenario investigates the possibility of having different combustible materials along the porch SCS that can be placed during summer. The ignition of the fuel packs is not simulated simultaneously, but it is modelled as starting in one FP and spreading to the others.

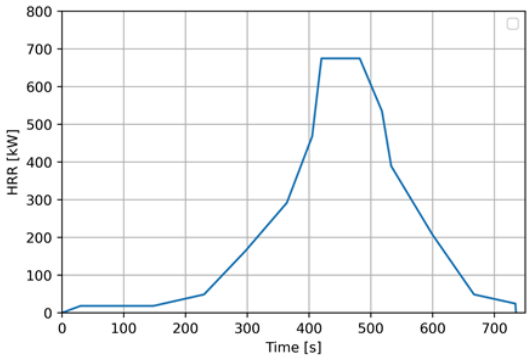

Figure 14: HRR curve for scenario 2a

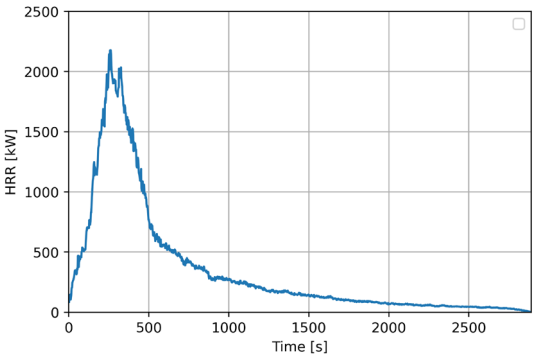

Figure 15: HRR curve for scenario 2b

As just plastic fuel is defined for this scenario, simple chemistry was used, and the soot yield (0.0594 g/g) and CO yield (0.023 g/g) were averaged from the three experiments involving a plastic chair (NIST, 2019).

Scenario 3

The third scenario examines the flat's vulnerability, focusing specifically on the glazing systems, composed of one window with a wood frame and the other two with an aluminum frame. Only one window (with aluminium frame) is protected by a shutter. The worst-case condition for the wind differs from the previous two scenarios. For this, the worst wind is the one coming from the SSW direction, blowing towards the vulnerable part of the flat. This type of wind has a 30% chance of occurring during summer (Weather Spark, 2024).

The hazard is given by the storage of wooden materials in front of the windows. With the possibility of firebrands igniting these combustible materials, this scenario simulates the simultaneous ignition of four packages as a worst case. The HRR is based on the one obtained for wooden pallets of 1.20 x 1.20 m, stacked up to 0.9 m high (Särdqvist, 1993), shown in Figure 16, with an HRRPUA of 3580.0 kW/m² and a burning period of 694 s (11.5 min). As the FPs have different areas (FP1 2.05 m², FP2 4.20 m², FP3 and FP4 each 2.16 m²), the corresponding HRR curve for each FP is shown in Figure 17. The location of each FP is shown in Figure 18.

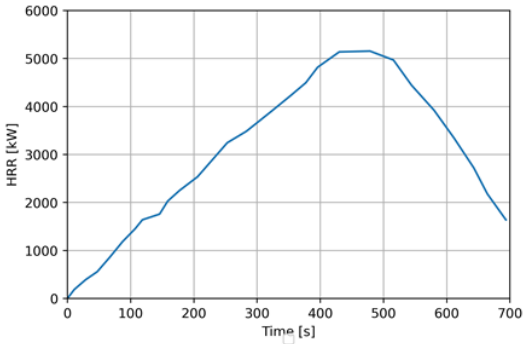

Figure 16: HRR for 0.9 m height stacked wooden pallets

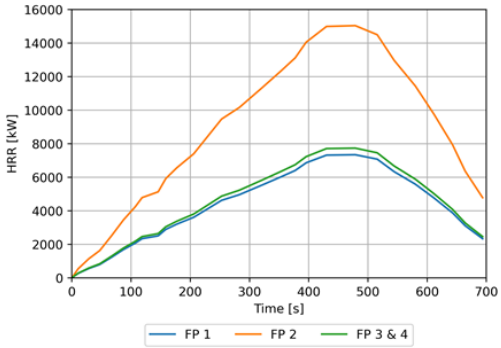

Figure 17: HRR curves for the fuel packages

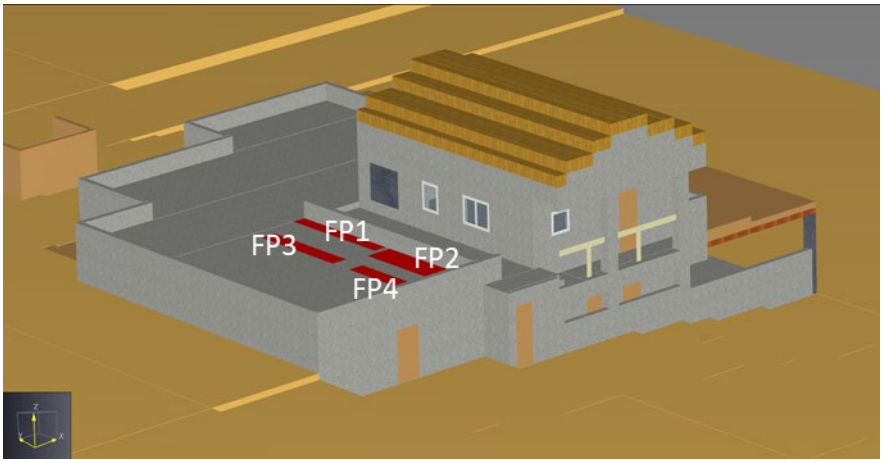

Figure 18: Representation scenario 3

1.2.4. Simulation parameters

Wind and environmental parameters

All the simulations are performed in FDS version 6.8.0, and all wind scenarios are modeled with the Monin-Obukhov Similarity, which generates a vertical wind profile. The model includes average high values for ambient temperature (28.5 °C) and wind speed (7 m/s at 10 m height) (Weather Spark, 2024). With this, the Pasquill stability class could be C or D, depending on the radiation levels. However, neutral stability (class D) is chosen to get the worst condition, with L = 1000000 m. Another critical factor is the roughness of the landscape. This parameter is set as very rough (z0 = 0.5 m), corresponding to a mix of fields, forest, and scattered buildings (McGrattan et al., 2023).

Simulations with wind profiles need a larger domain than usual to avoid numerical instability during FDS calculations. The domain size was selected based on the guidelines presented by Węgrzyński et al. (2018): 103.2 m x 104.0 m x 49.6 m for scenario 1 and 103.2 m x 104.0 m x 40.0 m for scenarios 2 and 3. A simulation with the north wind (0°) was performed to understand the timeframe in which the wind stabilizes, after which ignition is set to occur. According to this analysis, the time at which the wind profile reaches a steady state is 30 seconds.

Material properties

The materials used in all scenarios are displayed in Table 2. The ceiling of the porch is defined as a three-layered material with untreated yellow pine wood as an external material and EPS as an insulator. The total thickness of the ceiling is 20 mm, with 1.90 mm of wooden boards and 16.20 mm of EPS in the middle. Another component with layered material is the frame of the windows of the flat, which consists of a 3 mm aluminum or wood frame followed by 6 mm of float glass.

Table 2: Specification of the materials used in all scenarios

Material	Density [kg/m³]	Specific heat [kJ/(kg·K)]	Conductivity [W/(m·K)]	Emissivity [-]	Reference
Concrete	2280.00	1.04	1.80	0.90	Peacock et al., 1988
EPS	22.50	1.30	0.038	0.95	Greenspec, 2024
Glass	2600.00	0.84	0.80	0.90	Karlsson et al., 2022
Yellow pine	640.00	2.85	0.14	0.90	Thunderhead Engineering 2024
Aluminum	2700.00	0.89	218.00	0.05	Karlsson et al., 2022

Mesh size

The D* (fire diameter) method was used to choose the cell size of the finest mesh (McGrattan et al., 2023). A fine mesh with a cell size of 10 cm is chosen to get a better resolution near the fire and investigate objects such as glazing systems and wooden ceilings. This cell size also gives satisfactory results when it comes to modelling window breakage (Vacca, 2023). Other areas of the domain include meshes with cell sizes of 20 cm, 40 cm and 80 cm.

Outputs

Devices are placed to read the necessary data for the performance criteria. For scenarios 1 and 3, gauge heat flux (GHF) and wall temperature (WT) devices are placed on the glazing's surface at the positions indicated in Figure 19. Figure 20 shows a top view of the window's geometry within the simulation, where there is a layer of an aluminum shutter, an air gap, and the frame with the pane. Also, in scenario 1, WT and incident heat flux (IHF) devices were used. In addition, boundary files were implemented to measure wall temperature and the incident heat flux across the LPG canisters. WT, radiative heat flux (RHF) devices, boundary files, and PROF are placed in scenario 2.

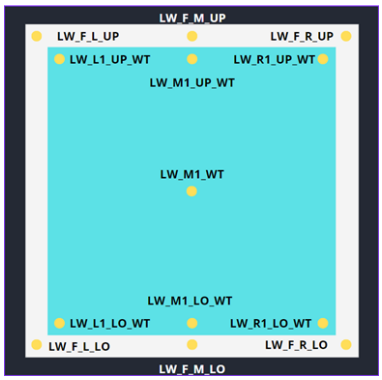

Figure 19: Location of the devices on the frame, glazing, and shutter

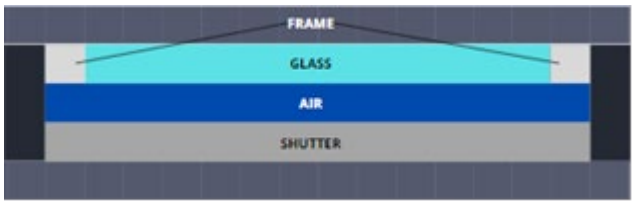

Figure 20: 2D representation of the glazing system with a protective shutter (top view)

Logic control for scenario 2b

In scenario 2b, a logic control is placed to simulate fire spread from one fuel pack to another. This depends on the auto-ignition temperature (AIT) of the polypropylene chairs, which is 357°C (Rompetrol Petrochemicals, 2008) and their critical heat flux, which Is 10 kW/m^2 (Hurley, 2016). Devices are placed by the fuel packs to measure temperature and radiant heat flux. The worst cases consist of starting the ignition of one of the four FP on the left (Figure 13), as they are closer to each other and have more chance of igniting the adjacent FPs. If one of the previously mentioned values is reached by an adjacent fuel pack, it will ignite.

1.2.5. Evaluation of the design against the assigned fire scenarios

Scenario 1

Figure 21 shows the development of the fire for scenario 1, starting with the quick burning of the wooden fence, followed by the garbage and the wooden walls. The peak HRR for this case is reached at 300 s. Figure 22 shows the labeling of the left window (LW) and right window (RW), with their three panes named 1 to 3, and the LPG canister.

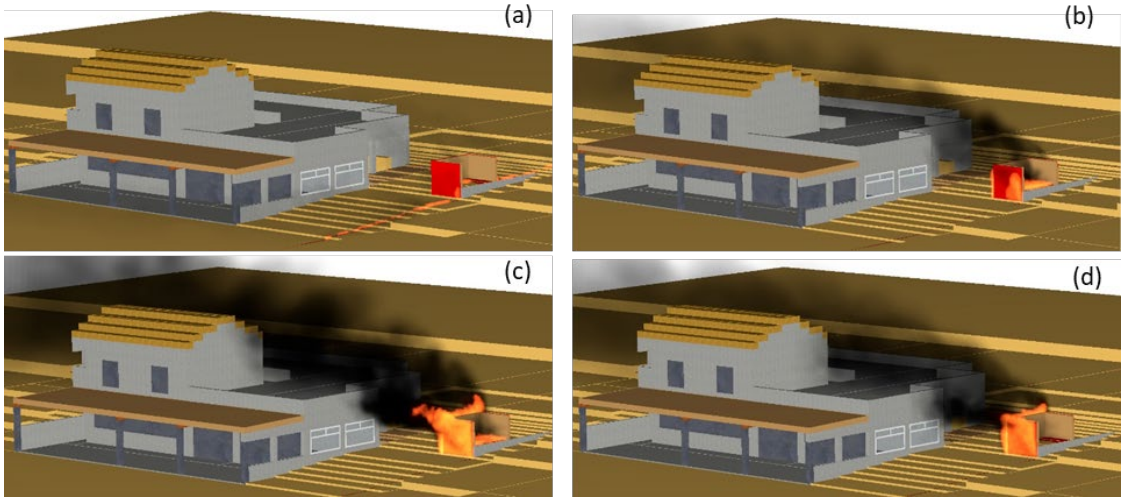

Figure 21: Scenario 1 at (a) 60 s of simulation, (b) 100 s, (c) 300 s, (d) 500 s

Figure 22: Label of the windows and LPG displayed in the representation of Scenario 1

None of the analyzed windows reach the surface temperature criterion. The lower devices on the first pane are those that record the peak surface temperatures of the left window (Figure 23), with a peak value of 70.4 °C. For the right window, the values are higher because it is closer to the burning items. Figure 24 indicates that the highest measured temperature is in the lower right device of pane 1, reaching a peak of 105.6 °C.

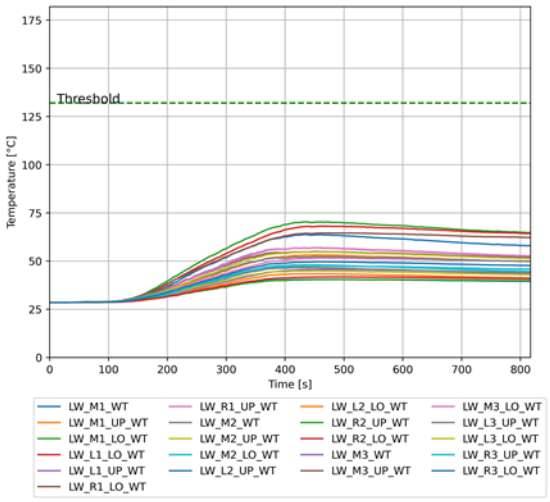

Figure 23: Surface temperature through time of the left window for scenario 1

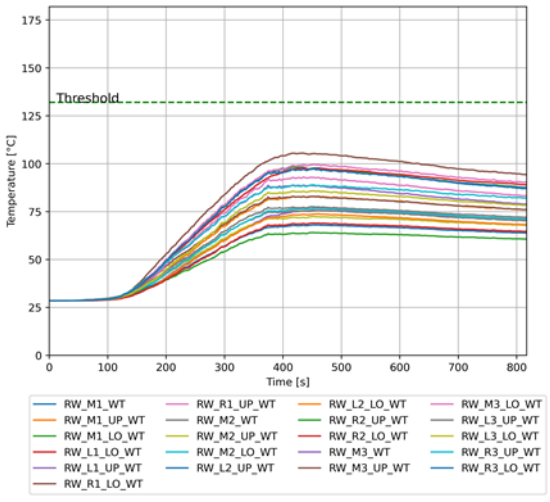

Figure 24: Surface temperature through time of the right window for scenario 1

None of the windows are expected to break for the temperature difference criterion. Figure 25 shows that the temperature difference in the left window reaches a peak of only 40°C, and for the right window (Figure 26), this maximum is 72.8°C. This value does not reach the chosen criterion of 83°C, however, considering alternative references which indicate a ΔT_{cr} of 52 °C for a 3 mm pane (Harada et al., 2000) and a ΔT_{cr} of 74 °C for a 6 mm pane (Wang et al., 2017), the obtained value could indicate glazing breakage.

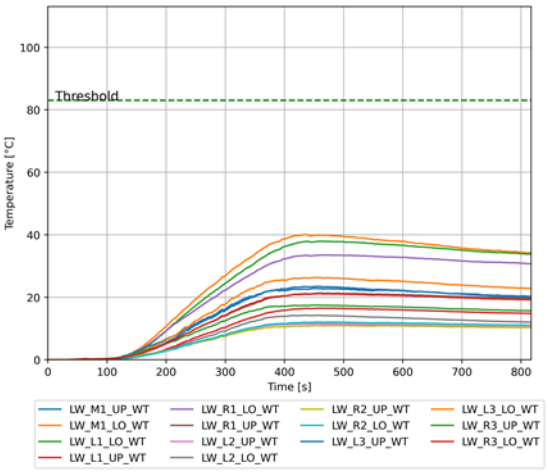

Figure 25: ΔT through time between the unexposed and exposed glazing in the left window for scenario 1

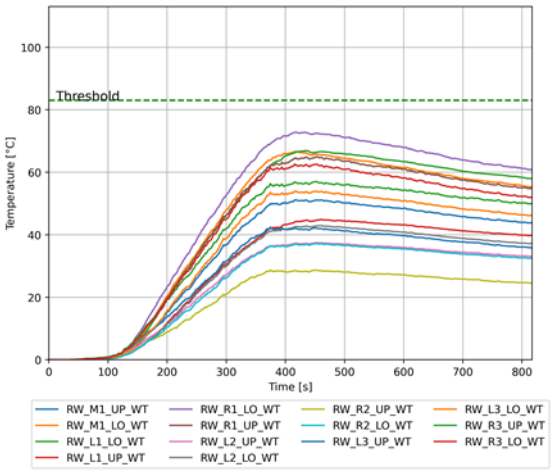

Figure 26: ΔT through time between the unexposed and exposed glazing in the right window for scenario 1

For the heat load criterion, both windows reach the threshold value, with the left window (Figure 27) reaching it almost 300 seconds (5 minutes) later than the right window (Figure 28). This difference in time is expected, as the right side of the right window faces the heat source directly, receiving more radiation and, consequently, the accumulation of the heat flux through time (HL) reaches a higher amount quicker.

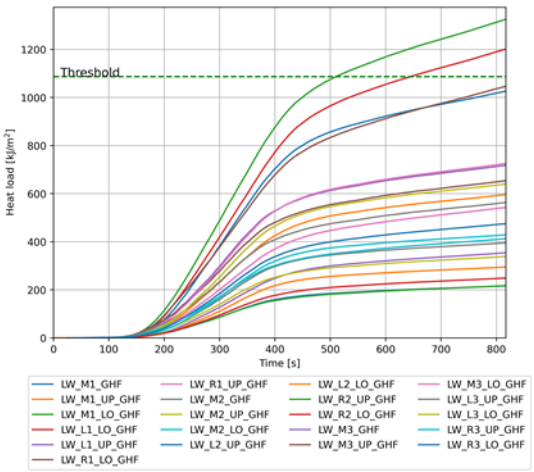

Figure 27: Heat load through time in the left window for scenario 1

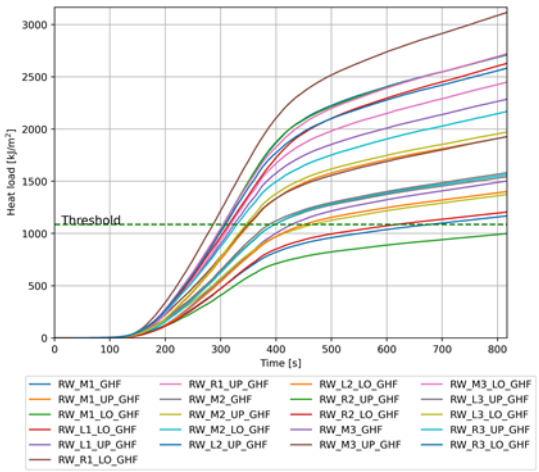

Figure 28: Heat load through time in the right window for scenario 1

The presence of LPG canisters does not present a risk for this scenario, as the incident heat flux reaches a maximum of 1.5 kW/m^2 (Figure 29) which is way below the 22 kW/m^2 threshold. Therefore, this does not require further examination. This safety can be explained by the LPG canister being at least 5.5 m distant from the fire source.

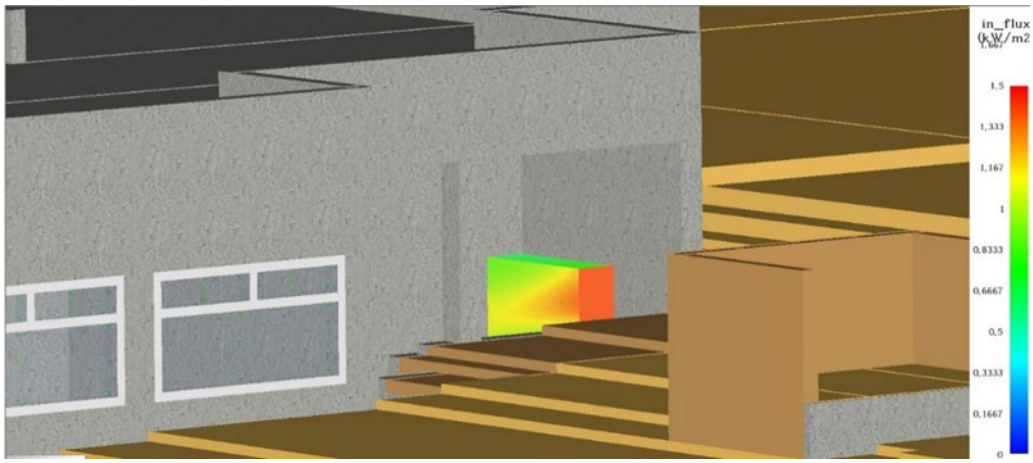

Figure 29: Boundary file for the incident heat flux on the LPG canister

Table 3 summarizes the time at which the performance criteria for each analyzed element are reached in scenario 1.

Table 3: Times at which performance criteria are reached in scenario 1

Performance criteria	Time of reaching the performance criteria [s]		
	Left window	Right window	LPG canisters
T_{surf}	-	-	NA
ΔT_{cr}	-	300 (Harada et al.)	NA
HL	507	287	NA
T_{surf} frame	-	-	NA
$\dot{q}''_{rad}$	NA	NA	-

NA: Not Applicable

Scenario 2a

Figure 30 shows the fire development in scenario 2a until 700 seconds. This scenario does not present a risk for the ignition of the wooden ceiling of the porch SCS, as the wall temperature devices, with data plotted in Figure 31, show a maximum temperature lower than 150°C and, consequently, below the threshold of 350°C. The other criterion is presented in Figure 32, where the radiative heat flux values peak around 4 kW/m^2, below the 12 kW/m^2 threshold.

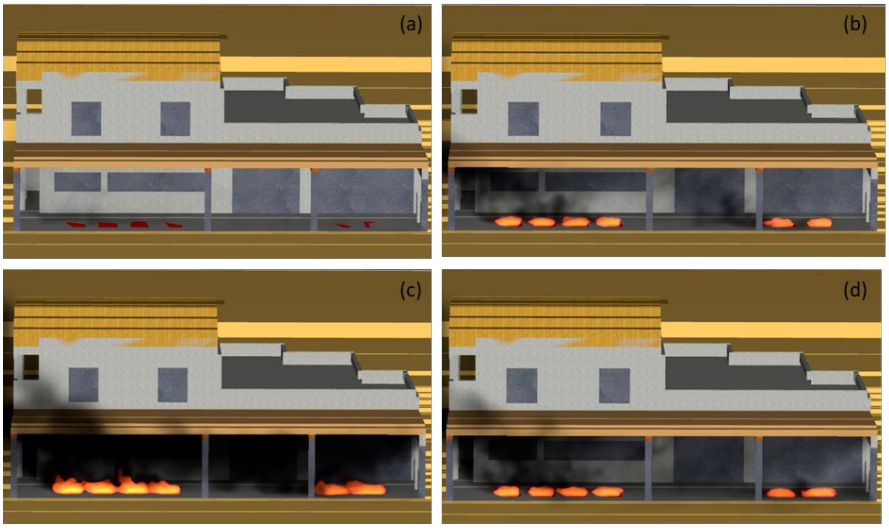

Figure 30: Scenario 2a at (a) 100 s of simulation, (b) 300 s, (c) 500 s, (d) 700 s

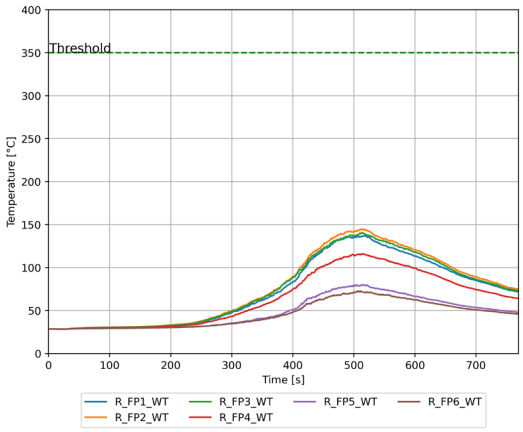

Figure 31: Surface temperature of the wooden ceiling for scenario 2a

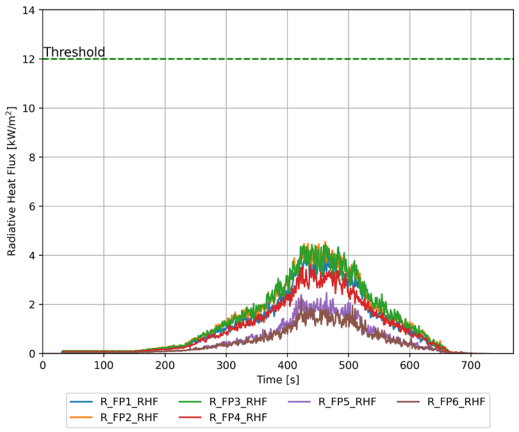

Figure 32: Radiative heat flux on the wooden ceiling for scenario 2a

Scenario 2b

This scenario has a higher HRRPUA for the FP than scenario 2a, as the FP consists of more combustible materials. This is evidenced by taller flames and more smoke production (Figure 33). Another indication of the impact of a higher HRRPUA is shown in Figure 35, with higher temperatures than the previous case, except for the devices above the FPs 5 and 6 (located on the right side of the porch), which did not ignite. The lower temperature detected by the FPs that did not ignite shows the influence of the SCS being open on three sides, experiencing air entrainment, and the wind blowing toward the ignited FP, cooling some regions and avoiding the smoke entrapment. The temperature readings above the fuel package most on the left (FP1, Figure 34) indicate that in 378 seconds, the ignition's threshold limit is reached. The peak is 357°C, which is 446 seconds in the simulation. The second criterion is shown in Figure 36, where FPs 1 and 2 present high peaks surpassing the limit safety value. The ignition of the wooden ceiling for the RHF criterion occurs at 295 s and reaches up to 16.3 kW/m^2 at 346 s. Following the same trend for temperature measurement, FPs 1 and 2 have higher readings, showing that this wooden ceiling is susceptible to combustion and, consequently, losing its integrity.

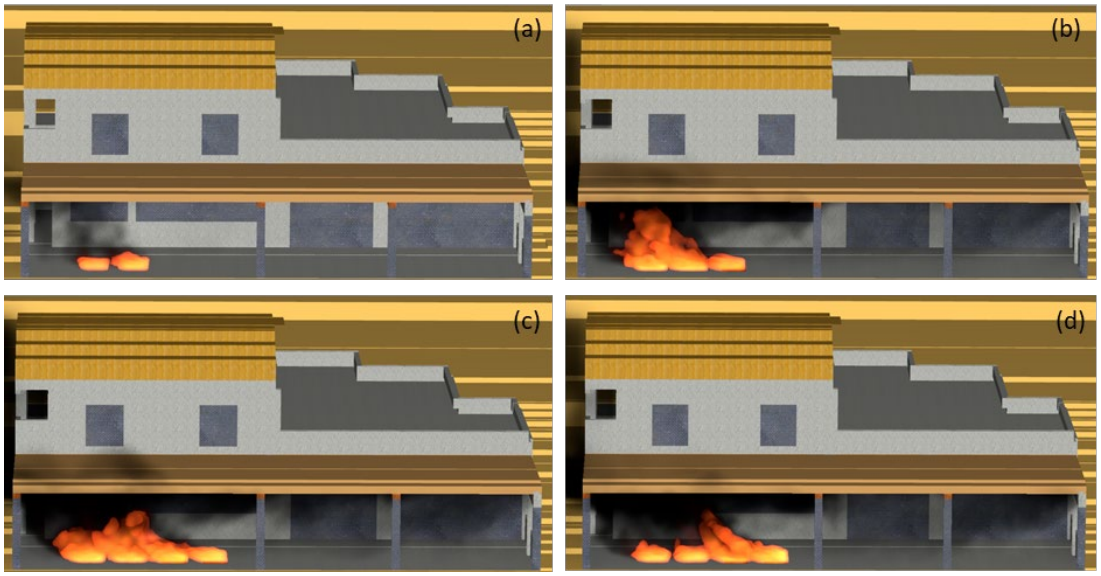

Figure 33: Scenario 2b at (a) 100 s of simulation, (b) 300 s, (c) 500 s, (d) 700 s

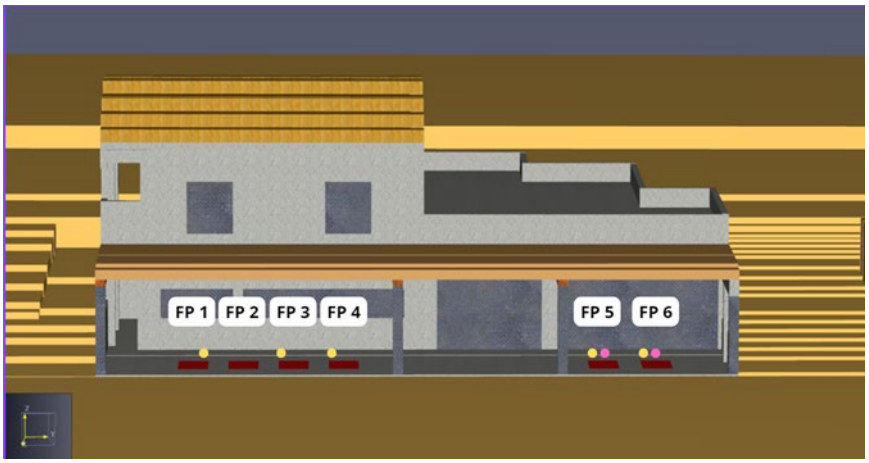

Figure 34: Scenario 2 identification of the FPs

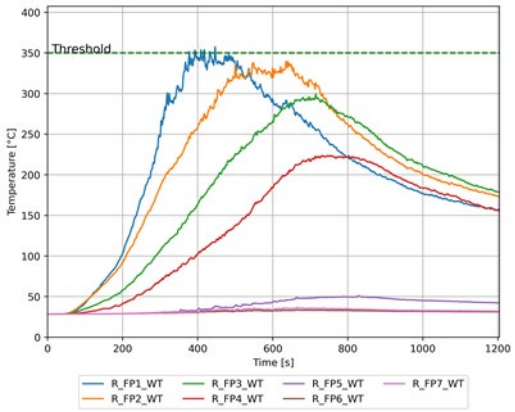

Figure 35: Surface temperature of the wooden ceiling for scenario 2b

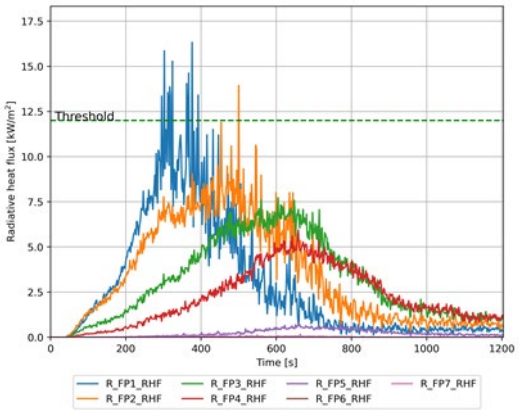

Figure 36: Radiative heat flux on the wooden ceiling for scenario 2b

As shown in Table 4, scenario 2a can be considered safe, as the temperature and heat flux values on the ceiling of the porch do not reach the set performance criteria. However, changing the typology and materials of the FP made the scenario unsafe, overpassing the RHF of 12 kW/m^2 at 295 s and the temperature of 350°C at 378 s, 83 s after the RHF criterion. The conclusion is that if elements similar to the fuel pack of scenario 2b are placed on the porch, combustion of the ceiling is possible.

Table 4: Times for the ceiling ignition according to the performance criteria of scenario 2

Performance criteria	Time of reaching the performance criteria [s]	
	Scenario 2a	Scenario 2b
T_{surf}	-	378
$\dot{q}''_{rad}$	-	295

Scenario 3

Figure 37 displays the labels utilized to identify the glazing systems of the flat in scenario 3. SH represents the window behind the shutter, LW stands for the left window, and RW indicates the right one. The evolution of the fire scenario is presented in Figure 38.

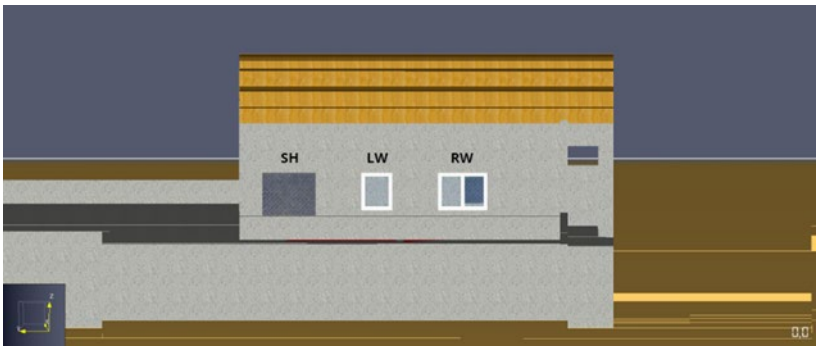

Figure 37: Label of the windows displayed on the representation of Scenario 3

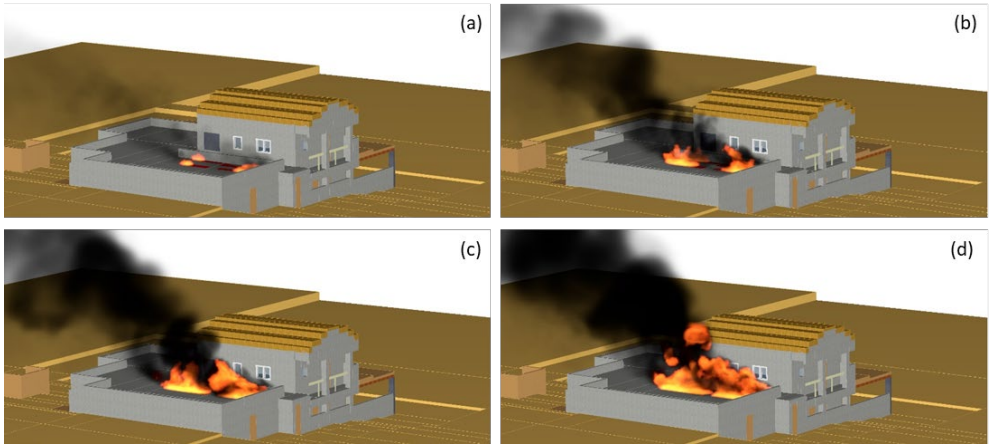

Figure 38: Scenario 3 at (a) 100 s of simulation, (b) 200 s, (c) 300 s, (d) 400 s

When it comes to the window protected by the shutter, the temperature of the glass remains almost at the ambient condition, as shown in Figure 39, not having a potential risk of breakage by this criterion. However, both unprotected windows reach the performance criterion on the upper sides of the panes. The left window breaks at 384 s (Figure 40), the left pane of the right window breaks at 393 s (Figure 41), while the right pane breaks at and 415 s (Figure 42).

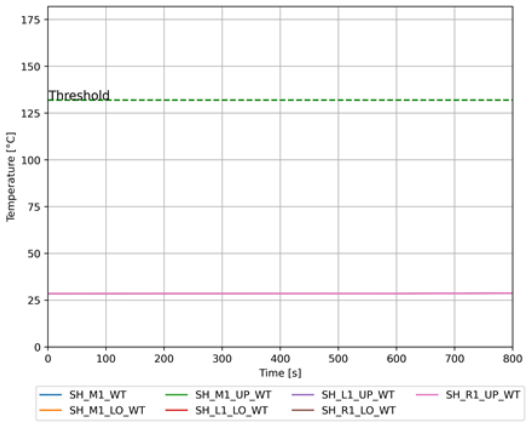

Figure 39: Surface temperature through time of the shuttered window for scenario 3

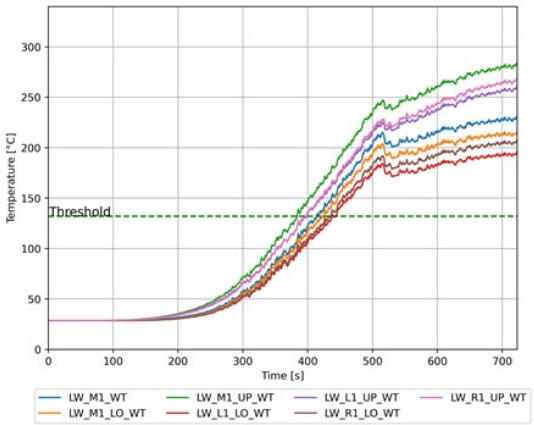

Figure 40: Surface temperature through time of the left window for scenario 3

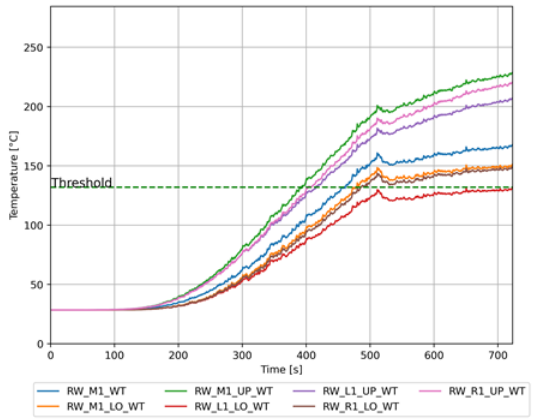

Figure 41: Surface temperature through time of the left pane of the right window for scenario 3

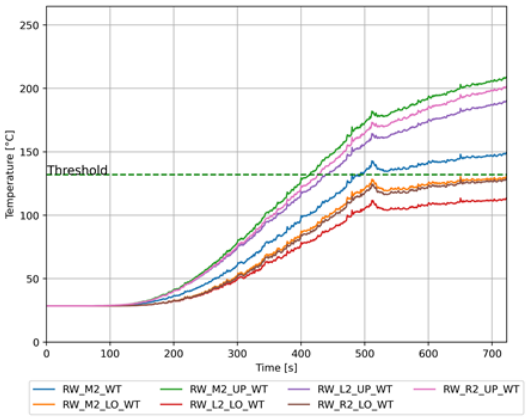

Figure 42: Surface temperature through time of the right pane of the right window for scenario 3

When it comes to the temperature difference criterion ΔT_{cr}, the window protected by the aluminum shutter does not experience a temperature difference between the protected and unprotected pane sections. In the unprotected glazing systems, the temperature difference threshold is reached for the right window earlier than the surface temperature criterion, at 362 s (Figure 44 and Figure 45), while for the left window the criterion is reached later, at 436 s (Figure 43).). The difference between the material of the frame causes this difference. Even though aluminum is a better heat conductor material, its surface temperature does not rise much, as shown in Figure 46. So, the conduction to the unexposed glazing does not reach high temperatures. In contrast, the wooden frame reaches higher surface temperatures (peak value of 336.5°C.

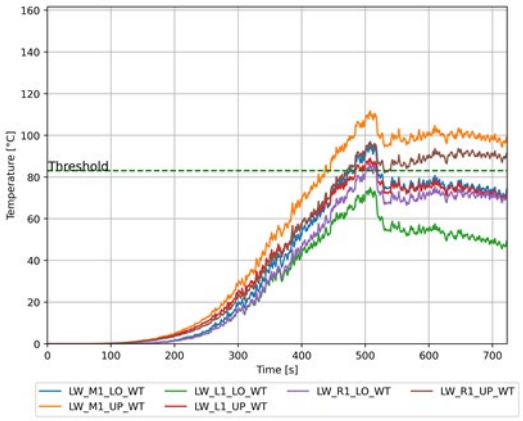

Figure 43: ΔT through time between the unexposed and exposed glazing in the left window (wooden frame) for scenario 3

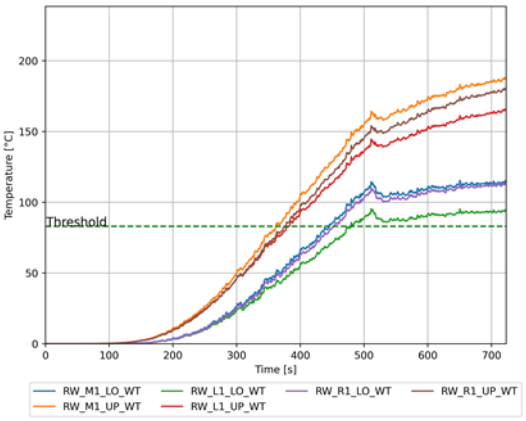

Figure 44: ΔT through time between the unexposed and exposed glazing in the left pane of the right window (aluminum frame) for scenario 3

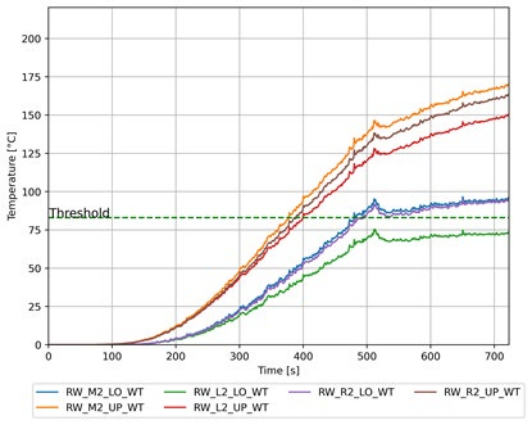

Figure 45: ΔT through time between the unexposed and exposed glazing in the right pane of the right window (aluminum frame) for scenario 3

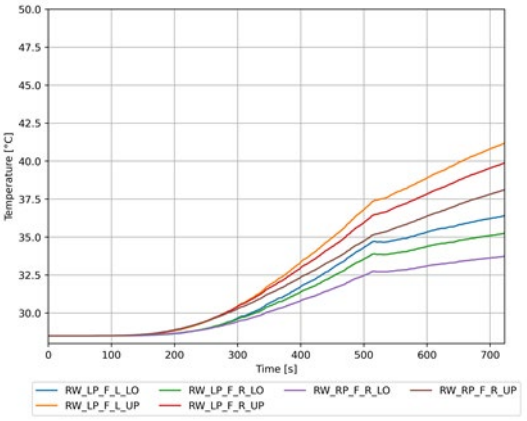

Figure 46: Temperature through time in the aluminum frame of the right window for scenario 3

Both unprotected windows fail for the heat load criterion, with the right window breaking first, compared to the left one, because it is positioned in the front of the FP with a higher HRR. Figure 47 and Figure 48 indicate that this threshold is reached earlier than the other criteria, between 300 to 350 s.

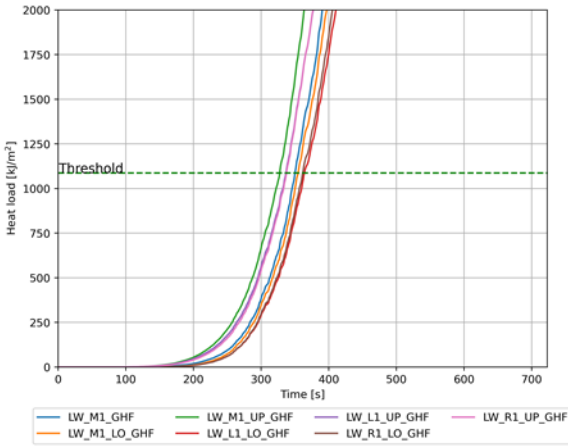

Figure 47: Heat load through time in the left window for scenario 3

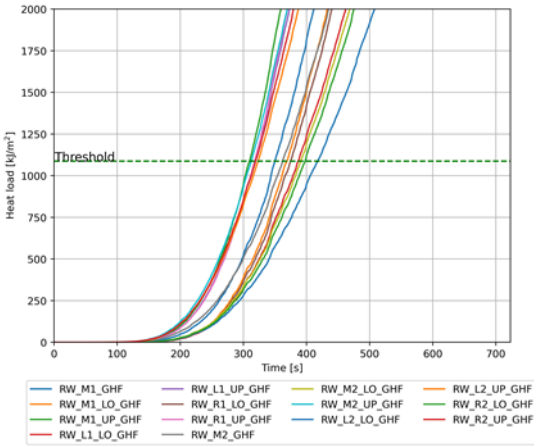

Figure 48: Heat load through time on the right window for scenario 3

When analyzing the measurement devices for the wooden frame, the temperature does not reach the threshold value, as the peak temperature is 336°C (Figure 49). However, the radiative heat flux reaches the set performance criterion and goes beyond it at 343 s (Figure 50). Unlike the aluminum material, which does not pose a danger to the window, the wooden frame is a problem in this case.

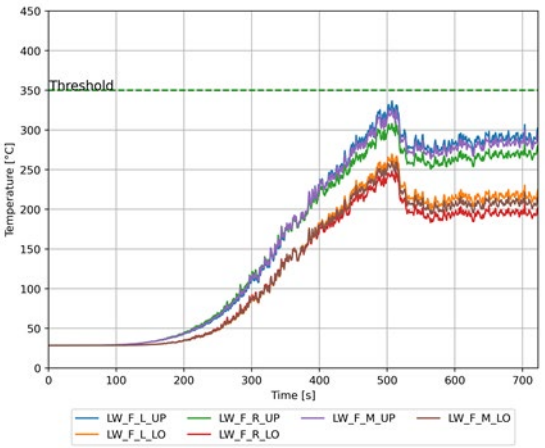

Figure 49: Temperature through time in the left window frame for scenario 3

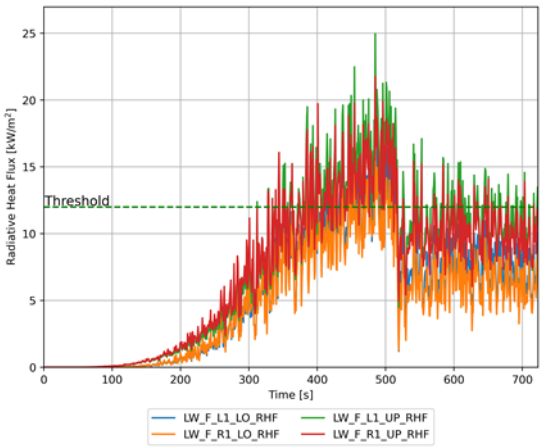

Figure 50: Radiative heat flux through time in the left window frame for scenario 3

When looking at the temperatures reached by aluminum shutter, it can be seen that it remains well below its melting point (Figure 51), therefore the shutter protects the glazing efficiently.

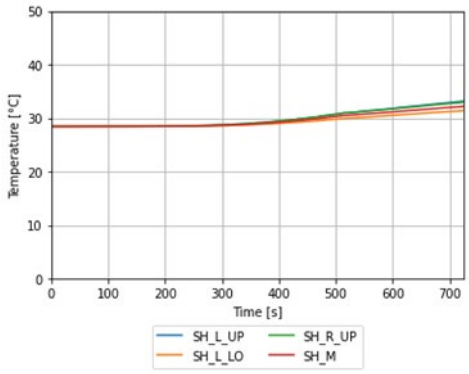

Figure 51: Surface temperature through time of the aluminum shutter for scenario 3

Table 5 summarizes the breakage of the glazing systems for scenario 3, showing that the heat load criterion is the first to be reached, followed by the radiative heat flux received by the wooden frame (which onsets ignition of the frame), then ΔT_{cr}, and finally, the T_{surf} of the pane. The shutter and aluminum frame criteria are not reached. As the windows break, allowing smoke and flames to enter the building, this scenario is not considered to meet the goal of property protection.

Table 5: Times for the failure of the windows according to the performance criteria of scenario 3

Performance criteria	Time of reaching the performance criteria [s]		
	Shuttered window	Left window	Right window
T_{surf}	-	384	393
ΔT_{cr}	-	436	362
HL	-	328	310
T_{surf} frame	-	-	-
$\dot{q}''_{rad}$ (wooden frame)	NA	343	NA

NA: Not Applicable

1.2.6. Design modifications and selection of the final design

Following the PBD framework, as the scenarios don't meet the set goal of property protection, it is necessary to change the design to meet the selected performance criteria. For the scenarios in which the fire led to the breakage of the glazing systems, the new design consists of placing an aluminum shutter in the same way as modeled for one of the windows in scenario 3.

Scenario 1 – Design suggestions

Scenario 1 is simulated again with the addition of aluminium shutters that protect the two windows located on the façade facing the garbage storage area (Figure 22). The surface temperature of the left shutter does not exceed 35℃ (Figure 52), while the one of the right shutter does not reach 40℃ (Figure 53). The heat transfer through the shutter is low, therefore the pane behind the shutter will not be impacted.

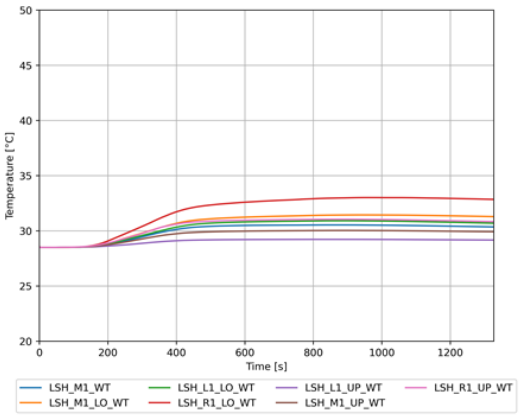

Figure 52: Surface temperature through time of the left shutter for Suggested Scenario 1

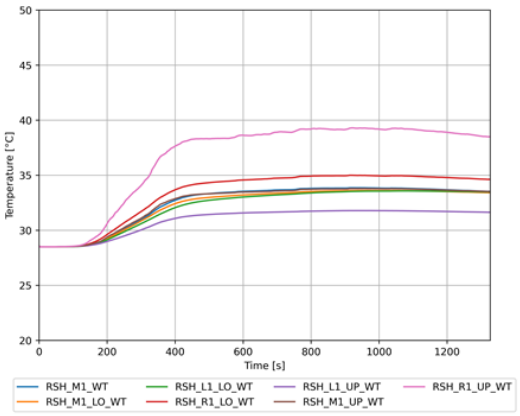

Figure 53: Surface temperature through time of the right shutter for Suggested Scenario 1

Scenario 2

When it comes to the ignition of the ceiling of the porch, no further simulations are made when it comes to changing the design of the building. It is recommended to ass a fireproof coating to the wooden ceiling and to remove the chairs and any other combustible material in the event of a wildfire.

Scenario 3 -Design suggestions

Scenario 3 is re-modelled with the placing of aluminium shutters on both exposed windows. Additionally, the damaged wooden frame of one of the windows is replaced by an aluminium one. The placed shutters protect the windows, as the temperature of the pane does not go above 28.6°C, only 0.1°C higher than the simulated ambient temperature (Figure 54, Figure 55 and Figure 56).

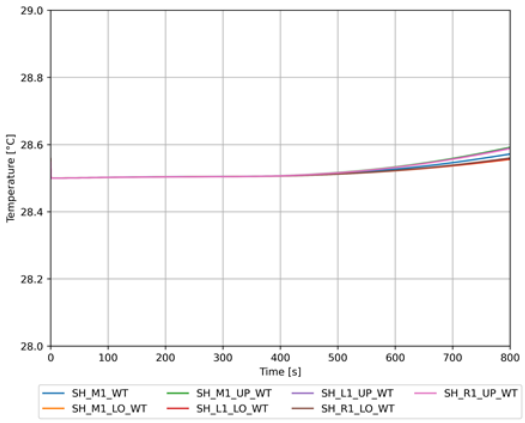

Figure 54: Surface temperature through time of the shuttered window 1 for Suggested Scenario 3

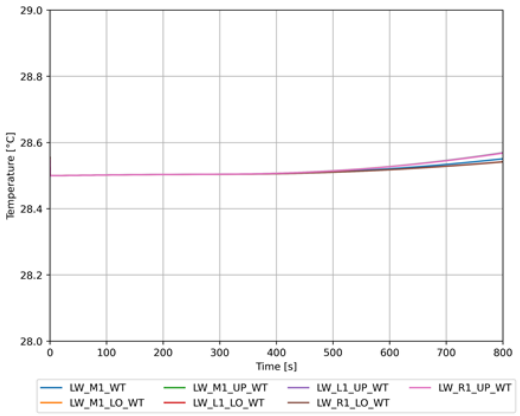

Figure 55: Surface temperature through time of the shuttered window 2 for Suggested Scenario 3

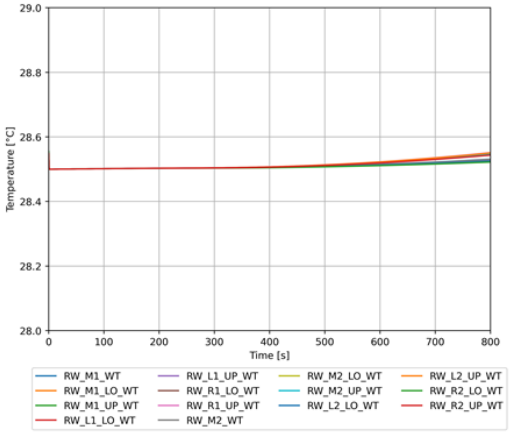

Figure 56: Surface temperature through time of the shuttered window 3 for Suggested Scenario 3

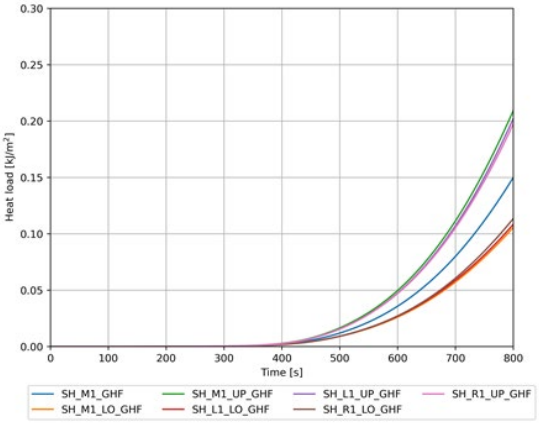

Figure 57: Heat load through time on the shuttered window 1 for Suggested Scenario 3

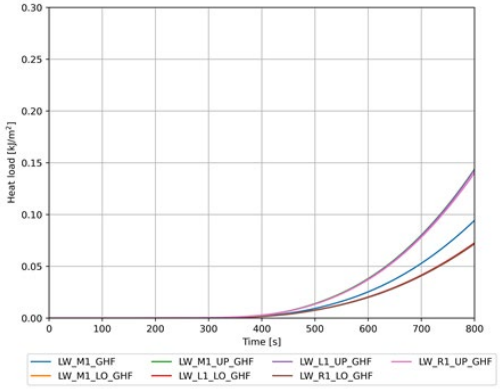

Figure 58: Heat load through time on the shuttered window 2 for Suggested Scenario 3

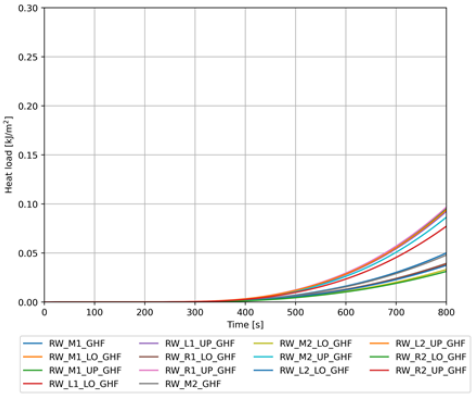

Figure 59: Heat load through time on the shuttered window 3 for Suggested Scenario 3

The HL criterion also made Scenario 3 unsafe. However, with the placement of the aluminum shutters in the front of the windows, the maximum HL imposed on the glazing (Figure 57, Figure 58 and Figure 59) is below 0.25 kJ/m2, which is deemed safe. Analyzing all the criteria means that the suggested scenario 3 is safe and achieves the goal of property protection. This scenario is also deemed safe for the shutter failure criterion, as the melting point is at 660.5°C and the temperature reached by the shutters is 32.7℃.

1.3. Conclusions of the study on Camping Punta Milà

Based on the results from the Performance-Based Design analysis, some modifications should be made to the building of the camping in order to meet the goal of property protection, and therefore to not have any great consequences to the structure of the building in case of wildfire.

The analyzed scenarios highlight the importance of protecting glazing systems from the heat load received in case of combustion of fuels located in their vicinity. It is therefore suggested to protect glazing systems located on the ground floor as well as on the first floor of the building by placing aluminium shutters. Additionally, it is recommended to apply a fireproof coating to the wooden ceiling of the porch, to avoid ignition and consequent failure of this structure. It is also suggested to remove all combustible materials from below the porch in the vent of a wildfire approaching, to avoid their ignition and subsequent impact onto the porch structure, and to seal the gap created by the shutter in the wall of the semi-confined space, to avoid firebrands and smoke entrance inside the building.

2. References

American Petroleum Institute (API), Fire-Protection Considerations for the Design and Operation of Liquefied Petroleum Gas (LPG) Storage Facilities, Washington, DC, 1996.

Babrauskas, V. Heat Release Rates, in: SFPE Handbook of Fire Protection Engineering, Springer New York, New York, NY, 2016: pp. 799–904. https://doi.org/10.1007/978-1-4939-2565-0_26.

Czerwinski, F. Thermal Stability of Aluminum Alloys, Materials 13 (2020) 3441. https://doi.org/10.3390/ma13153441.

Drysdale, D. An Introduction to Fire Dynamics: Third Edition, 2011. https://doi.org/10.1002/9781119975465.

Greenspec, Insulation materials and their thermal properties, (2024). https://www.greenspec.co.uk/building-design/insulation-materials-thermal-properties/ (accessed April 6, 2024).

Harada, K., Enomoto, A., Uede, K., Wakamatsu, T. An experimental study on glass cracking and fallout by radiant heat exposure, in: Fire Safety Science, 2000. https://doi.org/10.3801/IAFSS.FSS.6-1063.

Hurley, M.J. SFPE Handbook of Fire Protection Engineering, Springer New York, New York, NY, 2016. https://doi.org/10.1007/978-1-4939-2565-0.

Karlsson, B., Quintiere, J.G., Johansson, N. Enclosure Fire Dynamics, 2022. https://doi.org/10.1201/b22214.

Khan, M.M., Tewarson, A., Chaos, M. Combustion Characteristics of Materials and Generation of Fire Products, in: SFPE Handbook of Fire Protection Engineering, Springer New York, New York, NY, 2016: pp. 1143–1232. https://doi.org/10.1007/978-1-4939-2565-0_36.

McGrattan, K.B., Forney, G.P. Fire dynamics simulator: User's Guide (Sixth edition), Gaithersburg, MD, 2023. https://doi.org/10.6028/NIST.SP.1019.

NIST, Test7_4Pallet_r1, Fire Calorimetry Database (FCD): Multiple Item Transient Combustion Calorimetry (2019). https://www.nist.gov/el/fcd/multiple-item-transient-combustion-calorimetry/test74palletr1 (accessed March 26, 2024).

NIST, Test086_PatioChair_R3, Fire Calorimetry Database (FCD): Multiple Item Transient Combustion Calorimetry (2019). https://www.nist.gov/el/fcd/transient-combustion-calorimetry-tcc/test086patiochairr3 (accessed March 27, 2024).

Peacock, R.D., Davis, S., Lee, B.T. An experimental data set for the accuracy assessment of room fire models, Gaithersburg, MD, 1988. https://doi.org/10.6028/NBS.IR.88-3752.

Rompetrol Petrochemicals S.R.L., MSDS-01: Polypropylene - Material Safety Data Sheet, Constanta, Romenia, 2008. https://www.petrobul-bg.com/files/MSDS%20PP%20eng.pdf (accessed April 8, 2024).

Särdqvist, S. Initial Fires. RHR, Smoke Production and CO Generation from Single Items and Room Fire Tests, Department of Fire Safety Engineering and Systems Safety, Lund University, 1993.

SFPE, SFPE Engineering Guide to Performance-Based Protection. National Fire Protection Association., Quincy, MA, 2006.

Thunderhead Engineering, PyroSim, (2024). https://www.thunderheadeng.com/pyrosim (accessed March 25, 2024).

Vacca, P. Fire risk analysis framework at the wildland-urban interface, Universitat Politècnica de Catalunya, 2023. https://doi.org/10.5821/dissertation-2117-397449.

Vacca, P., Planas, E., Mata, C., Muñoz, J.A., Heymes, F., Pastor, E. Experimental analysis of real-scale burning tests of artificial fuel packs at the Wildland-Urban Interface, Safety Science, 146, 2022. https://doi.org/10.1016/j.ssci.2021.105568.

Wang, Y., Wang, Q., Wen, J.X., Sun, J., Liew, K.M. Investigation of thermal breakage and heat transfer in single, insulated and laminated glazing under fire conditions, Appl Therm Eng 125 (2017) 662–672. https://doi.org/10.1016/j.applthermaleng.2017.07.019.

Weather Spark, Climate and Average Weather Year Round in l'Escala, (2024). https://weatherspark.com/y/48990/Average-Weather-in-l'Escala-Spain-Year-Round (accessed March 26, 2024).

Węgrzyński, W., Lipecki, T., Krajewski, G. Wind and Fire Coupled Modelling—Part II: Good Practice Guidelines, Fire Technol 54 (2018) 1443–1485. https://doi.org/10.1007/s10694-018-0749-4.

Wildland-Urban Interface Fire Touristic Infrastructure Protection Solutions

WUITIPS

GA number 101101169

Co-funded by the European Union

Technical Note TN 5.2
Evacuation modelling of the Punta Milà campsite

WP - Task	WP5	**Version**	Final
File name	WUITIPS_Evacuation modelling of the Punta Milà campsite	**Dissemination level**	Public
Programmed delivery date		**Actual delivery date**	

Document coordinator	Enrico Ronchi (Lund University)
Contact	[enrico.ronchi@brand.lth.se]
Authors	Amina Labhiri (Lund University), Arthur Roahert (Lund University) Enrico Ronchi (Lund University),
Reviewed by	Elsa Pastor (UPC)

Abstract	This work uses simulation models for the assessment of evacuation strategies in touristic areas, with a specific case study related to the Punta Milà campsite. Recommendations in case of evacuation scenarios in the wildland-urban interface have been derived from the case study. This modelling work aimed at evaluating the effectiveness of available modelling approaches in representing tourist evacuations during wildfires and pinpointing the stages of the evacuation process that have the greatest impact on total evacuation time. Various evacuation strategies and modes have been investigated (both evacuation on foot and via private vehicles) through crowd and traffic modelling tools (the agent-based crowd model Pathfinder and microscopic traffic model SUMO respectively), along with the factors that influence them. The findings presented in this report offer recommendations for best practices that stakeholders can implement during wildfire evacuations in tourist areas.

Disclaimer

WUITIPS is co-funded by the European Union. Views and opinions expressed in this document are however those of the author(s) only and do not necessarily reflect those of the European Union or the European Commission. Neither the European Union nor the granting authority can be held responsible for them.

Table of Contents

Introduction 5

1. Wildfire evacuation modelling 7

1.1. Crowd and traffic evacuation modelling 7

2. The Punta Milà campsite 9

2.1. Background on Punta Milà campsite 9

2.2. Punta Milà campsite layout 10

2.3. Punta Milà campsite occupancy 10

3. Evacuation models in use 12

3.1. Pathfinder 12

3.2. Simulation of Urban Mobility 12

4. Evacuation scenarios 14

5. Pathfinder model configuration 17

5.1. Occupants' characteristics 18

5.2. Pre-evacuation time 18

5.3. Waiting time at the meeting point 22

5.4. Preparation time in the accommodation 23

6. SUMO configuration 24

6.1. Road network 24

6.2. Traffic Assignment Zone (TAZ) 24

6.3. Traffic demand 25

6.4. Background traffic 27

7. Evacuation simulation results 28

7.1. Scenario 1 (Traffic day evacuation) 28

7.1.1. Crowd evacuation modelling with Pathfinder 28

7.1.2. Traffic evacuation modelling with SUMO 30

7.1.3. Combination of Pathfinder and SUMO models 33

7.2. Results of Scenario 5 (traffic night evacuation) 35

7.3. Day vs night comparison 35

7.3.1. Traffic day evacuation vs traffic night evacuation 35

7.3.2. Day evacuation on foot vs night evacuation on foot 37

7.3.3. Day evacuation on foot with groups vs night evacuation on foot with groups 39

7.4. The impact of groups 40

7.5. The impact of archetypes 42

7.6. Results summary 44

8. Discussion 45
9. Conclusions 49
References 51

Introduction

The severity and frequency of fires affecting Wildland-Urban Interface (WUI) communities have increased rapidly over the past few decades worldwide. This increase has resulted in greater loss of human lives and destruction of structures (Haynes et al., 2020). In fact, changes in major driving factors have contributed to this escalation (Huang et al., 2015). Factors such as the climate crisis (Jolly et al., 2015), which leads to hotter and drier seasons, along with increased urbanization have intensified these fires as well. From this perspective, emergency managers are responsible for protecting people and ensuring safe evacuations when necessary. To achieve this goal, emergency managers prepare comprehensive plans and implement strategies designed to effectively manage such an event. Those strategies include different protective actions such as stay-and-defend, shelter-in-place, and leave early (Cova et al., 2009; Strahan, 2020). However, it is important to consider the potential delays in people taking proactive actions, which may result in negative consequences.

In this context, the WUI in touristic areas presents a real challenge compared to the other areas. This challenge arises because tourists are heterogeneous and the impacts of wildfires on tourism can cause economic losses and requires specific recovery strategies (Otrachshenko & Nunes, 2022). Several wildfires have occurred in touristic areas, such as the 2016 Cadiz fire in Spain (Ronchi et al., 2021), the 2023 Rhodes Fire in Greece (Bubola & Kitsantonis, 2023) and the 2023 Hawaii wildfires which were described as being more deadly than Hawaii's 1960 tsunami (Gupta, 2023). Tourists may exhibit behaviours different from those of local residents, as they may be unfamiliar with the area, speak different languages, or have different levels of risk awareness (Arce et al., 2017). These factors are crucial in defining how tourists will respond to a wildfire event and the protective actions they are likely to take.
Modelling the wildfire evacuation in Wildland-Urban Interface (WUI) areas can be challenging not only due to the complex nature of wildfires themselves which is influenced by multiple factors affecting wildfire spread behaviour (Sun et al., 2023) but also due to the research gap in terms of human behaviour response in case of wildfire scenario (Haghani et al., 2022).

Evacuation models can be used to assess the safety of individuals in wildland-urban interface fires. The evacuation modelling helps to determine the evacuation time needed to reach a safe area known as evacuation time curves. The different modelling layers depend on the evacuation mode (on foot, via private vehicles, via public transport or via alternative means) which is related to the required covered travel distance during the evacuation process (Ronchi, E. (2023)).

Crowd modelling represents a useful tool to aid evacuation design as it provides insight into the two major phases of evacuation which are the pre-evacuation and the movement process (Purser & Bensilum, 2001). Multiple traffic modelling approaches can be used to model the wildfire traffic evacuation (Intini et al., 2019).

In the case of a WUI fire in a touristic area, assessing the evacuation of individuals (whether this occurs on foot or via private vehicles) to estimate their time of arrival at a safe destination necessitates the consideration of the various behavioural elements.

Specifically, the behaviour of tourists during a wildfire is particularly significant. Nevertheless, while the scientific literature has largely explored wildfire evacuation behaviour in general (Kuligowski et al., 2020; Rohaert, Kuligowski, et al., 2023) there has been less focus on the specific behaviours of tourists (Labhiri et al., 2024). Furthermore, there is limited research that details the critical factors influencing the evacuation decision-making of tourists during a wildfire evacuation. This gap extends to specific scenarios such as the evacuation of tourist campsites, a context where the dynamics can significantly differ from other environments due to the unique layout and temporary nature of these accommodations as well as the high number of tourists during peak seasons.

In order to address this issue and to reduce this knowledge gap, this work makes use of evacuation modelling to investigate the impact of several variables on evacuation strategies. Those variables include time of the day (i.e., day vs night), and modes of evacuation (on foot vs by vehicle). Evacuation modelling is performed for a camping site (Punta Milà camping) through crowd and traffic modelling. This is performed respectively with a widely used agent-based crowd simulator called Pathfinder (Thunderhead Engineering, 2024) and a widely used open-source traffic simulator called SUMO (Simulation of Urban Mobility) (Lopez et al., 2018).

1. Wildfire evacuation modelling

Modelling the wildfire evacuation in WUI communities presents a unique challenge compared to building scenarios. This is due to several reasons. The first reason is that modelling wildfire evacuation requires different types of evacuation modes which are typically linked to pedestrian and traffic movement. Another reason is that wildland fire is seen as an event that triggers human responses at various scales, for instance, the temporal scale and the social-organizational (McCool et al., 2006). This is because the WUI communities differ from one another in terms of social, political, and environmental context (McCool et al., 2006). Overall, this was summarized by Ronchi et al., 2017 in one sentence "*The multi-dimensional nature of a WUI incident that further differentiates it from most building fires: spatial dynamism, temporal iterations, the range of influential factors and the multi-level organisational involvement.*"

Using evacuation models in WUI helps to provide an estimation of the time needed to leave the threatened area and reach a safe destination. Those tools help as well to evaluate the impact of various evacuation strategies in response to changing fire conditions (Ronchi & Gwynne, 2020). Different approaches can be used to represent different modelling components of evacuation modelling where three modelling layers exist, namely, people response, people movement, and traffic movement (Ronchi & Gwynne, 2020) . The first approach consists of modelling all three layers explicitly, the second is to include implicitly the representation of people's response and the third is to include an implicit representation of people's response and movement (Ronchi & Gwynne, 2020). The selection of the approach usually depends on modeler preferences as well as the computational resources, time and data needed for calibration, and the level of detail needed to be captured.

1.1. Crowd and traffic evacuation modelling

Crowd models can be used to calculate the time needed for evacuees on foot to reach a safe destination. Those are typically used for those scenarios in which evacuation takes place on foot, or in the initial stage of a multi-modal evacuation, i.e. to calculate the time needed for evacuees to reach on foot their private vehicles.

Traffic modelling is one of the key simulation layers in a WUI fire evacuation scenario. It typically consists of a four-step structure: 1) Travel Demand, 2) Trip Distribution, 3) Modal Split and 4) Traffic Assignment (Intini et al., 2019).

Travel demand involves trip generation, which, in the context of touristic areas, refers to the number of tourists departing from their original location. The trip distribution links origins and destinations. This can be presented by adopting either a trip-based or an activity-based modelling approach (Ronchi et al., 2017) where the difference between the two is the capability of the activity-based modelling to count for the individual activities of each person. In other words, the trip-based modelling approach ignores the intermediate trips (Ronchi et al., 2017). Modal split specifies the types of transportation chosen for travel (Ronchi et al., 2017). In the context of wildfire evacuations in tourist areas, especially in campsites, the modes of transportation can include either private vehicles or transportation arranged by authorities. Traffic assignment involves distributing a specified set of origin-destination pairs across an

appropriate road network, according to criteria chosen by travellers (Saw et al., 2015). Depending on the project goals and time variability, traffic assignment can either be static or dynamic. In static assignment, the traffic demand is assumed to remain constant over time where the traffic on the network is in a 'steady-state' (Ronchi et al., 2017). In contrast, the dynamic assignment implies that traffic loading and route choices changes over time.

Key outputs of evacuation modelling include the elements that describe the crowd and traffic movement (i.e., flows, travel times, delays) and the total evacuation time (Ronchi & Gwynne, 2020). It also assesses strategies to enhance evacuation efficiency, like reducing congestion. In the case of a wildfire evacuation scenario in WUI, the resolution of the results depends mainly on the scale of the modelling (i.e., microscopic, mesoscopic, macroscopic)

A macroscopic model typically represent evacuation behaviour with a lower level of detail, often using macroscopic relationships between speed (km/h), flow (veh/km/lane), and density (veh/h/lane) (Rohaert, Kuligowski, et al., 2023; Rohaert, Wahlqvist, et al., 2023). In contrast, a microscopic model allows a more detailed description of the evacuation by capturing the interactions between individual agents (Ferrara et al., 2018). It uses time as an independent variable, calculating each agent position, speed, and acceleration at each simulation step (Tapani, 2008). Nevertheless, this modelling approach often requires a detailed calibration of a high number of parameters to accurately simulate the scenario (Ferrara et al., 2018). Mesoscopic models occupy an intermediate position between the microscopic model and the macroscopic model (Ferrara et al., 2018). Mesoscopic models describe flow dynamics using aggregate probability distributions influenced by individual behaviours.

2. The Punta Milà campsite

The Punta Milà campsite is a major tourist destination in the northeastern part of Spain. This campsite features the typical infrastructure found in many other campsites across Southern Europe.

2.1. Background on Punta Milà campsite

A study trip was undertaken by the research team to the study area in September 2023, during which several campsites were visited. Conversations with campsite managers, who had previously experienced wildfire evacuations, as well as discussions with firefighters and municipality managers, provided insights into the tourism activity in the area, the types of visitors, specific weather conditions, and the fire management strategies implemented there.

The Punta Milà campsite is located in the heart of the Natural Park of Montgrí between the municipalities of l'Escala and Torroella de Montgrí. The discussion with the fire manager in the region indicated that those municipalities receive a high number of tourists mainly during the summer season with tourism services serving as the main economic activity. According to campsites managers, this region is attractive to tourists because of its proximity to beaches and forests, offering numerous entertainment activities.

However, the area where the Punta Milà campsite is located can present a real danger for tourists in case of a wildfire event. The wind behaviour in this region can be driven by the wind coming from the north known also as northern wind (Tramontana). This wind accelerates the spread of the fire as it is a very strong wind blowing from north to south, directly towards the Natural Park of Montgrí, where there is plenty of fuel (see Figure 1). Moreover, the final stage of these wildfires remains challenging even after the general northern wind disappears because the local winds which are influenced by the terrain (topographic winds) can still be active and may increase the fire activity in the flanks and back.

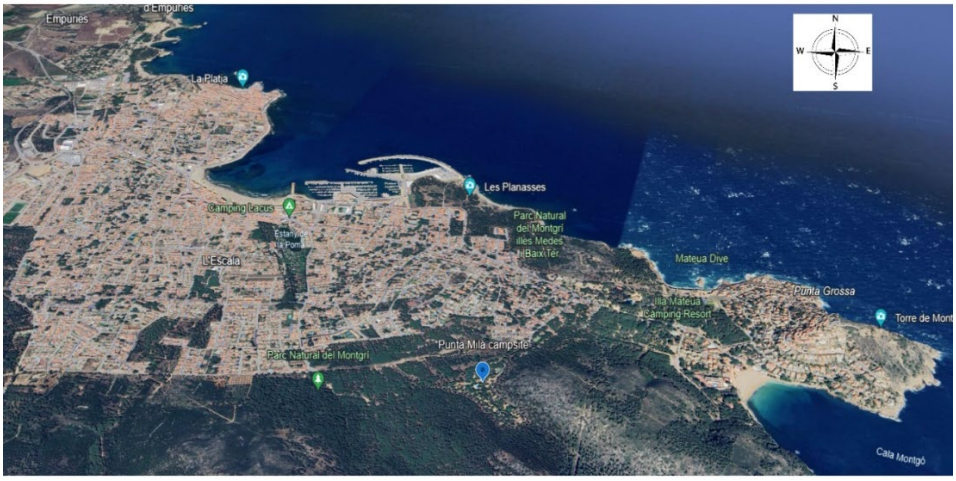

Figure 1. View of L'Escala region (Image: Google Earth).

2.2. Punta Milà campsite layout

Punta Milà camping site is a popular destination for tourists from the Netherlands, Belgium, and France because of its proximity to beaches (850 meters from Cala Montgó beach), natural park, and its Mediterranean climate. The total area of the camp is approximately 51810 m² and it provides various accommodation options including pitches for tents and caravans. The total number of parcels is 160 fully equipped for 5 persons each. The camp also includes several buildings to ensure that guests have access to services. The reception is located near the camp entrance where the staff assist tourists in obtaining information relevant for their holiday stay. Moreover, there is a building that houses a supermarket, a bar, and a restaurant.

Inside the camp all surfaces are designed to be easy to walk. A concrete path runs through the camp, providing a well-defined route for vehicles and pedestrians to navigate. The width of main paths within the camping site is approximately 5 m. Besides that, the camp has only one entrance/exit (permanently open exit door with a total width equal to approximately 10 m). Moreover, the vegetation within the camping includes tall, pruned pine trees and low scattered bushes, all of which are well maintained.

The yellow region in Figure 2 shows the campsite boundary from a satellite view (Google maps).

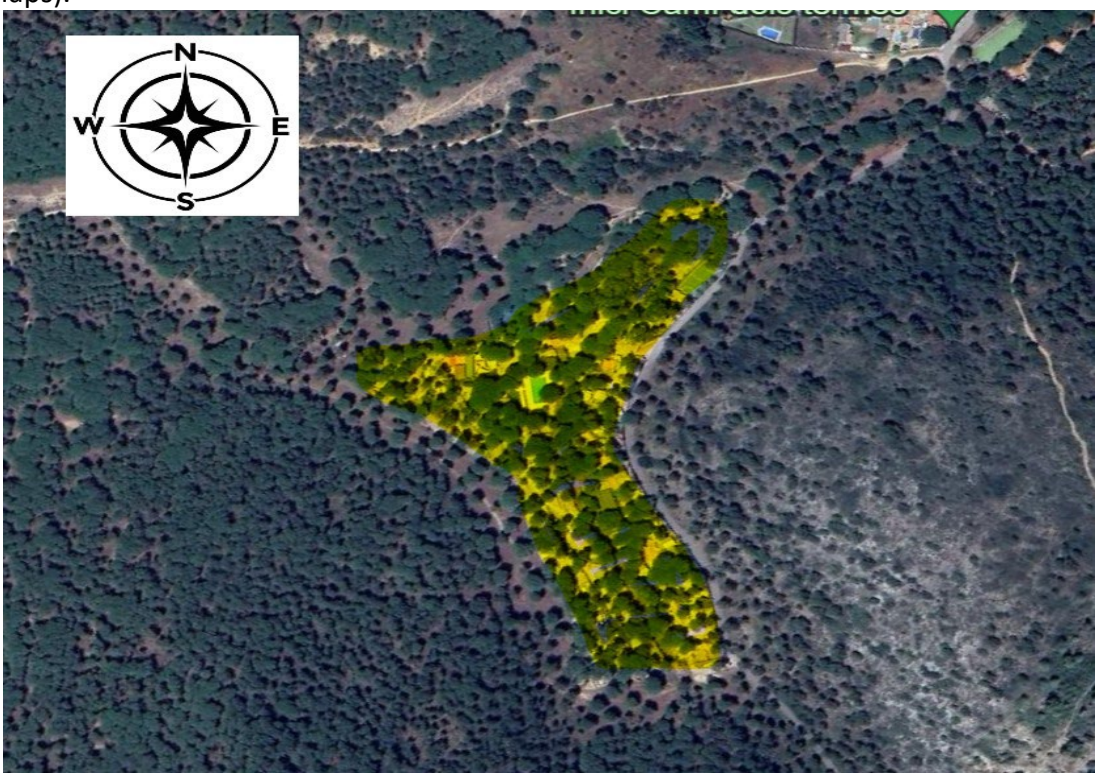

Figure 2. Satellite view of Punta Milà campsite, with the yellow region indicating the campsite boundary (Image: Google Maps).

2.3. Punta Milà campsite occupancy

During the peak season, Camping Punta Milà can host a maximum of 900 tourists with a staff of 14 individuals during the day and 10 individuals during the night.

A typical tourist population in the campsite includes families with 2-3 children aged 10-15 years old. This is alongside a number of older couples who also frequent the camp. While the majority of the tourists are from the Netherlands, there is also a considerable number of tourists coming from Belgium and France.

The maximum number of vehicles during peak season is 300 vehicles where 1/3 are caravans and 2/3 are passenger vehicles. Although parking spaces are limited both inside and outside the campsite, tourists have the option to park their vehicles in their parcels or in a parking area near the entrance.

3. Evacuation models in use

The simulations in this study have been performed with a crowd evacuation model (Pathfinder) and a traffic simulation model (SUMO). A brief introduction on both models is here presented.

3.1. Pathfinder

Pathfinder is an agent-based evacuation simulator developed by Thunderhead Engineering (2022). Widely adopted in both academic and commercial applications, Pathfinder is a commonly used pedestrian evacuation model (Lovreglio et al., 2020). It allows the use of two movement simulation modes. The first one is the steering mode where occupants use a steering mechanism to interact with others (Reynolds & others, 1999). The second one is the Society of Fire Protection Engineering mode which is based on a set of hand calculations and assumptions where agents do not avoid each other (Gwynne & Rosenbaum, 2016). The default configuration in Pathfinder is continuous movement based on steering behaviours. The spatial representation in Pathfinder is a triangulated mesh providing walkable areas and obstacles allowing agents' interactions within it.

3.2. Simulation of Urban Mobility

SUMO (Simulation of Urban Mobility) is a free and open-source traffic simulation tool. It is created by The Institute of Transportation Systems in Berlin, Germany and was released on the year 2001 (Lopez et al., 2018). SUMO is a multi-modal model which means that it integrates the movement of cars as well as the other transport systems and supports traffic lights. Moreover, the simulation in SUMO is space-continuous, and time-discrete traffic flow simulation (Lopez et al., 2018). The traffic flow is microscopic which means that each vehicle within the road network is represented individually by providing its specific position and speed through the network. Modelling vehicles at this granular level is important to get insights into the time when the last vehicle reached the safe zone as well as the speed distribution of the vehicles travelling to the safe destination.

The SUMO package includes a variety of tools, the main modules of the package are:

- SUMO GUI which is the graphical user interface that helps to visualize vehicles dynamic. It reads the input data, conducts the simulation, collects results, and generates output files.
- OsmWebWizard is a tool that allows to extract the road network from OpenStreetMaps (a free, open geographic database). After the configuration of randomized traffic demand, it is possible to run and visualize the scenario in the SUMO-GUI.
- For a visual network editor, Netedit or a command line can be used to modify the network or to create new features within the road (Lopez et al., 2018). It processes the input data, generates the input for SUMO, and saves the outcomes in different output formats, including XML.

The car-following model defines the speed of a vehicle in relation to the vehicle ahead of it (Song et al., 2014). This is an important feature as it illustrates that vehicle speeds influence overall traffic flow and can significantly impact evacuation times. The default

model used by SUMO is Krauß model (Krauß, 1998) which consists of selecting the maximum speed that allows one to stop at any time without any collision with the following vehicle (Lopez et al., 2018). The speed is referred to as the safe velocity (v_{safe}) (Krajzewicz et al., 2002). The car-following model is influenced by multiple factors such as individual characteristics (age, gender, risk-taking propensity, driving skills) but also by situational factors (time of day, road conditions, impairment due to alcohol, fatigue, trip purpose, driving length) (Ranney, 1999).

In terms of input, SUMO relies on two main files to initiate simulations. The first file, known as the routes file, serves a dual purpose. Firstly, it defines the traffic demand by specifying the routes that vehicles will take within the simulated network. Additionally, this file includes details about the characteristics of the vehicles involved, such as their type, acceleration, deceleration, length, and maximum speed. The second essential file is the net-file, which represents the network topology of the network. This file illustrates the spatial layout of roads, intersections, lanes, traffic lights, and other relevant infrastructure elements. Together, these two files provide SUMO with the necessary information to simulate the scenario.

As for output data, SUMO can generate several files for the simulated scenario. One of the key outputs is the XML file from the virtual induction loops (in case it was added to the network) which records detailed information about the movement of each vehicle in a specific lane. Another key output is the trip output which provides a table with all information about every vehicle including depart time, arrival time, arrival speed, duration, route length and waiting time (queuing). SUMO version 1.19.0 was used for building the model and an example of working interface of SUMO-GUI is shown in the Figure 3.

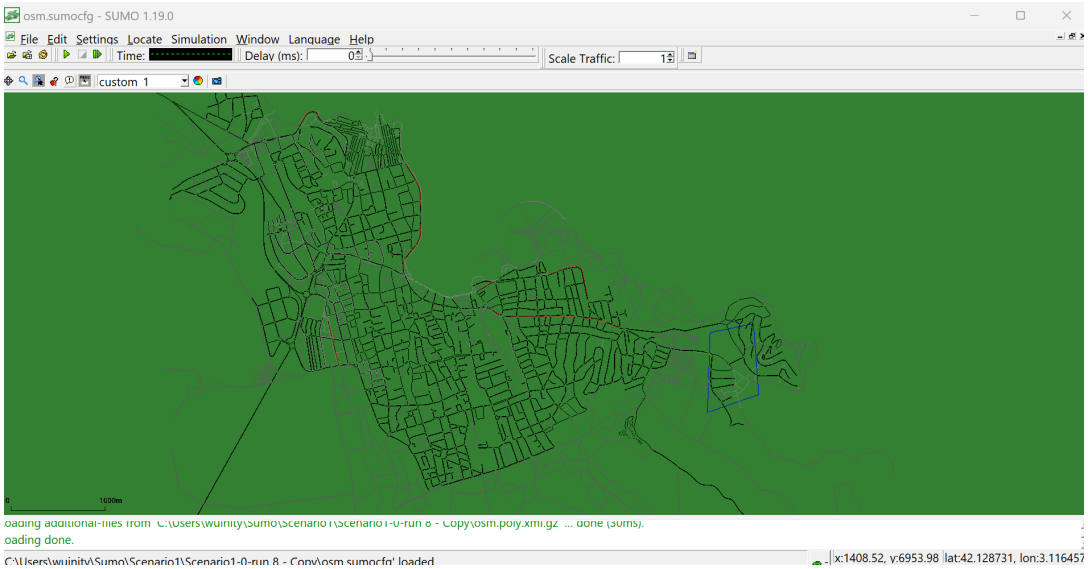

Figure 3. SUMO Graphic User interface.

4. Evacuation scenarios

A set of evacuation scenarios is here defined to assess the influence of various factors on the overall evacuation time. It should be noted that this study does not take into consideration shelter-in-place scenarios. The evacuation scenarios include therefore two types of strategies: one in which tourists evacuate on foot, and the other in which tourists use their private vehicles.

Figure 4 illustrates the first evacuation strategy (Evacuation on foot), tourists are initially located either in their accommodation or somewhere around the camp (starting point). They are then required to go to the meeting point by foot to receive evacuation instructions. After that, they are supposed to return to their accommodation to prepare for the evacuation. Finally, they evacuate on foot to the campsite's designated exit point before boarding buses arranged by authorities for further transport. This strategy requires good coordination and management between authorities to ensure the safe evacuation of all individuals.

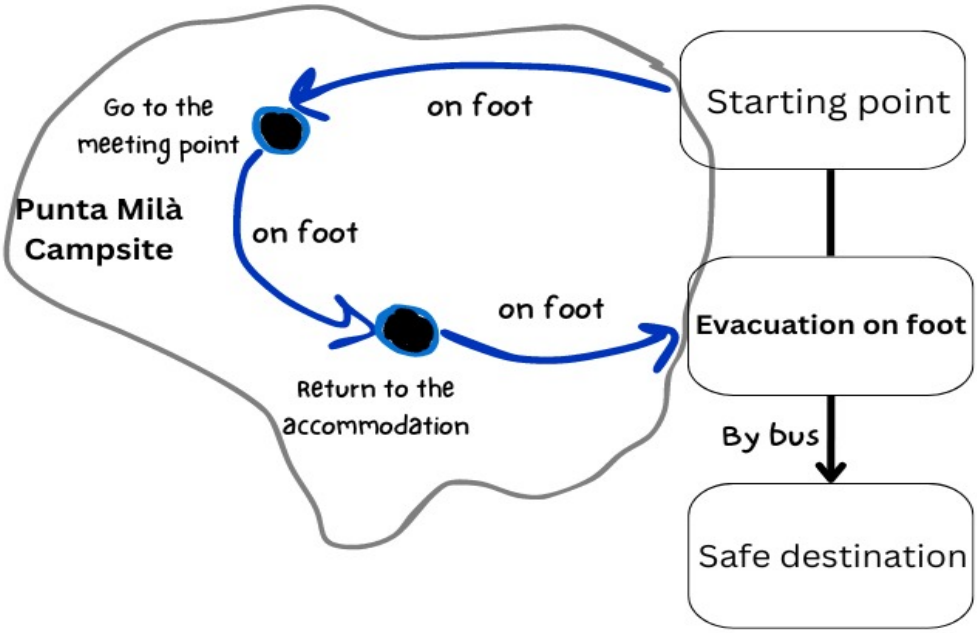

Figure 4. Evacuation on foot strategy process.

Figure 5 shows the second evacuation strategy (Traffic evacuation), tourists are initially located either in their accommodation or somewhere around the camp (starting point). They are then required to go to the meeting point by foot to receive evacuation instructions. Following instructions, they are supposed to return to their accommodation to prepare for the evacuation. Finally, they are required to drive by private vehicle to a dedicated safe area, specifically the area near the beach 'Platja de Montgó'. This evacuation strategy considers traffic congestion and good coordination to facilitate the safe departure of tourists from the campsite.

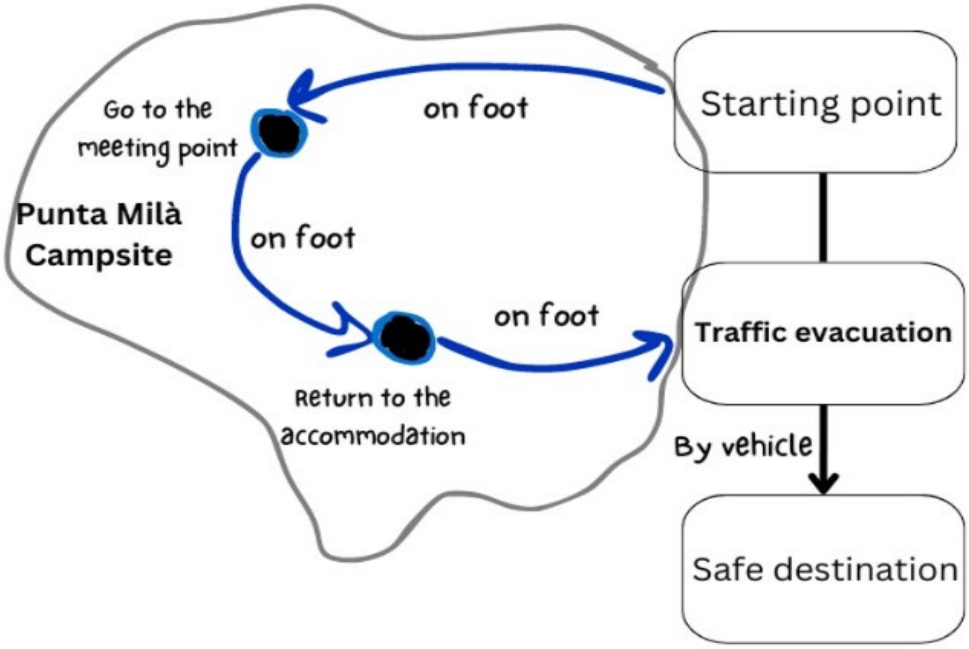

Figure 5. Evacuation by vehicle strategy process.

By evaluating these two evacuation strategies and their respective implications, it is possible to decide on the most effective approach for ensuring a secure evacuation of tourists from the campsite in case of a wildfire evacuation.

Table 1 outlines the total number of scenarios performed during the modelling, where in all scenarios the camp is operating at full occupancy.

Table 1. Description of the evacuation scenarios.

Scenario	Description	Moment of the day	Evacuation type	Groups	Archetypes
1	Traffic day evacuation	Day	Vehicles	No	No
2	Day evacuation on foot	Day	Foot	No	No
3	Day evacuation on foot with groups	Day	Foot	Yes	No
4	Day evacuation on foot with archetypes	Day	Foot	No	Yes
5	Traffic night evacuation	Night	Vehicles	No	No
6	Night evacuation on foot	Night	Foot	No	No
7	Night evacuation on foot with groups	Night	Foot	Yes	No

In scenario 1, which is the traffic day evacuation, tourists are randomly distributed around the campsite. Tourists will receive the evacuation notification from the staff or other tourists as there is no centralized alarm, then they need to go to the assembly point on foot to receive the instruction, and then return to their accommodation, take their private vehicle (generally a car or van), and then evacuate via their vehicle.

In scenario 2, which is a day evacuation on foot, tourists go to the assembly point on foot, receive instructions and then return to their lot and evacuate on foot to the outside of the camping to be taken by buses arranged by authorities.

In scenario 3, which is a day evacuation on foot with groups, tourists engage in the same process as in scenario 2. However, in this scenario, the fact of having group movement is introduced to evaluate its impact on evacuation time.

In scenario 4, which is a day evacuation on foot with archetypes (Labhiri et al., 2024; Strahan et al., 2018), tourists follow the same process as in scenario 2. Nevertheless, the concept of archetypes is introduced to examine how the added complexity in defining profiles can influence evacuation time.

Scenarios 5, 6, and 7 respectively represent traffic night evacuation, night evacuation on foot, and night evacuation on foot with groups. These scenarios aim to capture the influence of nighttime conditions on the evacuation process.

5. Pathfinder model configuration

The Pathfinder model configuration is based on the information available as well as a number of assumptions made. The model configuration includes the occupant's characteristics, occupants' distribution, the pre-evacuation time, the waiting time at the meeting point, the preparation time, and the effect of the topography on the walking speed.

Overall assumptions:

- Full occupancy of the campsite.
- The impact of potential obstacles on the road that might obstruct or impede movement is disregarded. The reason is based on the observations from a visit to the campsite, where all surfaces appeared easily navigable. There is a concrete path for vehicles and people to go through. Moreover, vegetation within the camping is very well maintained. Tall, pruned pine trees, and low scattered bushes (See Figure 6)
- Fire detection and alarm notification times are omitted as RSET calculations will start directly after the evacuation order is given.
- The area on the top left of the camp is excluded from the study as it was a renting area from the municipality (on the other side of the river, parcels 60-77 and 98-103).
- The toxic effect of smoke is not considered as we are assuming that the smoke is not yet reaching the campsite during the evacuation.
- Staff members are distributed randomly around the campsite.
- The campsite terrain is predominantly flat, but in an area where a moderate incline was observed a speed reduction factor equal to 0.97 was assumed.
- It is assumed that all vehicles are parked nearby the accommodation.

Figure 6. Punta Milà campsite (8 February 2024).

5.1. Occupants' characteristics

The total number of tourists at full occupancy is 900 people. The majority of the visitors are assumed families with 2-3 children aged 10-15 years. Additionally, older visitors are also accounted for in the demographic makeup of the campsite.

Table 2 (scenarios 1, 2,3 and 4) and Table 3 (scenarios 5, 6, and 7) present the occupant's number distribution as well as their walking speed for the different scenarios (Korhonen et al., 2008). The speed is given as uniform distribution to capture variability and the influence of factors such as congestion, density, and obstacles on pedestrian movement. The speed during nighttime is reduced due to the reduced visibility at night.

Table 2. Profile's characteristics for day scenarios.

Profile	Number	Speed in m/s (uniform distribution)	Size in m
Adult	450	Min= 0.95; Max= 1.55	Min= 0.44; Max= 0.58
Child	360	Min= 0.6; Max= 1.2	Min= 0.39; Max= 0.45
Elderly	90	Min= 0.5; Max= 1.1	Min= 0.46; Max= 0.54

Table 3. Profile's characteristics for night scenarios.

Profile	Number	Speed in m/s (uniform distribution)	Size in m
Adult	450	Min= 0.71; Max= 0.88	Min= 0.44; Max= 0.58
Child	360	Min= 0.46; Max= 0.91	Min= 0.39; Max= 0.45
Elderly	90	Min= 0.38; Max= 0.84	Min= 0.46; Max= 0.54

5.2. Pre-evacuation time

The pre-evacuation time is also referred to as pre-travel or pre-movement time, represents how long it takes for people to recognise the alarm and respond to it. This time varies depending on several factors, including the occupants' familiarity with the physical environment, their state of alertness (i.e., sleeping or awake), the type of alarm employed, and the level of management in place. In the case of the campsite and tourists, specific pre-evacuation times were not readily available, since limited behavioural research has been conducted on this topic. As a result, estimates were made considering the existing literature. These estimates were done to consider a credible pre-evacuation time for the campsite evacuation scenarios.

The pre-evacuation time was defined using Table E.2 from PD 7974-6:2019 standard (PD, 2019). For day scenarios the scenario category is B: awake and unfamiliar, while for night scenarios the scenario category is Ciii: Sleeping and unfamiliar. Management level M2 consists of having occupants and staff trained for fire safety management but have a lower staff ratio whereas for management level M3, represent standard facilities with basic minimum fire safety management. However, for the Punta milà campsite is still assumed a higher level of fire safety management compared to M3. Additionally, it is

not possible to assume that all tourists are trained or have knowledge about fire safety procedure because tourists may have different levels of preparedness and risk awareness. Therefore, the camping site cannot be classified level M2 as well.

Consequently, the suggested pre-evacuation time for day scenarios estimates 10 minutes for $\Delta t_{pre(1st\ percentile)}$ and 20 minutes for $\Delta t_{pre(99th\ percentile)}$ as reasonable mid-way between management level M2 and management level M3.

The suggested pre-evacuation time for night scenarios estimates 20 minutes for $\Delta t_{pre(1st\ percentile)}$ and 40 minutes for $\Delta t_{pre(99th\ percentile)}$.
$\Delta t_{pre(1st\ percentile)}$: pre-evacuation time of the first few occupants.
$\Delta t_{pre(99th\ percentile)}$: pre-evacuation time of the last few occupants.

The pre-evacuation time is typically represented by a log-normal distribution. This choice is based on the fact that variables like social influence or delayed responses can impact pre-evacuation intervals, leading to non-symmetrical distribution shapes (Purser & Bensilum, 2001; Ronchi & La Mendola, 2016). The log-normal distribution of the pre-evacuation time for daytime is estimated based on a set of calculation.

For day-time scenarios, the parameters of the pre-evacuation time are presented in Table 4.

Table 4. Pre-evacuation for day scenarios.

Min (s)	600
Max (s)	1200
Location (s)	159
Scale (s)	9

For nighttime scenarios, the parameters of the pre-evacuation time are presented in Table 5.

Table 5. Pre-evacuation for night scenarios.

Min (s)	1200
Max (s)	2400
Location (s)	201
Scale (s)	9

In scenario 4, where evacuation on foot with various archetypes is represented based on (Labhiri et al., 2024), accounting for different pre-evacuation times is crucial. The *Responsibility Deniers* tourists may experience prolonged delays, expecting authorities or camp managers to handle their safety. The *Experienced Independent* tourists may show a quick response and decide to evacuate as soon as possible. The *Worried Wavers* tourists can show a quick commitment to the evacuation order as well by using information from emergency services. The *Dependent tourists* can exhibit a slight delay as they are committed to evacuating but rely extensively on emergency services in their decisions. The *Considered tourists* are strongly committed to evacuating as soon as they become aware of the risk. The *Threat Deniers tourists* may show a very long delay before they evacuate as they may disregard the information or the evacuation order. The

Community Guided tourists present moderate behaviour as they fully rely on the community evacuation decisions.

In the absence of specific data for pre-evacuation times of archetypes in wildfire evacuations, a systematic approach is adopted to incorporate the archetype concept into the model. This involves classifying archetypes based on their evacuation likelihood and quantifying pre-evacuation times accordingly. The subsequent step consists of assigning the previously determined pre-evacuation time to archetypes exhibiting moderate behaviour. Adjustments are made by modifying the mean for archetypes showing delays and deducting time from the value of the location (μ) for those with shorter pre-evacuation times (see Table 6 for the resulting chosen values). The scale (σ), minimum, and maximum values remain consistent across all archetypes as we do not have data to support more detailed assumptions.

It should be noted that the pre-evacuation times for all archetypes have been accounted for in the simulations that did not consider archetypes explicitly, where the entire range of behaviours is captured. Nevertheless, adding a scenario with archetypes and comparing the two approaches can offer insights into the extent to which added complexity impacts the total evacuation time. Furthermore, this comparison helps in understanding the model's sensitivity to variations in pre-evacuation times across different archetypes.

Table 6. pre-evacuation times based on assumed archetypes.

Archetypes	**Pre-evacuation time in a qualitative way**	**Reason**	**Quantification of the Pre-evacuation time**
Experienced Independents tourists	Shortest	They are aware of the best route/procedures and are familiar with the area and with the protective actions to be taken in case of wildfire in the area.	Log normal distribution (μ= 156.6 s; σ = 9 s; minimum=600 s; max=1200 s)
Worried Waverers tourists	Shorter	They are knowledgeable about wildfires and well-prepared and well-informed.	Log normal distribution (μ= 157.4 s; σ = 9 s; minimum=600 s; max=1200 s)
Considered tourists	Short	They are prepared as they perceive wildfires as a possible risk.	Log normal distribution (μ=158.2 s; σ = 9 s; minimum=600 s; max=1200 s)
Community Guided tourists	Moderate	They are reliant on the evacuation decisions of the community.	Log normal distribution (μ= 159 s; σ = 9 s; minimum=600 s; max=1200 s)
Dependent tourists	Long	They heavily rely on emergency services in their decisions.	Log normal distribution (μ= 159.8 s; σ = 9 s; minimum=600 s; max=1200 s)
Responsibility Deniers tourists	Longer	They will stay as long as others will take care of their evacuation as they are neither aware of the best route nor familiar with the area and procedures.	Log normal distribution (μ= 160.6 s; σ = 9 s; minimum=600 s; max=1200 s)
Threat Deniers tourists	Longest	Do not believe the threat will affect them, ignore warnings until the last moment. They are not familiar with the area and the wildfire safety procedure.	Log normal distribution (μ= 161.4 s; σ = 9 s; minimum=600 s; max=1200 s)

5.3. Waiting time at the meeting point

Once tourists start their movement, they are required to gather at the designated meeting point to receive instructions on the evacuation process (See Figure 7). It is assumed that the waiting time will differ from one individual to another, influenced by a variety of factors including the language of the instructions, the time needed by each person or group to comprehend the information, and possible congestion at the meeting point. In the absence of relevant data, a normal distribution has been assumed.

Table 7 presents the waiting time for day-time scenarios, while Table 8 presents them for nighttime scenarios.

Table 7. Waiting time for day-time scenario.

Min (s)	60
Max (s)	600
Mean (s)	300
Standard deviation (s)	96

Table 8. Waiting time for nighttime scenario.

Min (s)	60
Max (s)	900
Mean (s)	480
Standard deviation (s)	138

Figure 7. The meeting point location is indicated in red (from the Punta Milà Self-protection plan).

5.4. Preparation time in the accommodation

It is expected that tourists will perform a number of actions before their evacuation. Previous research (Shi et al., 2009) defines pre-evacuation times according to a set of key influencing factors. Assuming that each tourist will perform each delay action once, then the mean delay time would be the sum of the mean times for each delay action. Similarly, the variance of the delay time would be the sum of the variances of each delay action's time, assuming the actions are independent of each other. (ignoring the action of calling fire brigade, rescue, and notify others).

Based on Shi et al., (2009), the delay time is presented in Table 9.

Table 9. Preparation time.

Delay Action	Mean Time (s)	Standard Deviation (s)
Inaction	60	18
Collect belongings	30	9
Telephoned others	30	9
Close/open doors/windows	5	1.5
Shut down equipment	20	6
Get dressed	60	18
Total	205	-

The resulting input data for the delay time due to the performed preparation activities are presented in Table 10.

Table 10. Preparation time distribution.

Mean (s)	205
Standard deviation (s)	30
Min (s)	120
Max (s)	290

6. SUMO configuration

SUMO (Simulation of Urban MObility) is used here to model the traffic evacuation of tourists from the campsite to the safety zone. The SUMO scenario will start after tourists reach their accommodation and pick up their private vehicles. Therefore, the model configuration of SUMO (Simulation of Urban MObility) relies on the output from Pathfinder. The input data for SUMO (Simulation of Urban MObility) includes the road network, vehicle data, traffic demand and configuration file data.

6.1. Road network

The first step to build the SUMO model is to import the road network that describes the lanes, intersections, distances and road speed to have a real-world scenario. The road network can be uploaded using OSM Web Wizard map, which is a tool of the SUMO package.

SUMO requires an xml file for inputs, in this case a lane is represented as follows:
<lane id="<ID>" index="<INDEX>" speed="<SPEED>" length="<LENGTH>" shape="<SHAPE>"/>

The generated road network is then edited in NETEDIT which is a graphical network editor program from the SUMO package. This step is necessary as the roads inside the campsite were not initially visible after the generation of the road network for the selected region as well as making the street outside the camp one directional to reproduce an evacuation scenario. NETEDIT allows for the creation and modification of roads within the campsite and outside of it, ensuring that the entire network accurately represents the simulation real environment. The speed limit inside the campsite is set to 20 km/h to account for possible pedestrians walking around, which may slow down the speed of cars. Outside the camp, the speed limit is fixed at 50 km/h.

6.2. Traffic Assignment Zone (TAZ)

The traffic assignment zone TAZ defines the area where vehicles depart (Origin) or arrive (Destination). The TAZ zones typically include multiple network edges. In this case study, the traffic assignment zone is designated as a destination for vehicles. This decision is driven by the high number of vehicles coming from the campsite and the limited parking space, leading vehicles to park in various locations near the beach. To simplify the model, the traffic assignment zone for the destination is placed near the beach. Figure 8 shows the location of TAZ, where the beach 'Platja de Montgó' is designated as a safe destination for evacuating people.

Figure 8. Location of the Traffic Assignment Zone (Image: Google Earth).

6.3. Traffic demand

In SUMO the traffic demand refers to the traffic that moves over the road network during the simulation. To generate the traffic demand, it is necessary first to define the type of vehicles and their characteristics in the XML file known also as the trip file, moreover, each vehicle's route in the network must be included as well.

As the tourists inside the campsite are using cars and vans, the specific type of van employed is assumed as a Class C motorhome. The vehicle characteristics were selected according to specifications outlined in the SUMO documentation (Lopez et al., 2018), where default values are provided for passenger cars. However, no specifications were mentioned in the documentation for vans, so values between those for passenger cars and trucks were used, as vans may fall somewhere in between.

The resulting string of .xml code was starting with vType:

```
<vType id="veh_passenger" vClass="passenger" accel="2.6" decel="4.5" sigma="0.5" length="5" maxSpeed="55.55" color="0,1,1"/>
<vType id="veh_van" vClass="passenger" accel="1.3" decel="4.25" sigma="0.5" length="12" maxSpeed="45.83" color="1,0,1"/>
```

Now that the vehicle characteristics are defined, the next step is to generate routes for the vehicles evacuating from the campsite. For this purpose, the outputs from Pathfinder are required as input for SUMO. This is because tourists will start driving their vehicles at different times. To elaborate, in Pathfinder, the movement of tourists is modelled by starting from their initial position, proceeding to the meeting point, and then returning to their accommodation. The Pathfinder simulation ended when they reached their accommodation, marking the moment when tourists would initiate driving their vehicles outside the campsite (after completing some preparation activities).

To solve this, a Python code was used to generate the trips for SUMO based on the outputs of Pathfinder simulation (See appendix D).

At Punta Milà campsite, in full occupancy, there are a total of 300 vehicles, comprising 1/3 caravans and 2/3 passenger vehicles. The distribution of vehicles was randomly selected based on the total number of occupants in each accommodation area, ensuring that the final composition consists of 1/3 caravans and 2/3 passenger vehicles.
The suggested distribution of cars and vans is shown in Table 11.

Table 11. Vehicles distribution in the campsite.

Location	Number of people	Number of cars	Number of vans
R32	47	10	5
R34	7	2	1
R35	49	11	5
R37	41	9	5
R38	50	11	6
R39	15	3	2
R40	17	4	2
R41	16	4	2
R42	70	15	7
R43	45	10	5
R44	16	4	2
R45	34	8	4
R46	16	4	2
R47	37	8	4
R48	61	14	7
R49	36	8	4
R50	63	14	7
R54	11	2	1
R61	13	3	1
R62	30	7	3
R63	38	8	4
R64	55	12	6
R65	7	2	1
R66	28	6	3
R68	23	5	3
R85	75	16	8
Total number of vehicles		300	

An example of a SUMO trip code is:

```
<trip id="veh0" depart="1138.51" departLane="best" from="E38" toTaz="taz_0" type="veh_passenger"/>
<trip id="veh1" depart="1241.09" departLane="best" from="E18" toTaz="taz_0" type="veh_van"/>
```

6.4. Background traffic

In a real scenario, there can be background traffic in other areas away from the evacuation zone which may have an impact on the evacuation time as it may create congestion on the road. This traffic may include emergency vehicles or vehicles headed to other destinations. Therefore, it is crucial to take this into account when generating the traffic demand.

In SUMO, a random trip has a predefined Python script that helps create vehicles with random routes which represent background traffic. The Python script 'randomTrips.py' generates a set of random trips for a specific road network. The resulting trips are provided as an XML file. The trips are distributed evenly based on a started time (option -b, default 0) and end time (option -e, default 3600) in seconds. The number of trips is defined by the repetition rate (option -p, default 1) in seconds (Lopez et al., 2018).

The command used to generate vehicles with the random trips script is:
python randomTrips.py -n osm.net.xml -r test.rou.xml -e 3600 -p 1 -l

7. Evacuation simulation results

This section presents the results of the various scenarios described earlier. The primary objective of these simulations is to evaluate the models' effectiveness in simulating tourist evacuations from the campsite and to assess how different factors influence the evacuation process. The assessment of those factors will help to gain a deeper understanding of how each factor contributes to the overall evacuation time. This ultimately helped identify a set of recommendations related to emergency strategies and evacuation procedures.

7.1. Scenario 1 (Traffic day evacuation)

In this scenario, the objective was to test the capability of implicitly integrating two distinct software programs, previously unlinked, to simulate the entire evacuation process. The evacuation scenario involves using Pathfinder to simulate pedestrian movement and SUMO to simulate vehicular traffic. Although it is possible to model vehicles in Pathfinder and to use a pedestrian model called JuPedsim (Wagoum et al., 2015) integrated within SUMO, it was chosen to not use those models together, as the JuPedSim integration within SUMO is not yet fully documented. Another objective is to demonstrate how such tools can be used to evaluate the total evacuation time for tourists leaving the campsite in private vehicles compared to scenarios where tourists evacuate on foot and are subsequently transported by pre-arranged buses.

7.1.1. Crowd evacuation modelling with Pathfinder

Since Pathfinder is a probabilistic model making use of pseudo-random sampling from distributions, it is necessary to run the model multiple times (Ronchi et al., 2014) and assess convergence of model results. A probabilistic approach is indeed used in Pathfinder to randomise occupants' positions and other characteristics (Ronchi et al., 2014).

For this scenario, the average total pedestrian evacuation time is 3094 seconds (52 minutes), as shown in Table 12. The total pedestrian evacuation time which in this case refers to the time at which tourists arrive at their accommodation is a result of a series of intervals. The time intervals are illustrated in Figure 9. It includes the pre-evacuation time, active time and waiting time at the meeting point.

The active time here refers to the duration during which a simulated person (or agent) is actively moving towards a goal. It indicates the time when an agent starts moving until they reach their goal or become inactive due to encountering an obstruction or reaching a temporary waiting point. This metric helps in understanding how long each tourist is actively involved in the evacuation process.

Moreover, the pedestrian evacuation time includes pre-evacuation time, active time, and waiting time at the meeting point. The pedestrian movement time comprises the sum of active time and waiting time at the meeting point.

Table 12. Average and standard deviation of the pedestrian evacuation time for scenario 1.

Scenario	Average pedestrian evacuation time		Standard deviation	
	(s)	(hh: mm: ss)	(s)	(hh: mm: ss)
1 (Traffic day evacuation)	3094	51:33	126	02:06

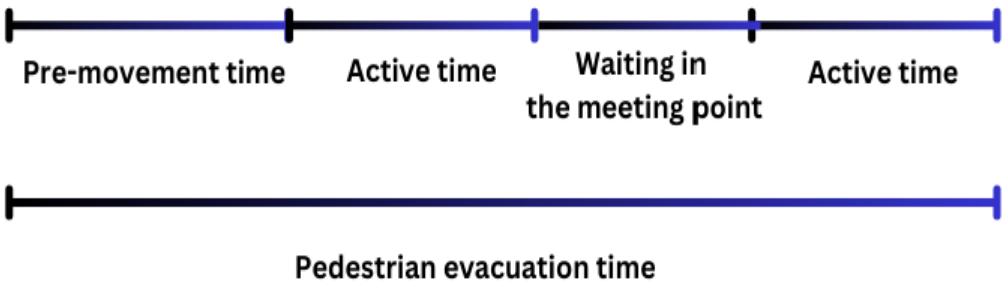

Figure 9. Timeline with intervals for pedestrian evacuation time.

Active time is defined as "*the amount of time the occupant is actively seeking a location in the model*" (Thunderhead Engineering, 2024). The average minimum active time is 27 seconds, while the average maximum active time is 1772 seconds (29 minutes). The difference between the minimum and maximum active time is around 30 minutes (see Figure 10).

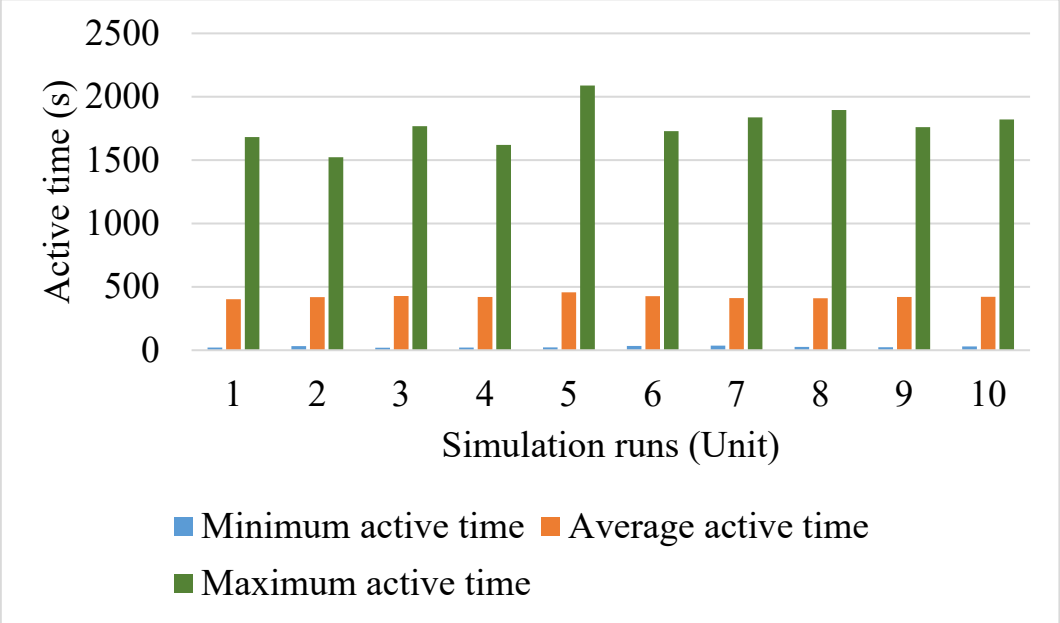

Figure 10. Active time analysis.

The average active time is around 422 seconds (e.g., approximately 7 minutes), providing a baseline for expected movement duration. However, understanding the reasons behind the extended or shorter active time is more important than focusing solely on the average value. In other words, analysing the factors influencing active time will help to capture the key elements impacting the total evacuation time as active time takes a considerable part in the time interval.

Figure 11 illustrates that the shortest and longest total pedestrian evacuation times do not correspond with the shortest and longest active times. This indicates that other factors are at play, such as pre-evacuation time, which can have a wide distribution and significantly impact the total evacuation time. Furthermore, the time spent at the meeting point follows a normal distribution, impacting the overall evacuation time.

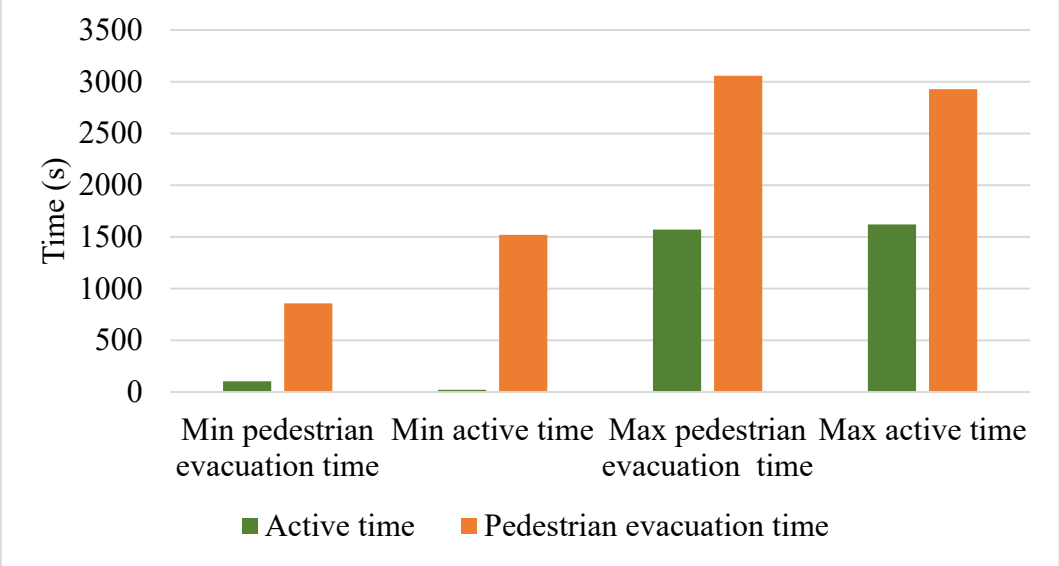

Figure 11. Active time vs total pedestrian evacuation time.

7.1.2. Traffic evacuation modelling with SUMO

The starting time of the vehicle movement from a specific lane in the campsite corresponds to the time tourists reach their accommodation and perform preparation activities. As mentioned previously, one of the key inputs in SUMO is the traffic demand. This key input is extracted from output results of Pathfinder. The Python code which is used to extract the necessary information requires a set of files from Pathfinder simulation:

- 'Scenario_occupants.csv' file from which the Python code extract the value of the 'last_goal_started time(s)' and the agent ID number to determine the time an agent reaches its accommodation.
- 'Scenario_occupant_params.csv' file is used to know the accommodation location of each agent.

Besides the files extracted from Pathfinder simulation, additional documents are needed:

- ‘From_To.csv’ file where the distribution of the vehicles around the campsite accommodation is defined as well as the ID of the starting lane and the ID of the destination which is in this case TAZ.

Figure 12 shows a view from the SUMO Graphic User Interface. In this visualization, cyan vehicles represent the passenger cars of tourists, fuchsia vehicles are camper vans, and yellow vehicles indicate background traffic.

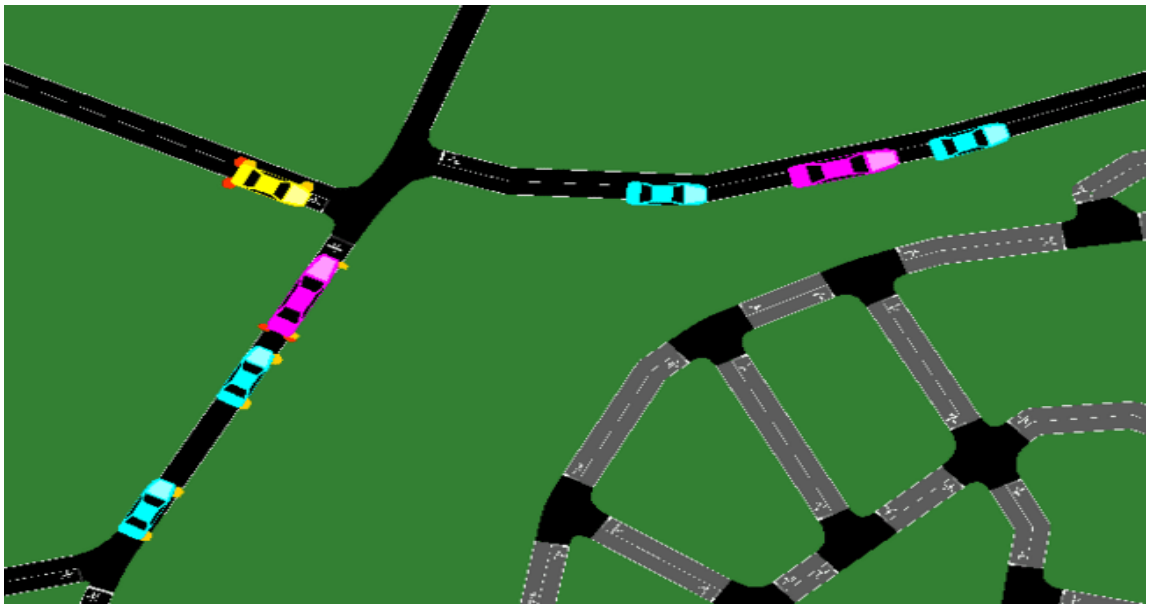

Figure 12. Screenshot from SUMO graphic user interface (yellow vehicles represent background traffic, cyan represents the evacuating passenger cars and fuchsia the camper vans).

One of the key elements in traffic simulations is the background traffic. Figure 13 shows the location of the campsite Punta Milà as well as the location of the TAZ.

Figure 13. View of the simulation in SUMO.

In this case study, a number of simulations were performed to assess the sensitivity of the SUMO model to the background traffic on the traffic evacuation of the vehicles coming from the campsite. The first case consists of running the SUMO simulation without background traffic. The second case includes a background traffic which consists of injecting 1 car per second during the total simulation time. The third case is more conservative as more vehicles were introduced (1 vehicle per 0.7 second). The number of vehicles introduced is selected by taking into account the total population in L'Escala region which is around 10 676.

Table 13 summarizes the sensitivity analysis conducted for background traffic. Changes in the number of vehicles in the background traffic did not affect the time it takes for the last tourists to drive and reach the safe zone (i.e. TAZ). This might be attributed to the short driving distance and the location of the safe zone. Congestion caused by background traffic has a greater impact within the city of L'Escala, rather than on the evacuation route.

Table 13. Sensitivity analysis of the background traffic on the traffic evacuation time.

Case	Background traffic	Number of cars in the background traffic	Time to reach TAZ for the last vehicle	
			(s)	(hh: mm: ss)
0	No	0	3388	56:27
1	Yes	3600	3424	57:03
2	Yes	5143	3401	56:40

As background traffic did not significantly affect the travel time of vehicles to the safe zone (TAZ), the simulation of tourist traffic evacuation was conducted without considering background traffic. Table 14 displays the duration of the traffic evacuation process, starting from the fastest tourists to begin driving their vehicle and ending with the slowest tourists arriving at the safety zone. The average duration of the traffic evacuation process may take 2214 seconds (36 minutes).

Table 14. Average duration and standard deviation of the evacuation process for scenario 1.

Scenario	Average duration of the evacuation process		Standard deviation	
	(s)	(hh: mm: ss)	(s)	(hh: mm: ss)
1 (Traffic day evacuation)	2214	36:54	125	02:04

The trip duration of each vehicle is presented in Figure 14 where more than 194 vehicles take only between 120 seconds (2 minutes) and 140 (2 minutes and 21 seconds) to reach the safe zone TAZ. However, the histogram also highlights outliers, notably the vehicle with the longest trip duration, which extends up to approximately 1009 seconds (16 minutes and 48 seconds). This considerable deviation from the typical trip duration is attributed to congestion within the campsite. The congestion likely slows down the progress of vehicles, leading to longer travel times for some.

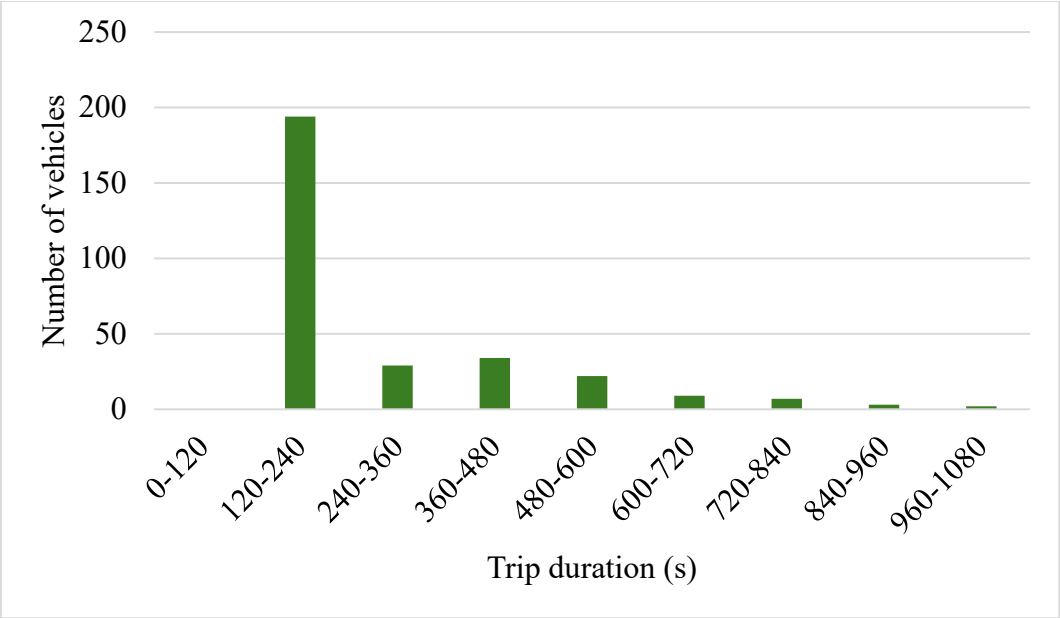

Figure 14. Trip duration of each vehicle in the simulation.

Figure 15 describes the number of vehicles passing by a simulated traffic detector (a device monitoring the number of vehicles passing a point) placed at the entrance of the safety zone. The first vehicle reaches the safety zone at around 1200 seconds (20 minutes) after the evacuation order was issued, while the last one at around 3388 seconds (56 minutes and 27 seconds).

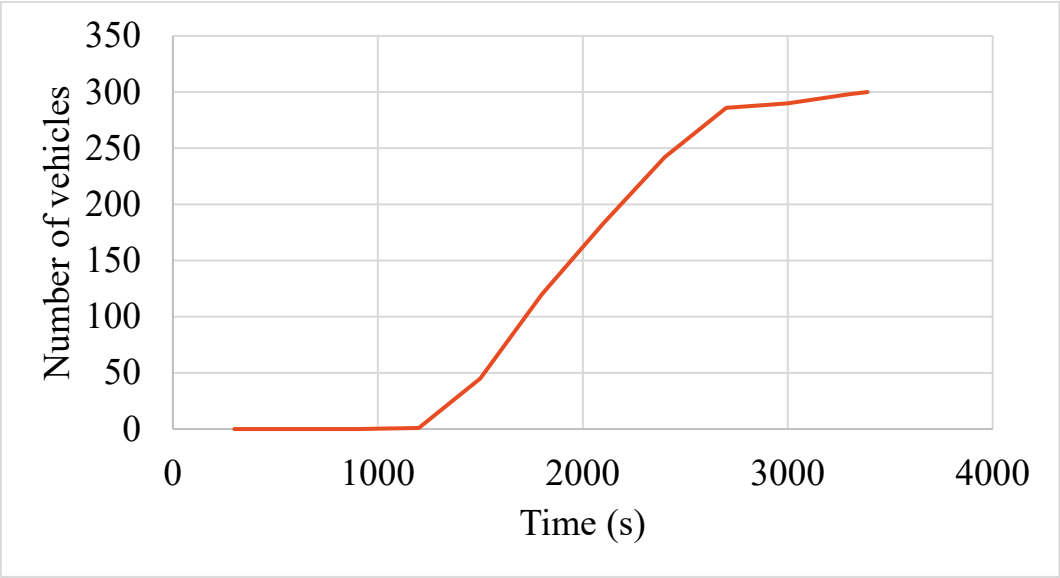

Figure 15. Number of vehicles passing by the traffic detector.

7.1.3. Combination of Pathfinder and SUMO models

The total evacuation time for Scenario 1 is the sum of the time when the last person arrived by foot (value from Pathfinder model) and the traffic evacuation time of the last person arriving by vehicle (value from Sumo model) which is in the case of the first run.

The average total evacuation time for scenario 1 is 3234 seconds (53 minutes), as shown in Table 15.

Table 15. Average total evacuation time and standard deviation for scenario 1.

Scenario	Average total evacuation time		Standard deviation	
	(s)	(hh: mm: ss)	(s)	(hh: mm: ss)
1 (Traffic day evacuation)	3234	53: 54	124	02:03

The timeline intervals for the overall evacuation process of tourists from the campsite is shown in Figure 16.

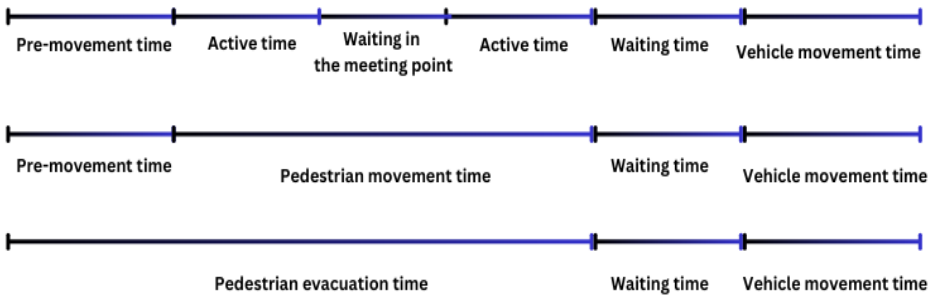

Figure 16. Traffic evacuation timeline intervals.

The simulation run with the highest evacuation time was used as a baseline to investigate the duration of each interval of the evacuation timeline. Figure 17 illustrates the total evacuation time for both the fastest tourist as well as the slowest one. After the evacuation order was issued, the fastest tourist arrived at the safe zone in 1191 seconds (19 minutes), while the slowest tourist took about 3388 seconds (56 minutes). As grouping (and people with mobility limitations) are ignored in this scenario, the fastest tourist's profile is classified as an adult, while the slowest profile belongs to a child. The fastest tourist's profile is classified as an adult, while the slowest profile belongs to a child, as grouping is not considered in this scenario. Notably, the tourists who arrived at the safety zone first were not necessarily the ones who reached the accommodation first. They had to wait for other members to join them before departing in the vehicle. This delay allowed another group, who gathered quickly, to arrive first.

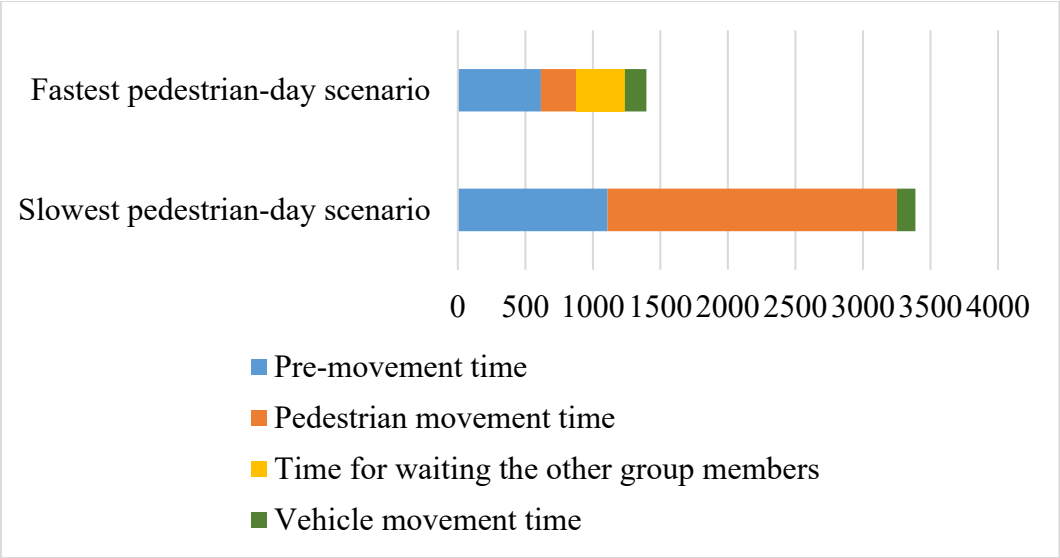

Figure 17. Slowest pedestrian vs fastest pedestrian comparison.

7.2. Results of Scenario 5 (traffic night evacuation)

The average total pedestrian evacuation time is equal to 5115 seconds (1 hour and 25 minutes). The average duration of the traffic evacuation process takes 3413 seconds (56 minutes and 48 seconds). The average total evacuation time for scenario 5 is 5242 seconds (1 hour and 27 minutes). By using a simulation run as a baseline, the fastest tourist to reach the accommodation arrived at the safe zone at time 1991 seconds (33 minutes) after the evacuation order was issued while the slowest tourist took about 5385 seconds (1 hour and 29 minutes) to arrive at the safety zone.

7.3. Day vs night comparison

7.3.1. Traffic day evacuation vs traffic night evacuation

Table 16 and Table 17 illustrate the impact of the time of the day on both the pedestrian evacuation time and the total evacuation time. The average total evacuation time for the scenario 1 (traffic day evacuation) is 3234 seconds (53 minutes) while for the scenario 5 (traffic night evacuation) 5242 seconds (1 hour and 27 minutes). Table 18 shows that the traffic night evacuation takes approximately 2,008 seconds (33 minutes and 40 seconds) longer compared to the traffic day evacuation. It can also be seen from Table 19 that the pedestrian evacuation time is nearly equal to the total evacuation time, suggesting that vehicle movement time does not have a significant impact on the total evacuation time. A Mann-Whitney U Test was employed to statistically compare the total evacuation times between scenario 1 (traffic day evacuation) and scenario 5 (traffic night evacuation). This test was used as data were not normally distributed (McKnight & Najab, 2010).

The results from the Mann-Whitney U Test indicate a significant difference in total evacuation time between scenario 1 (traffic day evacuation) and scenario 5 (traffic night evacuation). The U-Value is 0, which is less than the critical value (U, $p < 0.05$) of 23.

Additionally, the Z-score is equal to -3.74185 and the p-value is equal to 0.00018. Thus, the test result is significant ($p < .05$).

Figure 18 clearly illustrates the significant difference in total evacuation time between the two scenarios.

Table 16. Average and standard deviation of the total evacuation time (Scenario 1 vs scenario 5).

Scenario	Average total evacuation time		Standard deviation	
	(s)	(hh: mm: ss)	(s)	(hh: mm: ss)
1 (Traffic day evacuation)	3234	53: 54	124	02:03
5 (Traffic night evacuation)	5242	01:27:00	104	01:43

Table 17. Average and standard deviation of the pedestrian evacuation time (Scenario 1 vs scenario 5).

Scenario	Average pedestrian evacuation time		Standard deviation	
	(s)	(hh: mm: ss)	(s)	(hh: mm: ss)
1 (Traffic day evacuation)	3094	51:33	126	02:06
5 (Traffic night evacuation)	5115	01:25:12	101	01:40

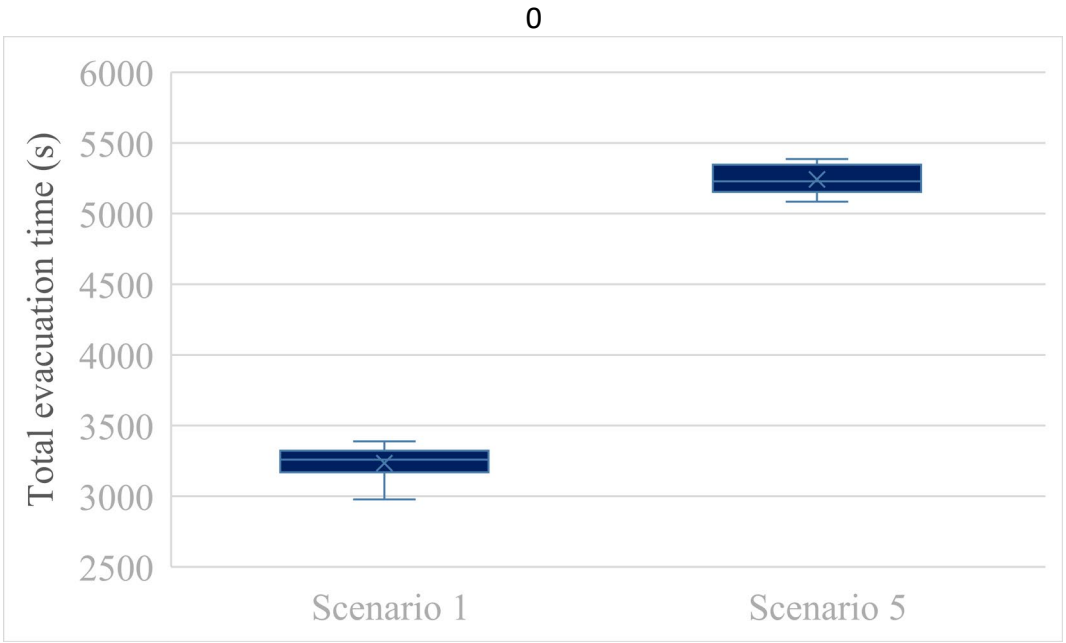

Figure 18. Statistical testing using Mann-Whitney U test (Scenario 1 is a traffic evacuation day scenario vs scenario 5 is a traffic evacuation nighttime scenario).

Figure 19 aims to compare the total evacuation time as well as its components between the fastest pedestrian who reach their accommodation and the slowest ones. The comparison also includes the nighttime vs day-time. This helps illustrating which part of

the interval mentioned previously has a more pronounced impact on the total evacuation time of tourists in the campsite. The first two bars indicate that the pre-evacuation time is the primary contributing factor to the total evacuation time for the fastest pedestrians, regardless of whether it is daytime or nighttime. However, the two last bars indicate that, when comparing daytime and nighttime evacuations for the slowest pedestrians, the extended total evacuation time can be attributed to both the pre-evacuation time and the pedestrian movement time. Here, the pedestrian movement time cover the majority of the interval.

Figure 19 demonstrates that vehicle movement time has the least impact on the total evacuation time. Additionally, waiting time is only visible in the case of the fastest pedestrians, as the last person to join the accommodation does not need to wait for anyone before leaving with the vehicle.

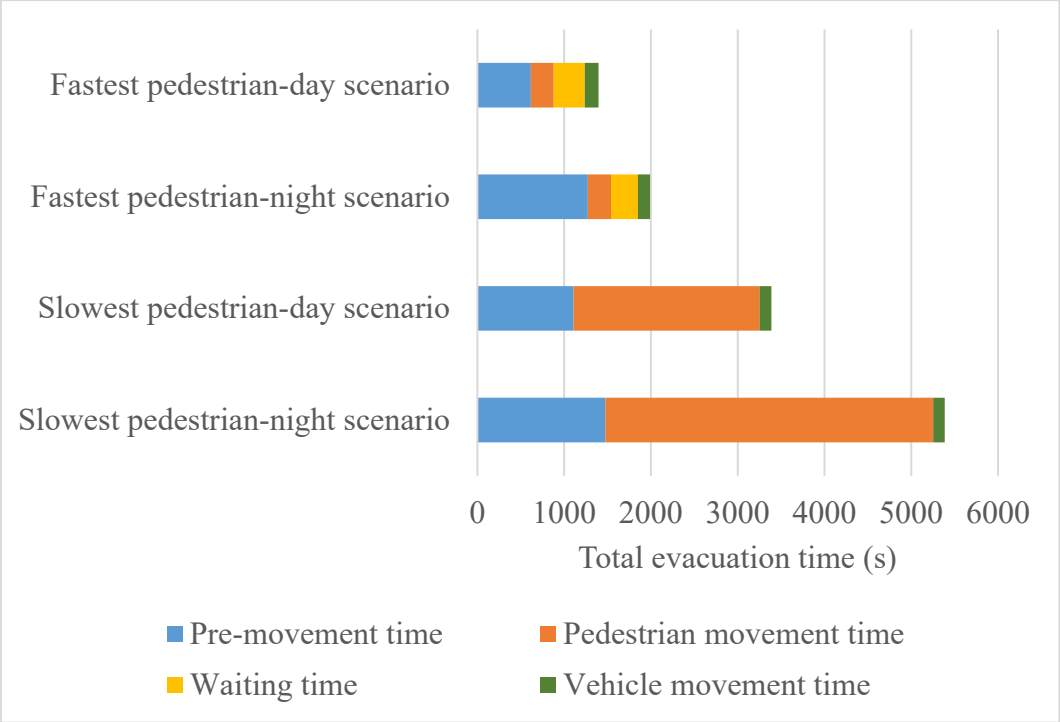

Figure 19. Fastest pedestrian vs slowest pedestrian total evacuation time.

7.3.2. Day evacuation on foot vs night evacuation on foot

Table 18 shows the average total evacuation time for scenario 2 (Day evacuation on foot) and scenario 6 (Night evacuation on foot). The average total evacuation time for scenario 2 (Day evacuation on foot) is 3249 seconds (54 minutes), while for scenario 6 (Night evacuation on foot) is 5098 seconds (1 hour and 24 minutes). The time difference in total evacuation time between day-time and nighttime evacuation on foot is approximately half an hour.

Results from a Mann-Whitney U Test indicate a significant difference in total evacuation time between scenario 2 (Day evacuation on foot) and scenario 6 (Night evacuation on foot). The U-value is 0, which is less than the critical value (U, $p < 0.05$) of 23. Additionally,

the Z-score is equal to -3.74185 and the p-value is equal to 0.00018. Thus, the test result is significant ($p < .05$).

Figure 20 clearly illustrates the significant difference in the total evacuation time between the two scenarios. The total evacuation time on foot does not account for the time it takes for the arranged bus to reach the safety zone, which may take around 4 minutes. Additionally, it does not include the time needed to board tourists onto the bus.

Figure 21 represents the number of evacuees leaving the campsite through the exit, termed 'unsafe evacuees' because this scenario only accounts for evacuation to the exit without considering the process of boarding the arranged bus. Evacuees are considered safe only when the bus reaches the safety zone. Figure 21 illustrates the impact of nighttime on the total evacuation time, with its main effect being a shift without altering the curve's shape. This shift is primarily due to the initially extended pre-evacuation time, the decrease in speed due to reduced visibility, and the prolonged waiting time at the meeting point.

Table 18. Average and standard deviation of the total evacuation time (Scenario 2 vs scenario 6).

Scenario	Average total evacuation time		Standard deviation	
	(s)	(hh: mm: ss)	(s)	(hh: mm: ss)
2 (Day evacuation on foot)	3249	54:09	101	01:40
6 (Night evacuation on foot)	5098	01:24:36	106	01:45

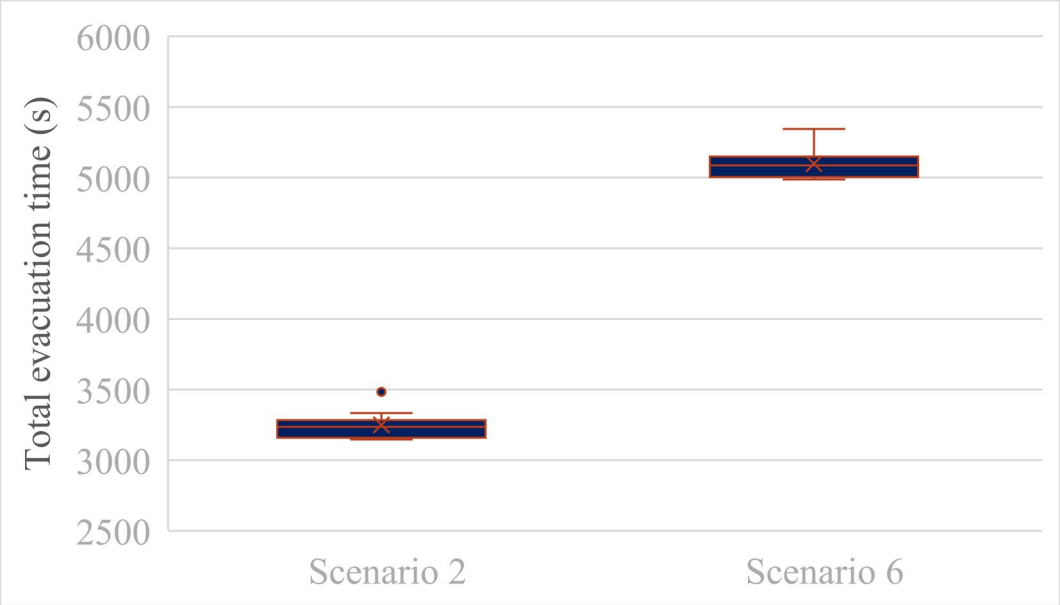

Figure 20. Statistical testing using Mann-Whitney U test (Scenario 2 vs scenario 6).

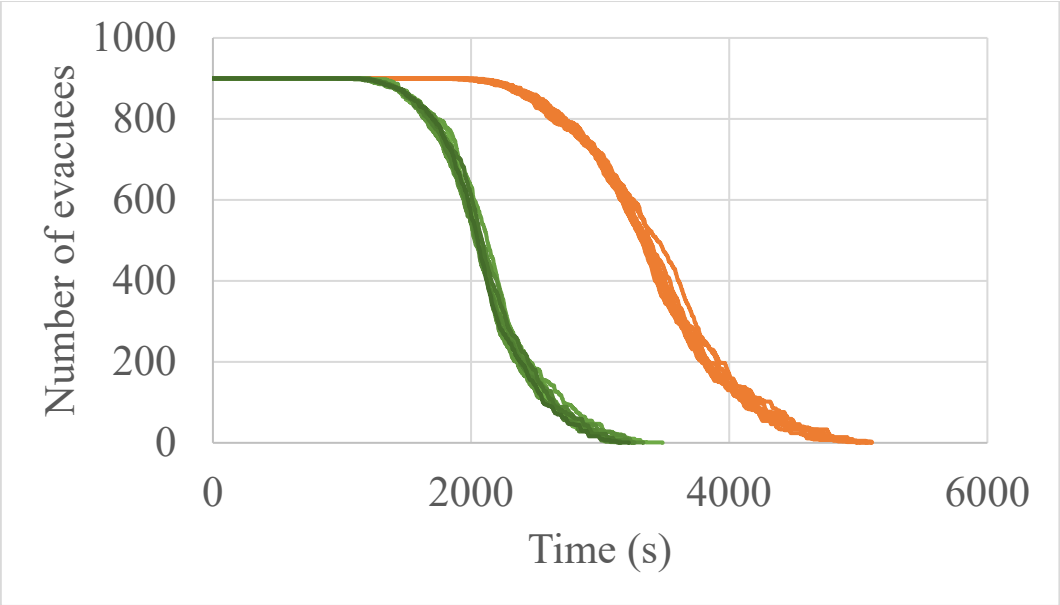

Figure 21. Evacuation time curve (Scenario 2 in orange vs Scenario 6 in green).

7.3.3. Day evacuation on foot with groups vs night evacuation on foot with groups

Table 19 presents the average total evacuation time for day and night evacuation on foot with groups. For a day scenario, the average total evacuation time of tourists for 3 (Day evacuation on foot with groups) is 3528 seconds (58 minutes), while for scenario 7 (Night evacuation on foot with groups) is 5640 seconds (1 hour and 33 minutes).

The results from the Mann-Whitney U Test indicate a significant difference in total evacuation time between scenario 3 (Day evacuation on foot with groups) and scenario 7 (Night evacuation on foot with groups). The U-value is 0, which is less than the critical value (U, $p < 0.05$) of 23. Additionally, the Z-score is equal to -3.74185 and the p-value is equal to 0.00018. Thus, the test result is significant ($p < .05$).

Table 19. Average and standard deviation of the total evacuation time (Scenario 3 vs scenario 7).

Scenario	Average total evacuation time		Standard deviation	
	(s)	(hh: mm: ss)	(s)	(hh: mm: ss)
3 (Day evacuation on foot with groups)	3528	58:48	93	01:33
7 (Night evacuation on foot with groups)	5640	01:33:36	97	01:36

Figure 22 highlights the difference in the total evacuation time between the two scenarios. Figure 23 clearly demonstrates the difference in evacuation time curves, showing that scenario 7 (Night evacuation on foot with groups) is shifted compared to scenario 3 (Day evacuation on foot with groups).

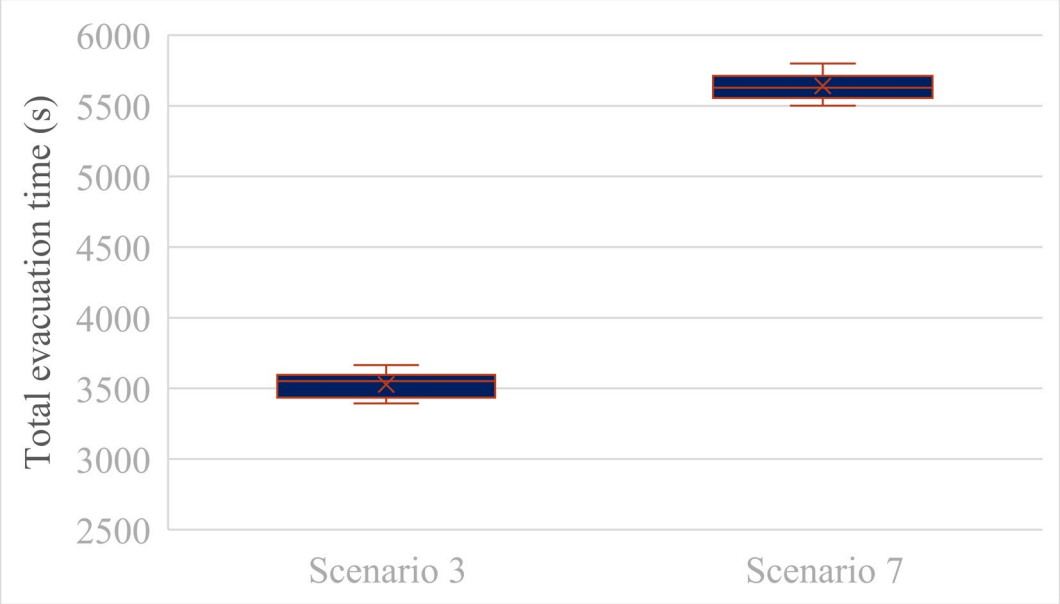

Figure 22. Statistical testing using Mann-Whitney U test (Scenario 3 vs scenario 7).

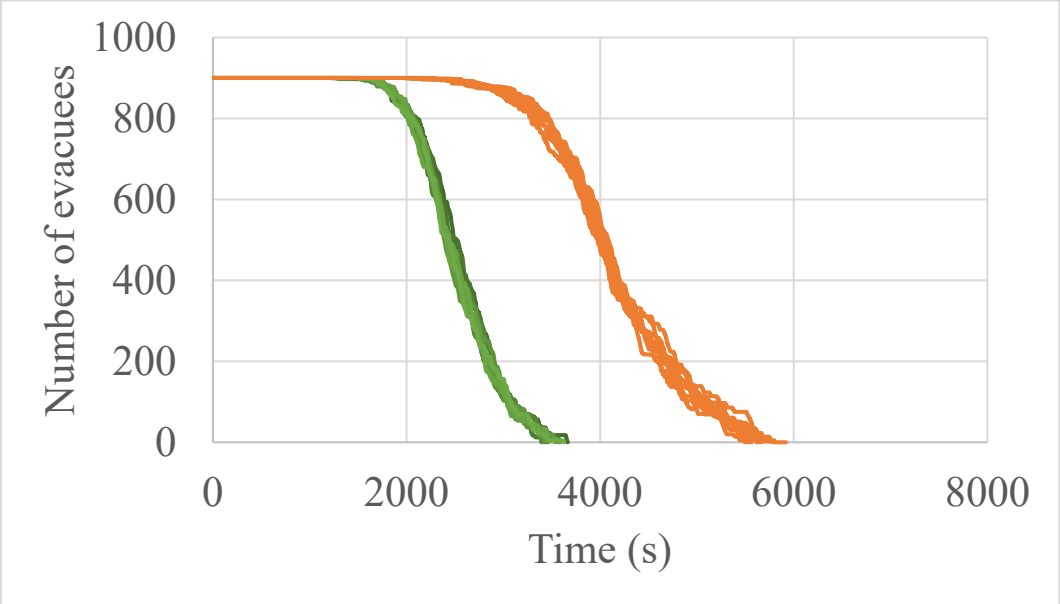

Figure 23. Evacuation time curves. Scenario 3 in green represents day evacuation on foot with groups vs Scenario 7 in orange represents night evacuation on foot with groups.

7.4. The impact of groups

This scenario aims to investigate the impact of adding a grouping feature to the model. In reality, tourists are likely to walk in groups and this may affect the total evacuation time. Table 20 presents the average total evacuation time for scenario 2 (Day evacuation on foot) and scenario 3 (Day evacuation on foot with groups). The average total evacuation time for the scenario scenario 2 (Day evacuation on foot) that did not consider the grouping feature is 3249 seconds (54 minutes) while for scenario 3 (Day evacuation on foot with groups) is 3528 seconds (58 minutes). The results show a 4-

minute difference, which is not as significant as the difference found in the day and night comparison.

The results from the Mann-Whitney U Test indicate a significant difference in total evacuation time between the scenario 2 (Day evacuation on foot) and scenario 3 (Day evacuation on foot with groups). The U-value is 4, which is less than the critical value (U, $p < 0.05$) of 23. Additionally, the Z-score is equal to -3.43948 and the p-value is equal to 0.00058. Thus, the test result is significant ($p < .05$).

Figure 24 illustrates the difference in the total evacuation time between the two scenarios. Compared to the previous tests where the U-Value was 0, the difference in the total evacuation time is slightly less pronounced in this case, as reflected by a higher U-Value of 4. Nonetheless, the test still indicates a significant difference between the scenarios.

Figure 25 clearly illustrates the effect of incorporating a group feature into the model. The curve is slightly shifted compared to the effect of nighttime, where the curve is more pronounced. This slight shift occurs because group members have to wait for each other, and they also need to synchronize their walking speeds.

Table 20. Average and standard deviation of the total evacuation time (Scenario 2 vs scenario 3).

Scenario	Average total evacuation time		Standard deviation	
	(s)	(hh: mm: ss)	(s)	(hh: mm: ss)
2 (Day evacuation on foot)	3249	54:09	101	01:40
3 (Day evacuation on foot with groups)	3528	58:48	93	01:33

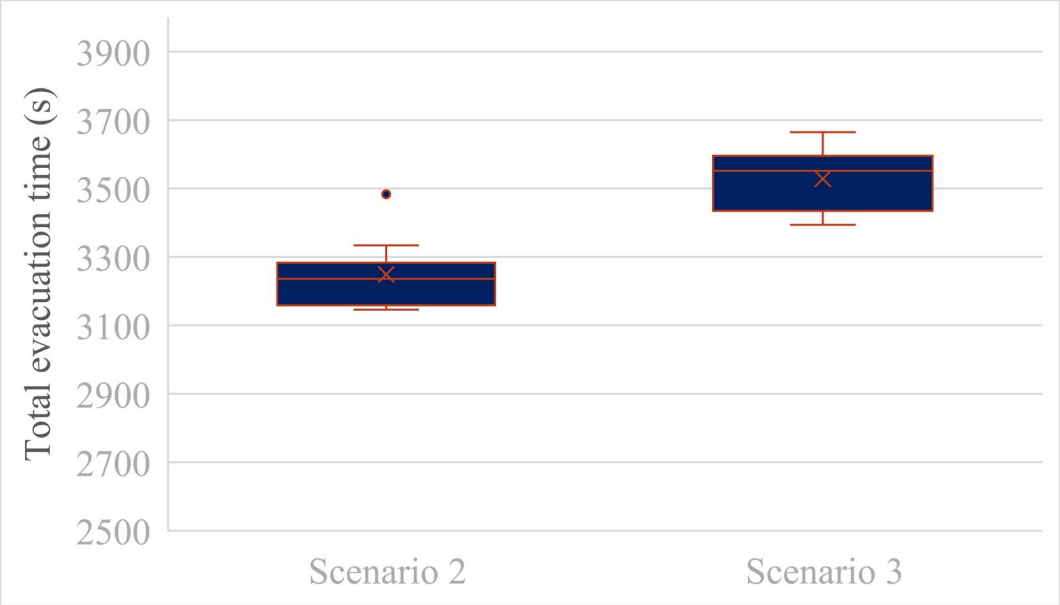

Figure 24. Statistical testing using Mann-Whitney U test (Scenario 2 vs scenario 3).

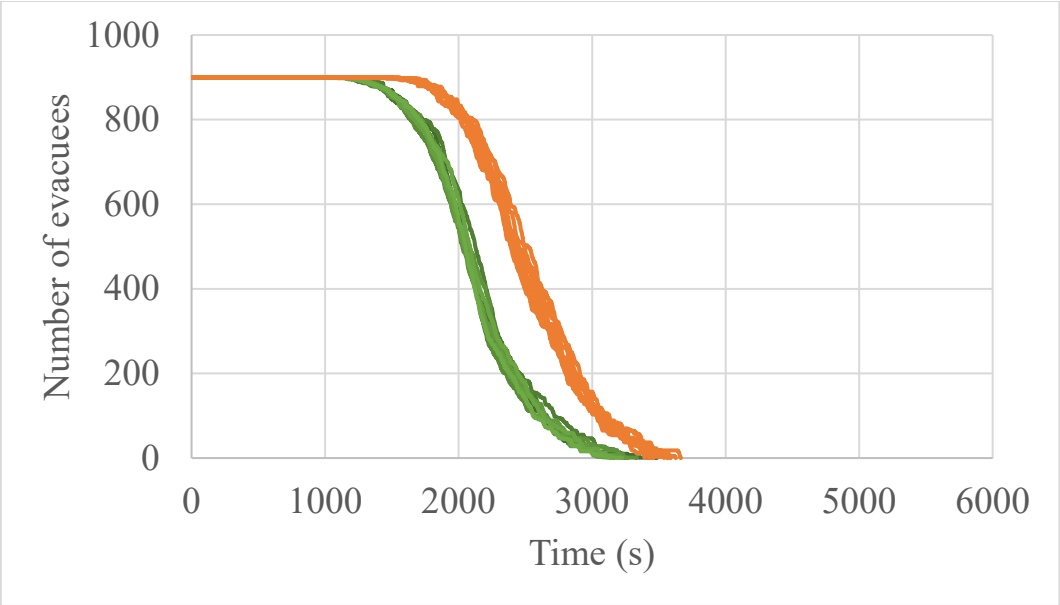

Figure 25. Evacuation time curve. Scenario 3 in orange represents day evacuation on foot vs Scenario 2 in green represents day evacuation on foot with groups.

7.5. The impact of archetypes

The use of archetypes was tested to investigate how added modelling resolution can influence the model results. Table 21 shows the average total evacuation time for scenario 2 (day evacuation on foot without archetypes) and for scenario 4 (day evacuation with archetypes). The average total evacuation time for scenario 2 (day evacuation on foot without archetypes) is approximately 3249 seconds (54 minutes), while for scenario 4 (day evacuation with archetypes) it increases to approximately 3894 seconds (1 hour and 4 minutes). The difference in total evacuation time between the two scenarios is about 10 minutes.

Table 21. Average and standard deviation of the total evacuation time (Scenario 2 vs scenario 4).

Scenario	Average total evacuation time		Standard deviation	
	(s)	(hh: mm: ss)	(s)	(hh: mm: ss)
2 (Day evacuation on foot)	3249	54:09	101	01:40
4 (Day evacuation on foot with archetypes)	3894	01:04:48	126	02:06

Figure 26 illustrates this difference in the total evacuation time between the two scenarios. The results from the Mann-Whitney U Test indicate a significant difference in total evacuation time between the scenario 2 (Day evacuation on foot) and scenario 4 (day evacuation with archetypes). The U-value is 0, which is less than the critical value (U, $p < 0.05$) of 23. Additionally, the Z-score is equal to -3.74185 and the p-value is equal to 0.00018. Thus, the test result is significant ($p < 0.05$).

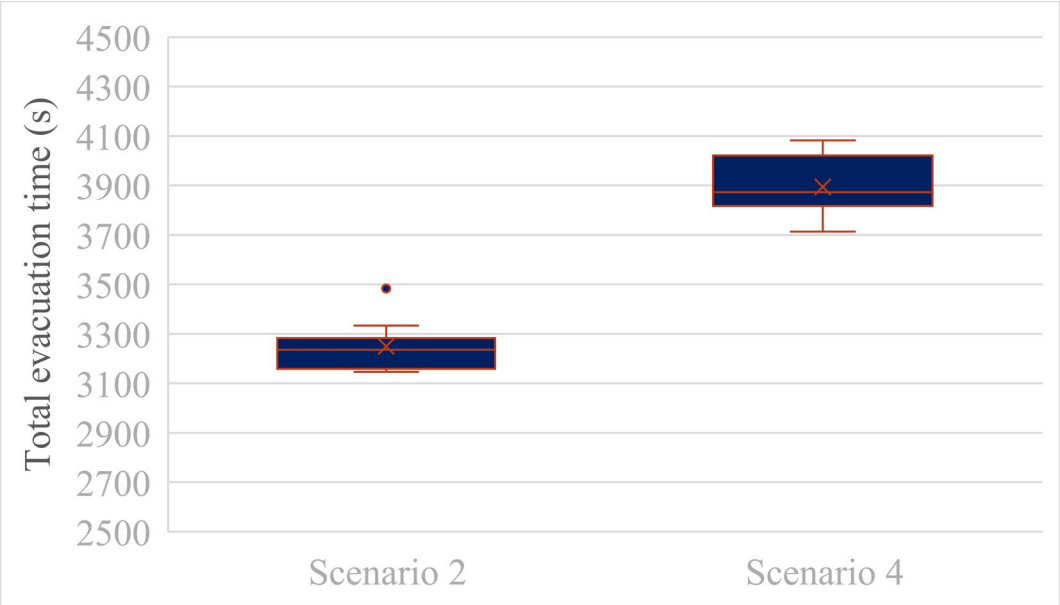

Figure 26. Statistical testing using Mann-Whitney U test (Scenario 2 vs scenario 4).

The effects of this added complexity are observable in Figure 27, where the curve for the scenario with archetype profiles differs noticeably from the curve for the scenario without them. This difference arises from the increased heterogeneity in tourists' profiles introduced by the archetype-based modelling approach.

From Figure 27 it can be seen that in the archetype-based model, tourists start their evacuation at slightly different times due to variations in mean pre-evacuation times. The curve of scenario 2 (day evacuation on foot without archetypes) reflects a more uniform evacuation process, while for scenario 4 (day evacuation with archetypes), the curve changes notably throughout the evacuation process. It begins with a gradual descent, followed by a steeper decline, and accelerates as the process progresses. It should be noted that these outcomes are based on the initial input assumptions and may vary depending on the initial model configurations.

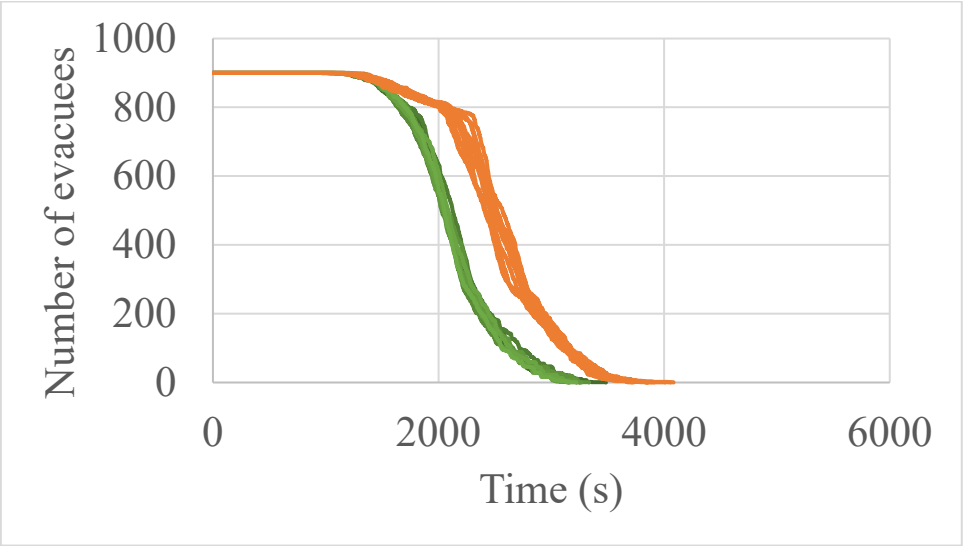

Figure 27. Evacuation time curve. Scenario 2 in gren represents day evacuation on foot vs Scenario 4 in orange represents day evacuation on foot considering archetypes.

7.6. Results summary

Table 22 shows a summary of the results of all scenarios.

Table 22. Summary of the total evacuation time for all scenarios.

Scenario	Average total evacuation time	
	(s)	(hh: mm: ss)
Scenario 1 (traffic day evacuation)	3234 seconds	53:54
Scenario 2 (day evacuation on foot)	3249 seconds	54:09
Scenario 3 (day evacuation on foot with groups)	3528 seconds	58:48
Scenario 4 (day evacuation on foot with archetypes)	3894 seconds	01:04:48
Scenario 5 (traffic night evacuation)	5242 seconds	01: 27:00
Scenario 6 (night evacuation on foot)	5098 seconds	01:24:36
Scenario 7 (night evacuation on foot with groups)	5640 seconds	1:33:36

8. Discussion

This section summarizes the key findings from the modelling case study. Figure 28 shows the vehicle movement time as a component of the timeline interval. It is evident from Figure 29 that this component is a smaller percentage of the total evacuation time in the Punta Milà case study. In this case study, vehicle movement time did not significantly impact the total evacuation time, as most vehicles took approximately 3 minutes to reach the safety zone. This is attributed to the campsite's proximity to the safe zone and the assumed limited impact of background traffic. This is in contrast with other wildfire events, for which vehicle movement time is very important in the case of wildfire evacuation, often serving as the primary contributor to the time required to reach safety zones, given the considerable distances that need to be covered (Ronchi et al., 2017). For instance, a study examining traffic dynamics during the 2019 Kincade wildfire evacuation reported a 5% reduction in road capacity during the event due to changes in driving behaviour (Rohaert, Kuligowski, et al., 2023). The study suggested that one reason for this change in driving behaviour could be drivers opting for unfamiliar routes (Rohaert, Kuligowski, et al., 2023). Therefore, this situation may also apply to tourists as they are typically unfamiliar with the area. This unfamiliarity with roads can result in different driving behaviours compared to residents, leading to reduced speeds and flow, ultimately resulting in longer evacuation times. The congestion inside the campsite is also a driving factor for the vehicle movement time as this will contribute to the speed reduction inside the camp caused by pedestrians walking around.

In this context, the limited interaction between pedestrians and vehicles in current evacuation models represents a limitation of this study. However, it also highlights a broader limitation within the field, as models have limited capabilities in providing a coupled pedestrian/traffic interaction fully validated with data related to wildfire scenario. Although multi-layer modelling platforms do exist (Ronchi et al., 2020; Wahlqvist et al., 2021), further research is needed for the explicit integration of different modelling layers relevant for wildfire evacuation (fire spread, pedestrian movement, and traffic movement).

Besides the vehicle movement time, the evacuation time interval includes other components. The first component of the timeline interval is the pre-evacuation time, which can significantly delay the evacuation process. Figure 32 shows that – in the present case study - the pre-evacuation time is predominant for the case of the fastest pedestrian. This finding provides insights into what can influence the evacuation dynamics of tourists without mobility limitations or those in close proximity to the meeting points. Therefore, it is of key importance to act to reduce pre-evacuation time by using methods backed up by human behavior theories to trigger the movement of tourists. This can be achieved by implementing strategies aiming at key variables affecting evacuation response (Labhiri et al., 2024), such as increasing risk perception, disseminating information in multiple languages, and providing detailed information about potential wildfire events in the area.

The second component of the timeline interval is the pedestrian movement time. Figure 32 demonstrates that this component is a major contributor to the total evacuation time

in the case of the slowest pedestrian. This could be attributed to the activities individuals undertake before returning to their accommodation, which are linked to their active time and waiting time at the meeting point.

One possible factor that can increase the active time is the initial location of the tourist which may lead to a longer travel distance. Congestion, particularly at gathering points, is another contributing factor that can prolong active time as it causes tourists to navigate through denser crowds, slowing their pace. Additionally, mobility limitations can influence active time, with age groups such as children and older populations having lower movement speeds. The campsite layout and design of the environment, including its topography, can also extend active time, as varying elevations or uneven terrains can reduce the walking speed. Besides that, route choice can have an influence on the active time especially if tourists are not yet familiar with the campsite layout.

Waiting time at the meeting point can be extended if the process of delivering the instructions is not well managed. In the case of tourists, this time may be influenced by several factors. The language and clarity of instruction delivery can represent a key element for lowering the waiting time. Moreover, the location, as well as the number of meeting points, are important as they influence travel distance and congestion. It is noteworthy that these factors may vary in different case studies.

The third component of the timeline interval involves waiting for other group members to join at the accommodation, and then board the vehicle to leave to the safe zone. This could potentially delay the evacuation process for tourists, as they may need to wait for other group members before departure.

In the case of the simulated daytime evacuation, tourists take more time to reach the campsite exit on foot (54:09 min) compared to when they use their vehicles to reach the safety zone (53:54 min). This difference is not large and can be attributed to several factors reflected in the modelling assumptions adopted, including variation in walking speeds among tourists, the distance they must walk, and the fact that using vehicles for evacuation enables faster movement. Additionally, the proximity of the safe zone to the campsite contributes to reduced driving time. Nevertheless, it is important to note that drivers would likely need to be more cautious at night and reduce their driving speed, a factor that is not fully accounted for explicitly in existing models.

In this case study, two evacuation strategies were investigated. The first strategy is the evacuation process using private vehicles. The second evacuation strategy is the evacuation on foot of tourists to the campsite exit followed by arranging a bus to transport them further. The transportation mode is identified as a key variable in the decision-making process of tourists in case of wildfire evacuation and resulting evacuation outcome.

On one hand, evacuation planning for large number of tourists from campsites using authority-arranged buses presents several challenges. One significant issue is logistical, especially considering the need for several buses to evacuate tourists safely. Additionally, narrow roads outside campsites may allow movement for only one vehicle,

thus obstructing access for emergency authorities (as in the current case study related to the need to reach the Parc del Montgrí during a wildfire event). Furthermore, compared to individual vehicles, buses may take longer to load, depart, and arrive, leading to delays in the evacuation timeline. Their main benefit is reduced congestion. Another challenge is managing the tourists' will to carry their luggage inside the buses, which can further complicate the evacuation process. Counting and waiting for all tourists to board the buses before departure can also prolong the evacuation time. Two of the key variables influencing tourists' evacuation behaviour are property attachment, which may have a significant negative relationship with evacuation (S.-K. Huang et al., 2016) and transportation mode. Therefore, an evacuation strategy using buses may affect tourists' decision-making regarding evacuation, as they may have a property attachment to their private vehicles, meaning they may not be keen on leaving them behind.

On the other hand, other challenges can also be associated with evacuation using private vehicles. One key challenge is the availability of private vehicles at the campsite to evacuate all tourists. Furthermore, research studies have explored the willingness to share resources during the evacuation (Wong et al., 2023), which may be necessary if not all tourists have access to private vehicles. Nevertheless, in their paper, Wong et al., 2023 did not specifically explore the willingness of tourists to share resources. However, they demonstrated that trust in strangers and neighbours significantly increases the willingness to share transportation among residents. From an overall perspective, future studies could investigate the key factors influencing tourists' willingness to share resources, such as transportation. This would make it possible to identify the elements that can lead to the sharing of private vehicles and use them to facilitate the evacuation process. Furthermore, travel distance in case of wildfire evacuation of tourists can present a key challenge as tourists may be unfamiliar with routes which can lead to a different driving behaviour and an extended evacuation time.

Different factors were introduced in the model to assess their impact on the total evacuation time. The results indicate that the evacuation process is prolonged during nighttime for all scenarios mainly due to the longer pre-evacuation time as well as the reduced walking speed. The impact of grouping on the evacuation process has also resulted in an extended evacuation time. In scenarios involving groups, individuals tend to move together, requiring group members to wait for each other and adjust their speed to match the group's pace. Those factors should explicitly be considered in evacuation planning.

The added complexity of defining profiles as archetypes did not result in a considerable increase in total evacuation time, but this is likely based on the way the archetypes have been implemented. In contrast, in the archetype-based model, the heterogeneity in occupants' mean pre-evacuation times leads to a distinctly different curve shape.

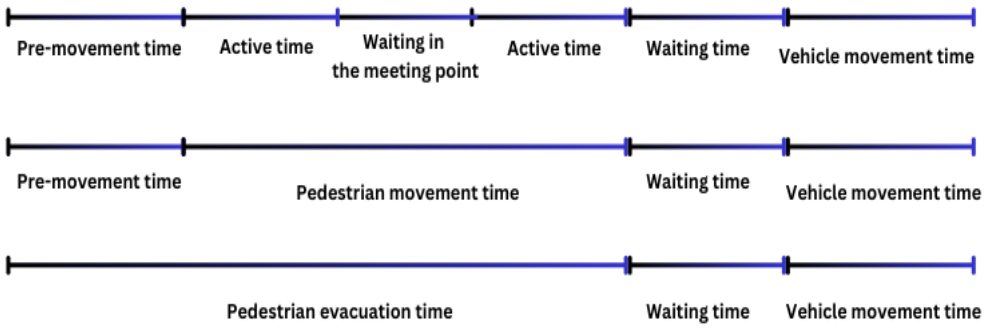

Figure 28. Traffic Evacuation timeline interval.

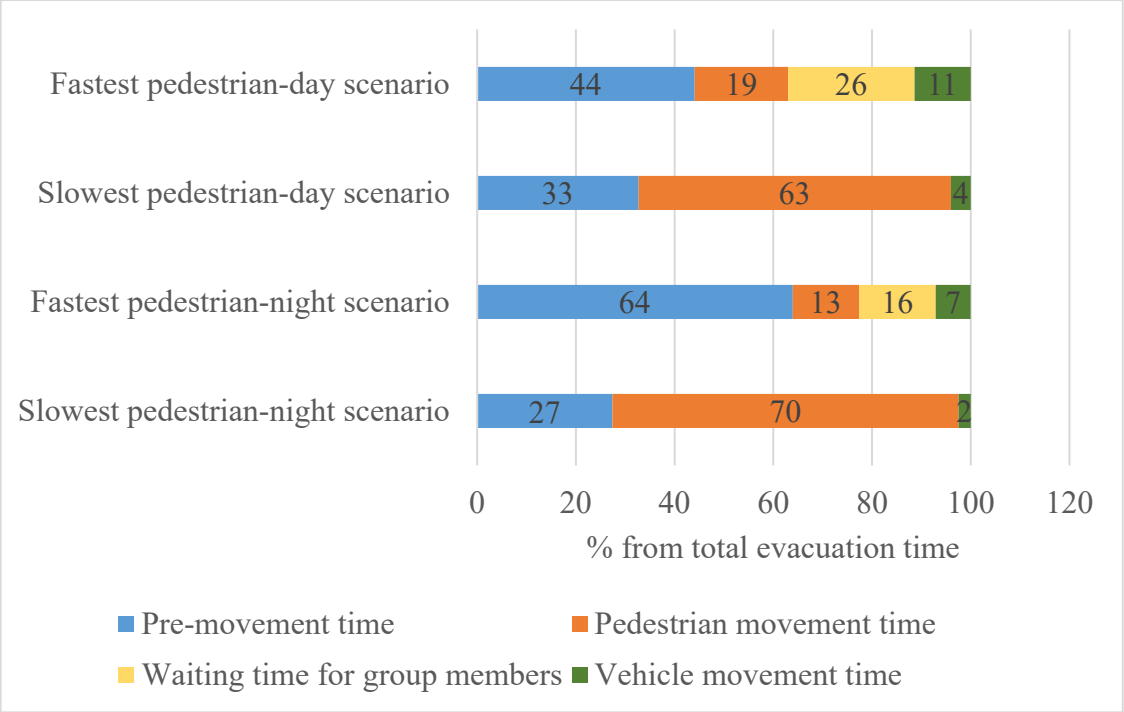

Figure 29. Percentage of each timeline interval component.

9. Conclusions

The findings from this work highlight the key variables influencing the decision-making of tourists which can be used for human vulnerability assessment of tourists' populations by stakeholders. Evacuation models were used to assess the capability of current simulation tools in modelling the wildfire evacuation of tourists at campsites. This included evaluating various evacuation strategies and optimizing total evacuation time. This was achieved by comparing a set of scenarios and examining the impact of different factors on evacuation times.

A timeline interval was established in this case study to explore which part of the interval contributes most significantly to the overall total evacuation time. Thus, it will be possible to identify the key elements affecting the evacuation process.

In this case study, both pre-evacuation time and pedestrian movement time emerged as significant contributors to the total evacuation duration. Addressing the pre-evacuation phase requires actions that stimulate tourists' decision-making processes, particularly by improving their risk perception and awareness, especially if they originate from regions where wildfire occurrences are rare or unfamiliar. Meanwhile, to reduce pedestrian movement time, enhancements to information provided, meeting point locations, route visibility, instructional delivery methods, and other factors associated with the campsite layout could be helpful.

Based on the findings from the model case study, a set of 10 recommendations have been defined.

1. In case of large travel distances and resources available, establish assembly points at various locations to minimize travel distances and reduce congestion.
2. If evacuation via private vehicle is planned, locate meeting points so that they do not represent an obstruction for vehicle traffic (especially in proximity of campsite exit areas).
3. Consider key factors in choosing an evacuation strategy (on foot or via vehicles), such as the number of tourists, their willingness to leave their private vehicles or to share transportation, and the travel distance to the safety zone.
4. Provide assistance for tourists with functional limitations to ensure their safe evacuation.
5. Provide tourists with detailed evacuation information upon arrival and inform tourists about the potential risk of wildfires to increase their risk perception, thus reducing their pre-evacuation time.
6. Ensure that tourists receive evacuation orders from an official source
7. Encourage tourists to fill in a document upon arrival that includes their contact information and spoken languages so that evacuation orders can be issued in multiple languages.
8. Increase the visibility of roads within the campsites at night to facilitate navigation in case of emergency.
9. Ensure that roads within the campsites are kept clear of any obstacles to help in easy navigation.
10. Install clear signage throughout the campsite towards the assembly point(s) and towards exit routes to guide tourists effectively.

A set of specific recommendations on how future evacuation models should be improved to better represent the tourist's evacuation in wildfire event is also provided.

1. Future evacuation models should explicitly incorporate the interaction between pedestrians moving on foot and vehicle movement to provide more realistic results backed up by behavioural research related to wildfire evacuation scenarios.
2. Integration of pedestrian modelling and traffic modelling into a single, cohesive model can help reduce uncertainties in evacuation predictions.
3. Human behaviour inputs specific to tourists and heterogenous groups should be accounted for. This could involve integrating factors that capture differences in driving styles (e.g., influenced by tourists' background), such as headways. This approach would reflect the findings of studies examining traffic dynamics during wildfire evacuation (Rohaert, Kuligowski, et al., 2023).
4. The time tourists spend waiting in their accommodation for others to join them can be represented more explicitly in the models and requires more behavioural research.

The insights derived from this study contribute not only to reducing the knowledge gap regarding wildfire evacuation in touristic areas but also offer practical recommendations that can be implemented by emergency planners to ensure safer and more efficient evacuations. Additionally, this work aims to highlight the limitations related to the current simulation tools in modelling tourist evacuation in a wildfire evacuation which may guide future research in this area.

References

Arce, R. S. C., Onuki, M., Esteban, M., & Shibayama, T. (2017). Risk awareness and intended tsunami evacuation behaviour of international tourists in Kamakura City, Japan. *International Journal of Disaster Risk Reduction*, *23*, 178–192.

Bubola, E., & Kitsantonis, N. (2023). Greek Hotels Fear a Burning Future:'Even the Animals Are Moving Away'. *International New York Times*, NA-NA.

Cova, T. J., Drews, F. A., Siebeneck, L. K., & Musters, A. (2009). Protective actions in wildfires: Evacuate or shelter-in-place? *Natural Hazards Review*, *10*(4), 151–162.

Ferrara, A., Sacone, S., Siri, S., Ferrara, A., Sacone, S., & Siri, S. (2018). Microscopic and mesoscopic traffic models. *Freeway Traffic Modelling and Control*, 113–143.

Gupta, G. (2023). The Maui fires are more deadly than Hawaii's 1960 tsunami. *The New York Times (Digital Edition)*, NA-NA.

Gwynne, S. M., & Rosenbaum, E. R. (2016). Employing the hydraulic model in assessing emergency movement. *SFPE Handbook of Fire Protection Engineering*, 2115–2151.

Haghani, M., Kuligowski, E., Rajabifard, A., & Kolden, C. A. (2022). The state of wildfire and bushfire science: Temporal trends, research divisions and knowledge gaps. *Safety Science*, *153*, 105797. https://doi.org/10.1016/j.ssci.2022.105797

Haynes, K., Short, K., Xanthopoulos, G., Viegas, D., Ribeiro, L. M., & Blanchi, R. (2020). Wildfires and WUI fire fatalities. *Encyclopedia of Wildfires and Wildland-Urban Interface (WUI) Fires*, 1073–1088.

Huang, S.-K., Lindell, M. K., & Prater, C. S. (2016). Who leaves and who stays? A review and statistical meta-analysis of hurricane evacuation studies. *Environment and Behavior*, *48*(8), 991–1029.

Huang, Y., Wu, S., & Kaplan, J. O. (2015). Sensitivity of global wildfire occurrences to various factors in the context of global change. *Atmospheric Environment*, *121*, 86–92.

Intini, P., Ronchi, E., Gwynne, S., & Pel, A. (2019). Traffic modeling for wildland–urban interface fire evacuation. *Journal of Transportation Engineering, Part A: Systems*, *145*(3), 04019002.

Jolly, W. M., Cochrane, M. A., Freeborn, P. H., Holden, Z. A., Brown, T. J., Williamson, G. J., & Bowman, D. M. (2015). Climate-induced variations in global wildfire danger from 1979 to 2013. *Nature Communications*, *6*(1), 7537.

Korhonen, T., Hostikka, S., Heliövaara, S., & Ehtamo, H. (2008). FDS+ Evac: Modelling social interactions in fire evacuation. *Proceedings of the 7th International Conference on Performance-Based Codes and Fire Safety Design Methods, SFPE, Bethesda, MD*, 241–250.

Krajzewicz, D., Hertkorn, G., Rössel, C., & Wagner, P. (2002). SUMO (Simulation of Urban MObility)-an open-source traffic simulation. *Proceedings of the 4th Middle East Symposium on Simulation and Modelling (MESM20002)*, 183–187.

Krauß, S. (1998). *Microscopic modeling of traffic flow: Investigation of collision free vehicle dynamics*.

Kuligowski, E. D., Walpole, E. H., Lovreglio, R., & McCaffrey, S. (2020). Modelling evacuation decision-making in the 2016 Chimney Tops 2 fire in Gatlinburg, TN. *International Journal of Wildland Fire*, *29*(12), 1120–1132.

Labhiri, A., Vaiciulyte, S., Kuligowski, E., & Ronchi, E. (2024). Evacuation decisions of tourists in wildfire scenarios. *International Journal of Disaster Risk Reduction*, *113*, 104836. https://doi.org/10.1016/j.ijdrr.2024.104836

Lopez, P. A., Behrisch, M., Bieker-Walz, L., Erdmann, J., Flötteröd, Y.-P., Hilbrich, R., Lücken, L., Rummel, J., Wagner, P., & Wießner, E. (2018). Microscopic Traffic Simulation using SUMO. *The 21st IEEE International Conference on Intelligent Transportation Systems*. https://elib.dlr.de/124092/

Lovreglio, R., Ronchi, E., & Kinsey, M. J. (2020). An online survey of pedestrian evacuation model usage and users. *Fire Technology*, *56*(3), 1133–1153.

McCool, S. F., Burchfield, J. A., Williams, D. R., & Carroll, M. S. (2006). An event-based approach for examining the effects of wildland fire decisions on communities. *Environmental Management*, *37*, 437–450.

McKnight, P. E., & Najab, J. (2010). Mann-Whitney U Test. *The Corsini Encyclopedia of Psychology*, 1–1.

Otrachshenko, V., & Nunes, L. C. (2022). Fire takes no vacation: Impact of fires on tourism. *Environment and Development Economics*, *27*(1), 86–101.

PD, B. (2019). 7974-6: 2019 Application of fire safety engineering principles to the design of buildings. *Human Factors. Life Safety Strategies. Occupant Evacuation, Behaviour and Condition (Sub-System 6)*.

Purser, D. A., & Bensilum, M. (2001). Quantification of behaviour for engineering design standards and escape time calculations. *Safety Science*, *38*(2), 157–182.

Ranney, T. A. (1999). Psychological factors that influence car-following and car-following model development. *Transportation Research Part F: Traffic Psychology and Behaviour*, *2*(4), 213–219. https://doi.org/10.1016/S1369-8478(00)00010-3

Reynolds, C. W. & others. (1999). Steering behaviors for autonomous characters. *Game Developers Conference*, *1999*, 763–782.

Rohaert, A., Kuligowski, E. D., Ardinge, A., Wahlqvist, J., Gwynne, S. M., Kimball, A., Benichou, N., & Ronchi, E. (2023). Traffic dynamics during the 2019 Kincade wildfire evacuation. *Transportation Research Part D: Transport and Environment*, *116*, 103610.

Rohaert, A., Wahlqvist, J., Najmanova, H., Bode, N., & Ronchi, E. (2023). The evaluation of data fitting approaches for speed/flow density relationships. *Pedestrian and Evacuation Dynamics 2023*. PED23, Eindhoven.

Ronchi, E., & Gwynne, S. (2020). Computational evacuation modeling in wildfires. In *Encyclopedia of wildfires and wildland-urban interface (WUI) fires* (pp. 115–124). Springer.

Ronchi, E., Gwynne, S. M., Rein, G., Wadhwani, R., Intini, P., & Bergstedt, A. (2017). *e-Sanctuary: Open multi-physics framework for modelling wildfire urban evacuation*.

Ronchi, E., & La Mendola, S. (2016). Evacuation modelling for underground physics research facilities. *Department of Fire Safety Engineering, Lund University*.

Ronchi, E., Reneke, P. A., & Peacock, R. D. (2014). A method for the analysis of behavioural uncertainty in evacuation modelling. *Fire Technology*, *50*, 1545–1571.

Ronchi, E., Wahlqvist, J., Gwynne, S., Kinateder, M., Rein, G., Mitchell, H., Benichou, N., Ma, C., & Kimball, A. (2020). *WUI-NITY: a platform for the simulation of*

wildland-urban interface fire evacuation (p. 80). Fire Protection Research Foundation.

Ronchi, E., Wong, S., Suzuki, S., Theodori, M., Wadhwani, R., Vaiciulyte, S., Gwynne, S., Rein, G., Kristoffersen, M., Lovreglio, R., & others. (2021). *Case studies of large outdoor fires involving evacuation*.

Saw, K., Katti, B. K., & Joshi, G. (2015). Literature Review of Traffic Assignment: Static and Dynamic. *International Journal of Transportation Engineering*, *2*(4). https://doi.org/10.22119/ijte.2015.10447

Shi, L., Xie, Q., Cheng, X., Chen, L., Zhou, Y., & Zhang, R. (2009). Developing a database for emergency evacuation model. *Building and Environment*, *44*(8), 1724–1729.

Song, J., Wu, Y., Xu, Z., & Lin, X. (2014). Research on car-following model based on SUMO. *The 7th IEEE/International Conference on Advanced Infocomm Technology*, 47–55.

Strahan, K. (2020). An archetypal perspective on householders who 'wait and see'during a bushfire. *Progress in Disaster Science*, *7*, 100107.

Strahan, K., Whittaker, J., & Handmer, J. (2018). Self-evacuation archetypes in Australian bushfire. *International Journal of Disaster Risk Reduction*, *27*, 307–316. https://doi.org/10.1016/j.ijdrr.2017.10.016

Sun, J., Qi, W., Huang, Y., Xu, C., & Yang, W. (2023). Facing the wildfire spread risk challenge: Where are we now and where are we going? *Fire*, *6*(6), 228.

Tapani, A. (2008). *Traffic simulation modelling of rural roads and driver assistance systems* [PhD Thesis]. Linköping University Electronic Press.

Thunderhead Engineering. (2024). *Pathfinder—Technical Reference*.

Wagoum, A. K., Chraibi, M., Zhang, J., & Lämmel, G. (2015). JuPedSim: An open framework for simulating and analyzing the dynamics of pedestrians. *3rd Conference of Transportation Research Group of India*, *12*.

Wahlqvist, J., Ronchi, E., Gwynne, S. M., Kinateder, M., Rein, G., Mitchell, H., Bénichou, N., Ma, C., Kimball, A., & Kuligowski, E. (2021). The simulation of wildland-urban interface fire evacuation: The WUI-NITY platform. *Safety Science*, *136*, 105145.

Wong, S. D., Yu, M., Kuncheria, A., Shaheen, S. A., & Walker, J. L. (2023). Willingness of Hurricane Irma evacuees to share resources: A multi-modeling approach. *Transportmetrica A: Transport Science*, *19*(2), 2017064.

Zhang, X., Li, X., & Hadjisophocleous, G. (2013). A probabilistic occupant evacuation model for fire emergencies using Monte Carlo methods. *Fire Safety Journal*, *58*, 15–24.

Wildland-Urban Interface Fire Touristic Infrastructure Protection Solutions

WUITIPS

GA number 101101169

Co-funded by the European Union

Technical Note TN 6.3
Building Vulnerability of FR Case Studies

WP - Task	WP6 – Task 6.4	**Version** (1)	Final
File name	WUITIPS_WP6_FR_Case_Studies_Building_Vuln	**Dissemination level** (2)	Public
Programmed delivery date	31/01/2025	**Actual delivery date**	05/02/2025

Document coordinator	Bruno Guillaume (EFR)
Contact	bruno.guillaume@efectis.com
Authors	
Reviewed by	Elsa Pastor (UPC)

Abstract	In this technical note we provide a vulnerability and protection assessment of the buildings in the FR case studies, using a PBD approach.

(1) *Draft / Final*
(2) *Public / Restricted / Internal*

Disclaimer

WUITIPS is co-funded by the European Union. Views and opinions expressed in this document are however those of the author(s) only and do not necessarily reflect those of the European Union or the European Commission. Neither the European Union nor the granting authority can be held responsible for them.

Content

1. Context 4
2. Pilot sites definition 5
2.1. Villa “Mas d’Amont” 5
2.1.1. Site location and fire history 5
2.1.2. Site hazard, vulnerability and existing protections 6
2.2. Campsite “Bois Fleuri” 9
2.2.1. Site location and recent fire history 9
2.2.2. Site hazard, vulnerability and existing protections 10
3. Adaptation of the WUITIPS methodology to the pilot sites 13
3.1. Villa “Mas d’Amont” modelling exercise 15
3.2. Campsite “Bois Fleuri” modelling exercise 16
4. Results and Discussion 19
4.1. Villa “Mas d’Amont” 19
4.2. Campsite “Bois Fleuri” 23
References 27

1. Context

It was convened in the initial proposal to develop during WP6.4 an assessment of vulnerability and protection of the different pilot sites, that had been selected during WP6.2. The vulnerability assessment methodology has been defined in WP4 (see D4.1 document [4]).

The selection of pilot sites was conducted between November 2023 and January 2024. Due to their configurations, these sites could be subject to one or more types of wildfire prevention study:

- Evacuation modelling;
- Building vulnerability and protection assessment based on objective input data;
- Webtool coarse vulnerability index calculation in the webtool (see TN6.3 document [5]), based on declarative data.

The identified sites are listed in Table 1-1. The construction vulnerability and protection assessment is focused on:

- The Mas d'Amont touristic villa, which can contain a bit more than 10 tourists;
- The "Bois Fleuri" campsite, which entrance building could possibly act as a temporary refuge (and effectively did when a fire did overcome the neighbouring campsite Les Chênes Rouges in the Argelès/Saint-André fire of August 2023).

Table 1-1: Selected pilot sites for the different types of wildfire prevention study

Category	WUITI	City	Evacuation modelling	Construction vulnerability and protection assessment	Coarse vulnerability index (declarative webtool)
Campsite	Bois Fleuri	Argelès	x	x	x
Campsite	Bois des Pins	Salses	x		x
Touristic villa	Mas d'Amont	Argelès		x	x
Touristic villa	Gîte Vandellos	Argelès (La Vall District)			x
Touristic villa	Gîte Tauzin	Argelès (La Vall District)			x
Touristic villa	Mas Llinas	Argelès			x

The current document is designed as follows:

- Section 2 provide details on the input data gathered at the two French pilot sites;
- Section 3 details the common methodology used to assess vulnerability and protection of the refuge building of these two sites;
- Section 4 details the simulation results and the recommendations on protection.

2. Pilot sites definition

2.1. Villa “Mas d’Amont”

2.1.1. Site location and fire history

Mas d’Amont (city of Argelès) is the geographic name, and its current commercial name is “Wanakaset” (see Figure 2-1). It is fully exposed to winds: hill slopes down the Mas are often aligned with the direction of “Tramontane” wind (originating from North-Western direction). The Garbí wind (originating from South-Eastern direction) is coming very dry and hot, due to Foehn effect after crossing the Pyrenees. It is accessible by two small unpaved roads, at 20min and 30min from the nearest harbour. The surrounding vegetation is composed of oaks with shrub understory (“maquis”).

Figure 2-1 Mas d’Amont location, surrounding vegetation and access path

The building can host a bit more up to 15 guests, and has been rebuilt after full destruction by a wildfire in 1969. The fire of August 2023 that occurred at the foot of the hill below Mas d’Amont (adjacent to site “Bois Fleuri”) did not go uphill, but smoke, in low concentration but largely reducing visibility, has been experienced by the tourists and housekeeper in Mas d’Amont.

According to the territorial regulation approved by DDTM66, the Mas d’Amont is located in the red zone in the PPRIF Argeles (see Figure 2-2), meaning that no specific construction constraints are to be applied to buildings. Moreover, the building is classified as “Etablissement Recevant du Public” (ERP). All protection means evaluated in the present study only concern auto-protection. All other protection means, preparing for potential intervention by fire brigades (“Défense Extérieure contre l’Incendie”, “Défense des Forêts contre les incendies”) or

concerning vegetation cleaning (“Obligations Légales de Débroussaillement”) are assumed to be already implemented by the owner.

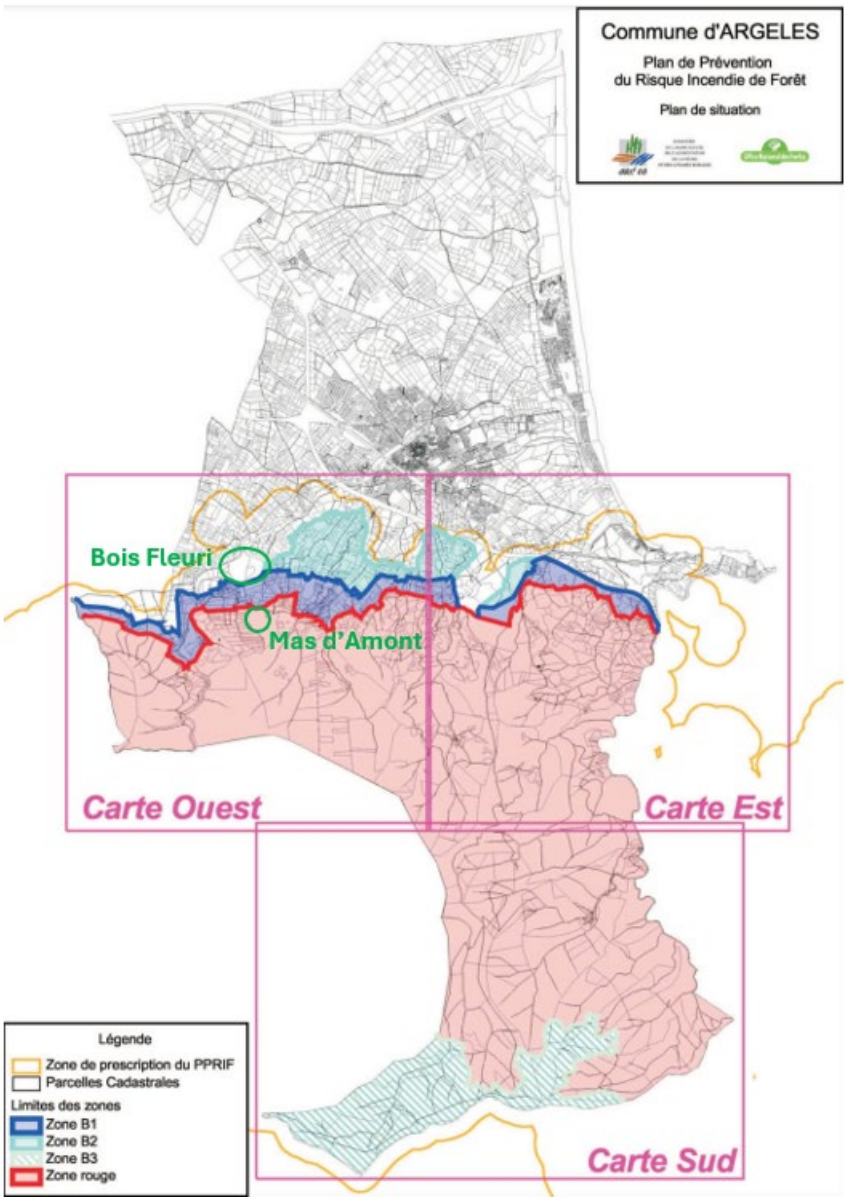

Figure 2-2 Location of Bois Fleuri in the PPRIF risk map

2.1.2. Site hazard, vulnerability and existing protections

The single building will be evaluated as potential refuge. Efectis could visit with SDIS66 the Mas d’Amont in December 2024. Numerical or paper plans could not be retrieved. The interview on site did allow to identify all combustible materials and vegetation present in the vicinity of the building and all building vulnerable items. Some photos could be taken.

(a) 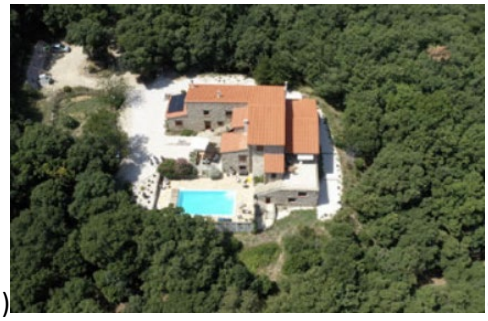 (b) 

Figure 2-3 Mas d'Amont: (a) aerial image and (b) view from swimming pool pointing to North

The inventory of combustible materials and vegetation was conducted in the last 100meters to the building, and the vulnerable elements which are exposed. These elements are summarized in Tab 2-1.

Table 2-1: Hazard items, exposed vulnerability items and existing protections for the building of Mas d'Amont (in orange: the items that will be assessed following WUITIPS methodology)

Hazard item	**Exposed vulnerability item**	**Already existing or ongoing protection measures (incombustible material, protections…)**
Surrounding forest of cork oaks, maintained clean with no understory (see Fig2-3(a)) on 100 m distance from the building	Full building envelope, particularly: - windows (double glazing) at Northern facade have no shutter - wooden lintel above each window	- Stone walls (no ext/int insulation) - Most window (double glazing) have wooden frames and shutters - Each foot of façade is mineralized on 5m to 15m depth (see Fig2-2(a)) - Masonry roof frame, mineral tiles assembly with no openings - Masonry between roof and wall - Steel gutters
Ornamental vegetation at Northern façade (directly under window, and 4m from wall)	Windows with no shutter, Wooden lintel	- Vegetation just below the window will be removed - Shutters are planned to be installed
Wooden pergola with reed roof	Window with shutter, Wooden lintel	
Many light combustible garden furniture (wood, fabric)		Will be removed when fire is approaching (housekeeper always present when tourists are present)
Small wood storage (for BBQ /chimney) at Western facade		Will be put at distance (at least 10m)
Gas bottle storage against wall at Western facade		Will be put at distance (at least 10m)
Car parks		Cars will be move from closest park to the other one

Figure 2-4 Locations of different hazard and vulnerability items around building: (a) cleaned surrounding cork oak forest, (b) Northern façade with ornamental vegetation, (c) pergola on Western façade, (d) and (e) garden furniture

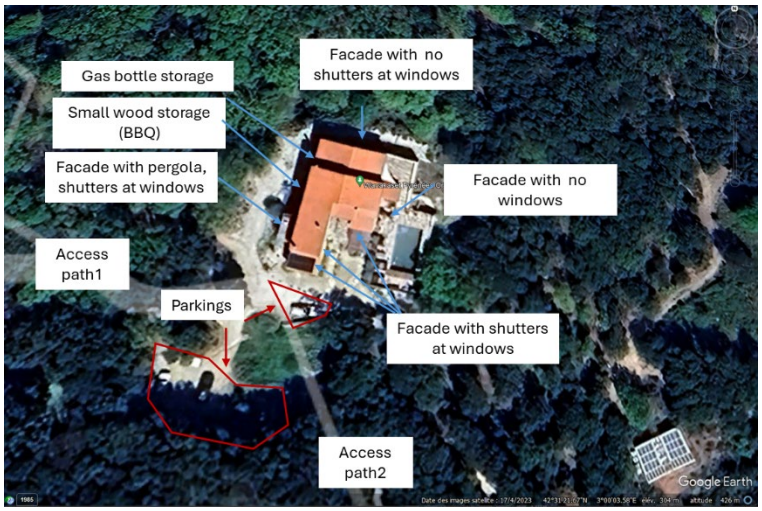

Figure 2-5 Locations of other hazard and vulnerability items around building

2.2. Campsite “Bois Fleuri”

2.2.1. Site location and recent fire history

“Bois Fleuri” is located in the city of Argelès, with good road access, at less than 5min of Argelès city centre. It is located at mountain foot, is largely exposed to “Tramontane” and is quite protected from strong winds by the mountain in case of Garbí wind.

The vegetation is largely present in the campsite, therefore named “Bois fleuri”, with no large continuous vegetated zone, but rather hedges of trees and shrubs separating the individual places of light structures.

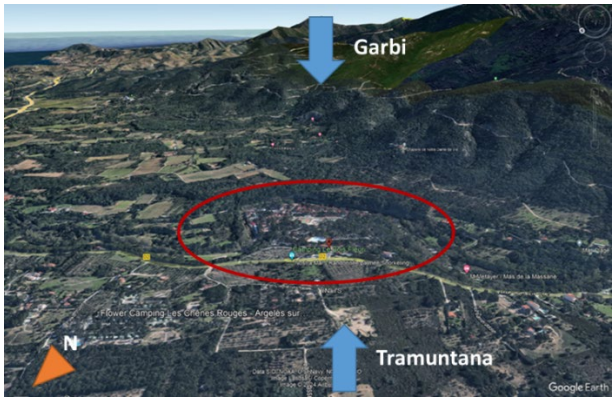

Figure 2-6 “Bois Fleuri” location

The campsite was very close to the wildfire of August 2023, the “Argelès/Saint-André fire”, that fully destroyed the neighbour campsite “Les Chênes Rouges”. This fire was mostly under Garbí wind, changing 3 times its direction.

(a)  (b) 

Figure 2-7 Fire of August 2023: (a) destroying olive tree plantation in campsite “Les Chenes Rouges” as seen from the entrance road of “Bois Fleuri” (courtesy of SDIS66), (b) no understory left under olive trees 6months after fire

According to the territorial regulation approved by DDTM66, the campsite is located in the white zone in the PPRIF Argelès (see Figure 2-2), meaning that no specific construction constraints are to be applied to buildings. Moreover, the entrance building (see next section) is not classified as “Etablissement Recevant du Public” (ERP). All protection means evaluated in the present study only concern auto-protection. All other protection means, preparing for potential intervention by fire brigades (“Défense Extérieure contre l’Incendie”, “Défense des Forêts contre les incendies”) or concerning vegetation cleaning (“Obligations Légales de Débroussaillement”) are assumed to be already implemented by the campsite owner.

2.2.2. Site hazard, vulnerability and existing protections

The campsite is essentially composed of:

- light structures (mobil homes) (very few places devoted to camping tents), separated by ornamental hedges;
- one large restaurant room, with wooden structure, located near the main swimming pool;
- the entrance building, also hosting a small grocery store.

(a)  (b) 

Figure 2-8 Bois Fleuri: (a)aerial view and (b) entrance building seen from entrance road

The entrance building will be evaluated as potential refuge. Efectis could visit with Entente Valabre the "Bois Fleuri" in December 2023. Digital or manual plans could not be retrieved. The interview on site did allow to identify all combustible materials and vegetation present in the vicinity of the building and all building vulnerable items. Some photos could be taken.

The inventory of combustible materials and vegetation was conducted in the last 100meters to the building, and the vulnerable elements which are exposed. These elements are summarized in Tab 2-2.

Table 2-2: Hazard items, exposed vulnerability items and existing protections for the building of "Bois Fleuri"

Hazard item	**Exposed vulnerability item**	**Already existing or ongoing protection measures (incombustible material, protections…)**
Unmanaged olive tree plantation in neighbouring campsite "Les Chenes Rouges" (large shrub understory) (before Aug 2023 fire – after fire, no more understory)	Window bays of entrance hall, exposed on Northern façade (10m long) and Western façade) at ground floor - No impact at first floor due to protections	- Masonry balcony cuts the impact to first floor windows - Masonry roof frame, mineral tiles assembly with no openings - Masonry junction btw wall and roof - Aluminium gutters
Cypress hedge at 14m from Northern facade	Window bays of entrance hall, exposed on Northern façade (10m long) at ground floor - No impact at first floor due to protections	- Cypress hedge currently being cut from 5-6m height down to 2m height - Masonry balcony cuts the impact to first floor windows
Large individual pine collocated to Northern facade	Window bay at first floor	- Branches of pine are being cut at 3m distance - Window bay will be replaced by a masonry wall

Hazard item	**Exposed vulnerability item**	**Already existing or ongoing protection measures (incombustible material, protections…)**
Gas bottle storage at 15m of Southern façade		Masonry wall high enough to protect building
Plastic trash containers at 8m of cypress hedge, itself at 14m of Northern facade	Cypress hedge	
Different flammable shrubs near the Western and Southern facades, particularly: - shrubs very close to window bay of Northern faced - planters very close to window bay of Western facade - 1 small palm tree located 5m from window bay of Southern facade	Windows and window bays with no shutter at Northern, Western and Southern façades	All the flammable species <10m distance of windows will be removed Most species are hardly flammable species (large leafs deciduous trees) : they can be kept
Car park, 10m from Northern facade	Iron garage doors	Cars will be removed when fire is approaching (housekeeper always present when tourists are present)
Mobile home close to Eastern facade		No window, masonry wall at first floor, high enough to protect the windows at first floor (located behind large balcony)

(a) 

(b) 

(c) 

(d) 

(e) 

(f)

Figure 2-9 : Locations of different hazard and vulnerability items around entrance building: (a) unmanaged olive tree plantation on other roadside (historical photo before the 2023 fire), (b) cypress hedge at Northern façade being cut at 2m height, (c) large pine collocated to first stage of Northern façade, (d) isolated shrubs close to the window bay of entrance hall in Northern facade, (e) single small palm tree at Southern façade (among hardly flammable deciduous trees), (f) Mobile home close to Eastern facade

(a) 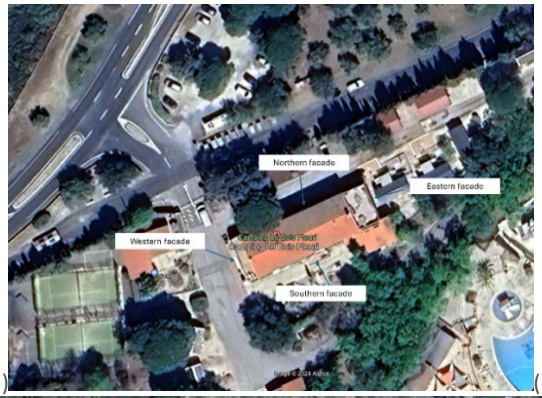

(b) 

(c)

(d) 

(e) 

Figure 2-10 : Locations of other hazard and vulnerability items around entrance building: (a) view of facades, (b)view from Northern and Western facades, (c) view from Western and Southern facades, (d) view from Eastern and Northern facades, (e) ground floor basemap

3. Adaptation of the WUITIPS methodology to the pilot sites

The methodology developed in WUITIPS (see D4.1 document [4]) has to be adapted according to the available input data on hazard and vulnerability characteristics.

The table 3-1 summarizes the performance criteria to be obtained to secure the building envelope as a refuge. It also precise how the method is adapted according to availability of the characteristics.

On both sites, no info has been made available on walls and openings characteristics, (structural and material composition). The adaptation consists on:

- Evaluating first the exposure level of the vulnerable items;
- Evaluating the vulnerability: according to the exposure level, if it appears to be critical, either standardized characteristics will be assumed to quantify the criteria, or alternatively qualitative recommendations will be used.

Table 3-1: Performance criteria as defined by the WUITIPS methodology (source: D4.1 document [4])"

	Quantitative PBD criteria (2min)	**Quantitative PBD criteria (30min)**	**Vulnerable items in the pilot sites**	**Possibility of application to the FR case studies**
Non ignition of walls or roof (target = exterior face) (Auguin et al., 2008, French Order of 29/07/2015)	<1800 $(kW/m^2)^{4/3}s$	<8kW/m^2	Wood shutters, window wood frames and lintels	Quantitative assessment possible, using SWIFFT model
Non explosion of the windows (target = exposed face) (3criteria, Vacca et al, 2020)	<1840 $(kW/m^2)^{4/3}s$	<8kW/m^2	Windows and window bays	Quantitative assessment possible, using SWIFFT model
	ΔT(middle-edge)<58°C	ΔT(middle-edge)<58°C	Windows and window bays	No knowledge of openings characteristics – If calculation is needed , standardized material properties will be assumed
	<150°C	<150°C	Windows and window bays	No knowledge of openings characteristics – Risk can be estimated as soon as 150°C is the temperature of the plume reaching the window
Tenability in the room for people (target = center of room, or interior face) (Auguin et al., 2008, LCPP 2017)	<60°C	<60°C	Building interior	No knowledge of openings & walls characteristics – If calculation is needed , standardized material properties will be assumed
Firebrands			Pergola with reed roof,	Qualitative assessment (NIST recommendations)

			lintel debording the facade	
Toxicity			Building interior	The different critical thresholds of n50 will be recalled. A way of measuring the n50 will be described. If more etancheity is needed, qualitative measures will be detailed to achieve this goal.

Only passive protections are evaluated in the 2 French pilot sites, no active protection.

The SWIFFT model (see TN3.1 document [5] for complete model description) is run in "no spread mode": the flame front is positioned during an extended exposure time of 5 min, covering the presence of the fire at the forest interface closest to the building as well as the pre-heating from the approaching fire in the forest before reaching the interface. It takes as inputs:

- the position of the flame front;
- the vegetation properties on the fix fire position, adding effect of forest fire and fire in the ornamental vegetation;
- the topography map;
- the wind scenario.

Let us recall that SWIFFT model has a strong safety approach of assuming that the hot gases plume do dissipate on the ground, which can be coherent here in the configuration of alignment of wind and slope. In reality, the hot gases plume is pushed by the highly chaotic and transient gusty wind, which can push hardly enough to have the plume on ground, but more often pushes the plume in altitude.

The non-ignition of wall and roof combustible material is evaluated by using the SWIFFT output of the total incident heat flux ($q_{incident}$), summing the contributions of radiative and convective thermal transfers, calculated as :

$$q_{incident} = h\left(T_{plume} - T_{wall}\right) + q_{rad}$$

where:

- T_{plume} and q_{rad} are issued by SWIFFT;
- h is the coefficient of heat transfer by convection along a wall, taken at a value of 25 W/m²/°C, in conformity with Eurocode 1-1-2 [7];
- T_{wall} Is taken as cold wall temperature of 20°C.

The non-glazing breakage of the window criterium of T<150°C is calculated on T_{plume} issued by SWIFFT.

Let us note that the topography is extracted for the 2 pilot sites from the European EU-DEM open data topography at 25m resolution (SWIFFT is in ongoing adaptation towards EU Sentinel-

2 topography map at 10m resolution, but not yet validated on this data in the zone of the pilot sites).

3.1. Villa “Mas d’Amont” modelling exercise

For this pilot site, only the building exposure to the fire burning the oak forest and the ornamental hedge in Northern façade requires complex modelling, using SWIFFT model.

Impact of pergola fire to windows and lintel is treated separately, assuming the pergola has been ignited by firebrands.

The cork oak forest contains no pines. The forest is fully clean (no understory, vegetation of oak litter and little shrubs <30cm, removal of dead trees) in the last 100m to the buidling, however full crown continuities (housekeeper refuses to cut trees). From INRAE (pers. comm.) and Efectis experience, no possibility for a fire without understory to travel independently in oak canopies over 50m distance: fire will only be a ground fire in the oak litter and little shrubs<30cm.

Forest vegetation properties are summarized in Tab 3-2.

Table 3-2: Vegetation properties for clean oak plantation (source: Efectis own database)

Vegetation property	**Value**
Vegetation type	Cleaned oak forest
Fuel load	0.3kg/m^2
Fuel depth	0.3m
Area-to-volume ratio	4600m^{-1}
Wood density	510kg/m^3
FMC	5%

SWIFFT deduces a flame height of around 1m.

Concerning ornamental vegetation, they are a mix of succulent plants, laurels and tall grasses, no other shrubs: max 1m height. Flame height can be considered between 0.5 and 3 times the vegetation height (Butler, 2014 [1]), so 3m is considered here for the 1m height vegetation. As mentioned by Filkov et al (2023) [2], average temperature in flames, for such small vegetation, is around 600-800°C, so 800°C is considered here, so an emittance of 75kW/m^2, under blackbody assumption.

Table 3-3: Fire properties in ornamental vegetation (source: Efectis own database)

Vegetation property	**Value**
Vegetation type	Ornamental hedge with flammable species (tall grasses, laurels) and non-easily flammable species (succulent plants)
Height	1m
Flame height	3m
Emittance	75W/m^2

The local topography just behind building on Northern façade is extracted from the European EU-DEM data. The slope is evaluated at 25%, taken securely for the fire propagation at Northern and Western facades, though topography is in reality smoother on Western facade.

The wind scenario is “Tramontane” (NW origin) at 5min-averaged value of 50km/hr.

(a)

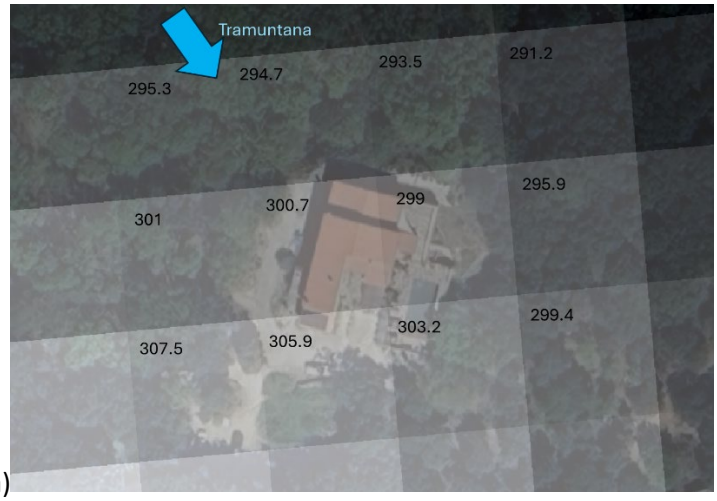

(b)

Figure 3-1 : Input data used for the SWIFFT simulation on cork oak forest and ornamental vegetation: (a) altitudes (meters) and wind direction, (b) vegetation positions and fireline position at interface

3.2. Campsite “Bois Fleuri” modelling exercise

For this pilot site, only the building exposure to the fire burning the unmanaged olive tree plantation and the cypress hedge on Northern façade requires complex modelling, using SWIFFT model.

Concerning the cypress hedge, they are managed to be kept at 2m height. This hedge cannot be dedensified or removed, since it serves as “privacy hedge”. Flame height can be considered 3 times the vegetation height (Butler, 2014 [1]), so 6 m is considered here. As mentioned by Filkov et al (2023) [2], average temperature in flames, for such small vegetation, is around 600-800°C, so 800°C is considered here, so an emittance of 75kW/m^2, under blackbody assumption.

The low grassland on the roadside is ignored since its fire will have only low additional impact to the olive tree plantation fire. The isolated olive tree on the roadside outside the plantation are being modelled since it brings the flames closer to the building.

Table 3-4: Fire properties of olive tree plantation

Vegetation property	**Value**
Vegetation type	Understory of unmanaged olive tree plantation (maquis)
Height	1m
Flame height	3m
Emittance	75W/m^2
Vegetation type	Olive tree in the plantation or isolated on roadside
Height	2.5m
Flame height	8m
Emittance	75W/m^2

Table 3-5: Fire properties of cypress hedge

Vegetation property	**Value**
Vegetation type	Cypress hedge
Height	2m
Flame height	6m
Emittance	75W/m^2

Note that the terrain can reasonably be assumed flat, since there is no main variations in elevation between the olive tree plantation and the “Bois Fleuri” entrance building.

Two scenarios of most unfavourable “Tramontane” winds are considered:

- Tramuntana1: wind of origin North-North-West, most unfavourable from cypress hedge;
- Tramuntana2: wind of origin West-North-West, most unfavourable from olive tree plantation.

Two separate simulations were conducted:

- Simulation n°1: Tramuntana1, with fire simultaneously in olive tree plantation and in the cypress hedge;
- Simulation n°2: Tramuntana2, with fire simultaneously in olive tree plantation and in the cypress hedge.

(a) 

(b)

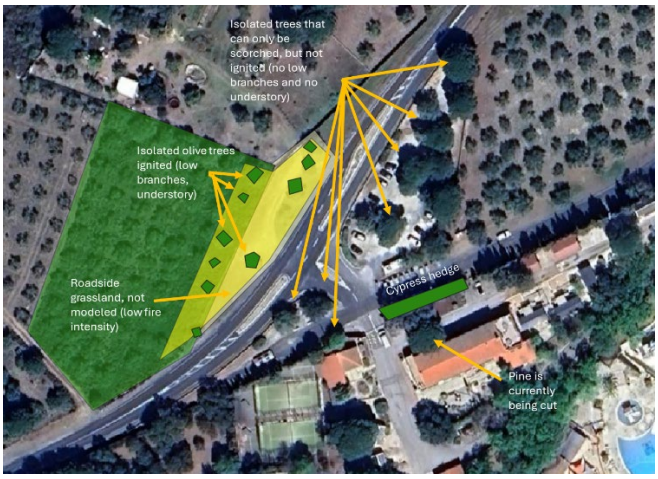

Figure 3-2 : Input data used for the SWIFFT simulation on olive tree plantation and cypress hedge: (a) wind directions, (b) vegetation positions and fireline position at interface

4. Results and Discussion

4.1. Villa "Mas d'Amont"

Exposure to the fire in the oak forest and flammable ornamental hedge - Non ignition of lintels and shutters and non explosion of windows

The non-ignition of wall and roof combustible material and non explosion of the window require total incident heat flux ($q_{incident}$) and the hot gases temperature (T_{plume}), which are displayed in Figs 4-1 and 4-2.

(a)

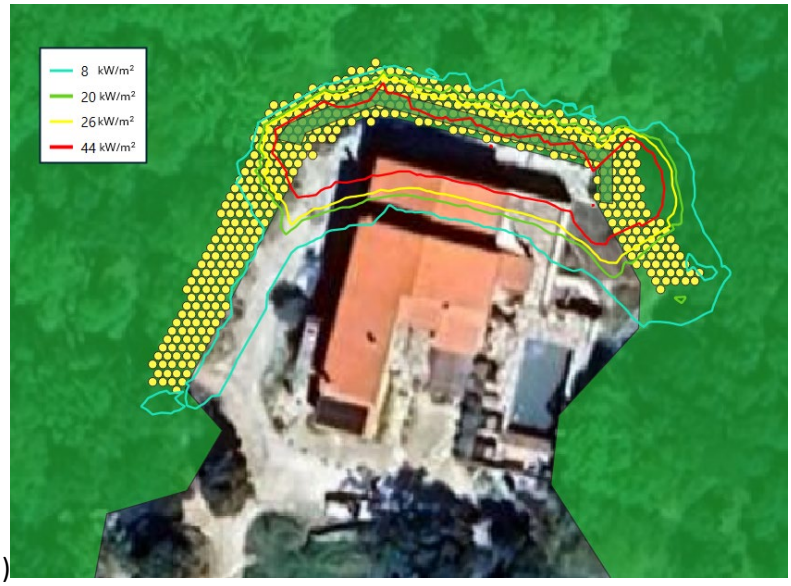

(b)

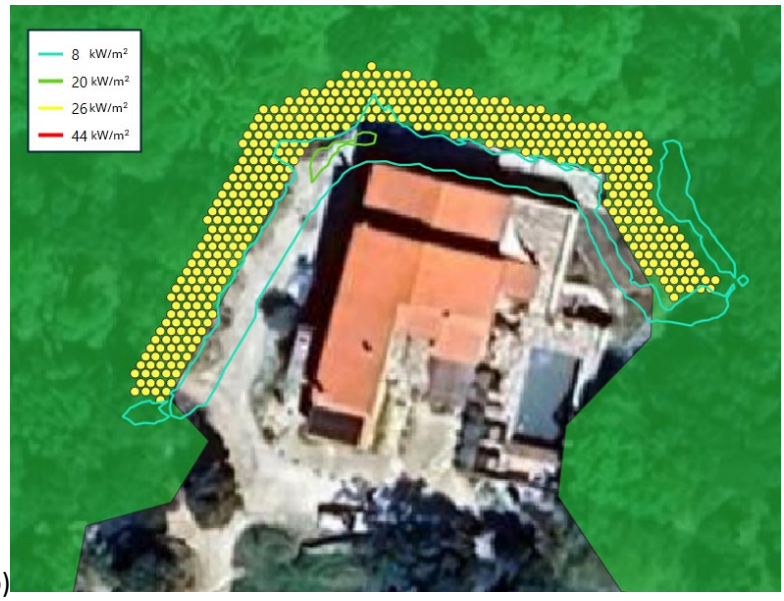

Figure 4-1 : incident heat flux isolines issued by SWIFFT model: (a) with flammable ornamental hedge, (b) with non-easily flammable ornamental hedge

(a)

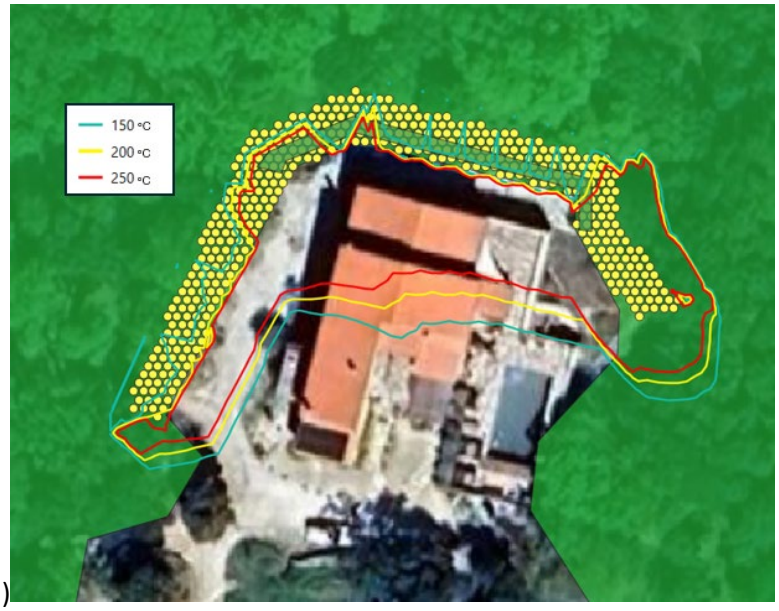

(b)

Figure 4-2 : incident temperature isolines issued by SWIFFT model: (a) with flammable ornamental hedge, (b) with non-easily flammable ornamental hedge

Table 4-1: Evaluation of the performance criteria for walls and openings

	Quantitative PBD criteria (2min)	**Quantitative PBD criteria (30min)**	**Application to case with flammable hedge**	**Application to case with non-easily flammable hedge**
Non ignition of walls or roof (target = exterior face) (Auguin et	<1800 $(kW/m^2)^{4/3}s$	<8kW/m^2	Wooden frames and shutters and lintels in danger by fluxes up to 44kW/m^2	Wooden frames and shutters and lintels not in

al., 2008, French Order of 29/07/2015)				danger by fluxes lower than 8kW/m^2
Non glazing breakage of the windows (target = exposed face) (3criteria, Vacca et al, 2020)	<1840 (kW/m^2)$^{4/3}$s	<8kW/m^2	Windows in danger by fluxes up to 44kW/m^2	Wooden frame not in danger by fluxes lower than 8kW/m^2
	ΔT(middle-edge)<58°C	ΔT(middle-edge)<58°C	Not evaluated	
	<150°C	<150°C	Windows in danger with hot gases much higher than 250°C	Windows in danger with hot gases up to 250°C

The solution is to:

- ***Remove all flammable elements (tall grasses, laurels) in the hedge, keeping only broad-leaf species and succulent plants (and removing any dead material that would appear) -This type of hedge will not ignite under the wildfire in the oak forest,***

- ***Install window shutters on Northern facade, which will not be ignited by the fire burning the forest oak nearby. Due to very good insulation capacity of wood shutter, the glass will be protected. (This modification is now performed in nov-2024)***

Exposure to pergola fire (Western façade) - Non-ignition of lintels and non-explosion of windows

The reed roof of the pergola is the main cause of danger, since its ignition will surely expose directly the window and shutter, with flames very close to these vulnerable elements, probably even with direct flame contact. The wooden purlins would also contribute to increase the fire effects. The protection will consist in replacing the reed roof by mineral tile roof.

Tenability in the room of Northern facade

The tenability in the room is ensured by the following combination of factors:

(1) low exposure (<8kW/m^2 incident heat flux);

(2) the fire resistance of walls and openings;

(3) very large walls with very insulating material (stone wall);

(4) low window coverage of the façade <30% (small windows).

Firebrands

No additional vulnerable points were identified in the envelope, directly endangered by firebrands. The cleaned oak forest is also poorly subject to emitting large firebrand showers.

Toxicity

According to the D4.1 document [4], two types of thresholds can be chosen on the allowed maximum air renewal rate without any active ventilation (n50):

- a very strong criterium of n50=0.30hr^{-1} , following the Australian 2014 Performance Criteria General Guidance for Wildfire Shelter Constructions;
- a more permissive criterium of n50=7.7hr^{-1}, authorizing CO concentrations in the room to be up to its irreversible effect threshold over 2h (SEI_{2h})

An ancient house, with no particular glazing, will rarely be at n50<1.

Here a n50 infiltrometry measurement needs to be performed in the rooms of the Northern facade, and according to the n50 value and the chosen criterium (strong or more permissive), some work shall be performed to increase etancheity of the room.

To improve room etancheity, the following measures need to be applied at minimum:

- Install 3-point closing windows, with French opening (interior);
- Install a “punch stop” command “punch stop” command to closing traps, for ventilation, for heating device and climatization;
- If needed, for access doors to the confinement room:
    - Replace with solid core doors, with a sealing bar;
    - Install a system of door closing on command;
- Caulk the cable passages;
- Caulk all interface zones:
    - ceiling-wall (ex. adding a plaster band);
    - Joineries-wall (install joints),
    - elements crossing the walls (crossing of air-water piping, electricity cables).

4.2. Campsite “Bois Fleuri”

Non explosion of window bays facing fire in the olive tree plantation and cypress hedge

As can be seen in Figs 4-3 and 4-4, the window bays are subject to fluxes and temperatures higher than the critical thresholds, due to the presence of the 2m cypress hedge. The olive tree plantation will not contribute significantly to this problem.

(a)

(b)

Figure 4-3 : incident heat flux isolines issued by SWIFFT model: (a) under scenario Tramuntana1, (b) under scenario Tramuntana 2

(a)

(b)

Figure 4-4 : temperature isolines issued by SWIFFT model: (a) under scenario Tramuntana1, (b) under scenario Tramuntana 2

Table 4-2: Evaluation of the performance criteria for openings

	Quantitative PBD criteria (2min)	**Quantitative PBD criteria (30min)**	**Application to case with hedge**
Non explosion of the windows (target = exposed face) (3criteria, Vacca et al, 2020)	<1840 $(kW/m^2)^{4/3}s$	<8kW/m^2	Windows in danger by fluxes up to 26kW/m^2
	ΔT(middle-edge)<58°C	ΔT(middle-edge)<58°C	Not evaluated
	<150°C	<150°C	Windows in danger with hot gases much higher than 250°C

The entrance hall cannot be seen as a refuge. However, if wall with fire resistance REI30 can be installed between entrance hall and office, the office and rooms with no window can make compartment.

Thermal tenability in the room

Following the PPRT guide, the wall between entrance hall and the personal entrance shall be reinforced to fire resistance REI30, then the thermal tenability can be ensured in the office and in the undefined rooms and grocery (see Fig 2-9).

Firebrands

No additional vulnerable points were identified in the envelope, directly endangered by firebrands. The cleaned oak forest is also poorly subject to emitting large firebrand showers.

Toxicity

According to the D4.1 document [4], two types of thresholds can be chosen on the allowed maximum air renewal rate without any active ventilation of n50:

- A very strong criterium of n50=0.30hr^{-1} , following the Australian 2014 Performance Criteria General Guidance for Wildfire Shelter Constructions;
- A more permissive criterium of n50=7.7hr^{-1}, authorizing CO concentrations in the room to be up to its irreversible effect threshold over 2h (SEI_{2h})

An ancient house, with no particular glazing, will rarely be at n50<1.

Here, a n50 infiltrometry measurement needs to be performed in the office and rooms with no window, and according to the n50 value and the chosen criterium (strong or more permissive), some work shall be performed to increase etancheity of the room.

To improve room etancheity, the following measures need to be applied at minimum:

- Install 3-point closing windows, with French opening (interior);
- Install a “punch stop” command “punch stop” command to closing traps, for ventilation, for heating device and climatization;
- If needed, for access doors to the confinement room:

    - Replace with solid core doors, with a sealing bar;
    - Install a system of door closing on command;
- Caulk the cable passages;
- Caulk all interface zones:
    - ceiling-wall (ex. adding a plaster band);
    - Joineries-wall (install joints),
    - elements crossing the walls (crossing of air-water piping, electricity cables).

References

[1] Butler BW (2014) Wildland firefighter safety zones: a review of past science and summary of future needs. International Journal of Wildland Fire 23, 295–308.

[2] Filkov A.I, Tihay-Felicelli, V., Masoudvaziri, N., Rush, D., Valencia, A. et al (2023), «A review of thermal exposure and fire spread mechanisms in large outdoor fires and the built environment,» Fire Safety Journal, vol. 140: 103871.

[3] Mell W., Maranghides A., McDermott R., and Manzello S.L. (2009) Numerical simulation and experiments of burning douglas fire trees, Combustion and Flame, vol. 156, no. 10, pp. 2023–2041.

[4] D4.1 document -WUITIPS project - Deliverable 4.1 – Protection of buildings and touristic assets against wildfires: goor practices and methodology for performance assessment

[5] TN3.1 document – WUITIPS project – Technical Note 3.1 – WUI risk analysis toolbox

[6] TN6.3 document - WUITIPS project – Technical Note 6.3 –Web tool specification document

[7] Eurocode 1991-1-2: 2002 Eurocode 1. Actions on structures. Actions on structures exposed to fire

Wildland-Urban Interface Fire Touristic Infrastructure Protection Solutions

WUITIPS

GA number 101101169

Co-funded by the European Union

Technical Note TN 5.1
Evacuation modelling of French campsites

WP - Task	WP5	**Version**	Final
File name	TN5.1_WUITIPS_Evacuation modelling of French campsites	**Dissemination level**	Public
Programmed delivery date		**Actual delivery date**	

Document coordinator	Enrico Ronchi (Lund University)
Contact	[borja.rengel@efectis.com]
Authors	Borja Rengel (Efectis France]
Reviewed by	Elsa Pastor (UPC)

Abstract	Evacuation simulation models have proven highly effective in planning and optimizing strategies for evacuating wildland areas. These models are crucial for evaluating evacuation plans by identifying the safest routes, optimizing resource allocation, and facilitating scenario analysis to identify potential bottlenecks. This study examines the evacuation strategies for two south-eastern French campsites that differ significantly in surface area, number of occupants, evacuation mode (by private vehicle or on foot), and types of accommodation. Crowd-modelling simulations using Pathfinder were conducted to predict tourist movements within the campsite. Additionally, traffic-modelling simulations with SUMO estimated the travel time of tourist vehicles from the campsite to a distant safety site. The results indicate that pre-evacuation and waiting times at various locations significantly influence overall evacuation time. The distance between assembly points/exits and individual plots also greatly affects total evacuation time, particularly in larger campsites. The mode of evacuation, whether on foot or by car, substantially impacts the time required for tourists to reach a safety point.

Table of Contents

Introduction 5
1. Emergency evacuation of campsites 7
1.1. Evacuation strategy 7
1.2. Methodology of assessment 8
2. French campsites selection 9
2.1. Le Bois de Pins 9
2.2. Le Bois Fleuri 12
3. Pathfinder modelling features 14
3.1. About Pathfinder 14
3.2. Occupant profiles 16
3.3. Distribution of occupants 16
3.4. Pre-evacuation times 17
3.5. Group movement 19
3.6. Waiting times 19
3.7. Evacuation modelling scenarios 19
4. SUMO modelling features 20
4.1. Overview of the model 20
4.2. Building traffic simulations 20
4.3. Car-following model 21
4.4. Vehicles characteristics 21
4.4.1. Size and speed 21
4.4.2. Intersections 22
4.5. Road network 22
4.6. Traffic modelling scenarios 23
5. Results and discussion 25
5.1. Summary of the input and output data 25
5.2. Le Bois de Pins 26
5.2.1. Evolution of the number of occupants 26
5.2.2. Evacuation times and travel distances 28
5.2.3. Cumulative space utilisation maps 30
5.2.4. Cumulative high-density maps 30
5.3. Le Bois Fleuri 35
5.3.1. Evolution of the number of occupants 35
5.3.2. Evacuation times and travel distances 36

5.3.3. Cumulative space utilisation maps 37
5.3.4. Cumulative high-density maps 39
5.3.5. Evolution of the number of vehicles 41
5.3.6. Maximum arrival time for campsite vehicles 42
5.3.7. Mean trip duration for campsite vehicles 43
6. Conclusions 44
7. Acknowledgements 46
References 47

Introduction

Wildfires pose a serious threat to populations in the wildland-urban interface (WUI), where vegetation and urbanized populated areas intersect (Benichou et al. 2021). This risk is of special importance to tourist areas characterized by a mix of people with different cultures, languages, infrastructure, and emergency strategies. Tourists, as transient populations, may come from non-wildfire-prone regions and are often unfamiliar with their temporary surroundings, making them more vulnerable during wildfire events (Labhiri et al. 2024).

Tourists' lack of familiarity with local emergency protocols and the specific risks associated with wildfires can lead to increased exposure and confusion during evacuation processes. This situation is worsened by the fact that tourist destinations frequently have infrastructure that is not designed to handle large-scale emergency evacuations, especially when dealing with a multilingual and culturally diverse population. Moreover, tourists' transient nature means they might not have established communication channels or local contacts to rely on for timely information and assistance.

The dangers posed by wildfires to tourist areas have been tragically underscored by several high-profile incidents around the world. The 2016 Madeira fire in Portugal (Ronchi et al. 2017), the 2023 Maui fire in the USA (Gupta 2023), and the 2023 Rhodes fire in Greece (Bubola and Kitsantonis 2023) are notable examples. These incidents highlight the difficulties tourists face during such events, from understanding evacuation routes and procedures to dealing with the emotional stress of being in an unfamiliar place during a crisis.

These events underscore the critical need for tailored evacuation strategies and improved communication systems in tourist areas prone to wildfires. Ensuring that tourists receive adequate information about wildfire risks and emergency procedures upon arrival, along with multilingual support, can significantly enhance their safety and preparedness. Additionally, developing robust evacuation plans that account for the unique challenges posed by transient populations can help mitigate the impact of wildfires on these vulnerable groups.

Campsites, often situated in remote areas or in wildland-urban interfaces, represent some of the most at-risk vacation spots in case of wildfires due to the possibly rapid spread of fire. The number of tourists at campsites typically peaks during the holiday season, coinciding with the highest risk of wildfires. These locations often have limited access roads and narrow pathways, significantly impeding the evacuation process during emergencies. The primary challenge lies in ensuring the safety of tourists and staff, especially when faced with the urgent need to evacuate accommodations that often lack adequate fire protection measures, both active and passive.

Effective evacuation strategies are essential for mitigating risks in wildfire-prone camping areas. However, many campsites develop their own strategies based on

available resources and specific needs, which may not always be the most effective. This variability highlights the need for standardized and optimized evacuation plans.

Evacuation simulation models have proven highly effective in planning and optimizing evacuation strategies in wildland-urban interface areas (Ronchi 2023). These models are invaluable for evaluating evacuation strategies by identifying the safest routes, ensuring optimal resource allocation, and facilitating scenario analysis to uncover potential bottlenecks. They also consider the impact of variables such as weather and terrain on evacuation times, informing policy and decision-making for more effective evacuation strategies.

This study aims to assess the evacuation strategies proposed in two southeastern French campsites, Le Bois de Pins and Le Bois Fleuri. These campsites differ significantly in surface area, number of occupants, evacuation mode (by private vehicle or on foot), and types of accommodation. To achieve this, crowd-modelling simulations have been performed using Pathfinder (Thunderhead Engineering 2023), an agent-based microscopic evacuation model which predicts the movement and behaviour of tourists within the campsite. These simulations account for tourist groups (e.g. families), reaching assembly points, returning to their accommodations to pick up belongings, and then either leaving the campsite or taking their vehicles. Additionally, traffic-modelling simulations with SUMO (Alvarez Lopez et al. 2018) have been conducted to estimate the travel time of tourist vehicles from the campsite to a distant site of relative safety.

The main findings show the importance of comprehensive evacuation planning and the need for campsite managers to adopt standardized - approaches to ensure the safety of tourists in wildfire-prone areas.

1. Emergency evacuation of campsites

1.1. Evacuation strategy

Unlike a conventional building, where occupants must evacuate upon receiving a fire alarm signal, the evacuation process at a campsite generally unfolds differently, as illustrated in Figure 1.

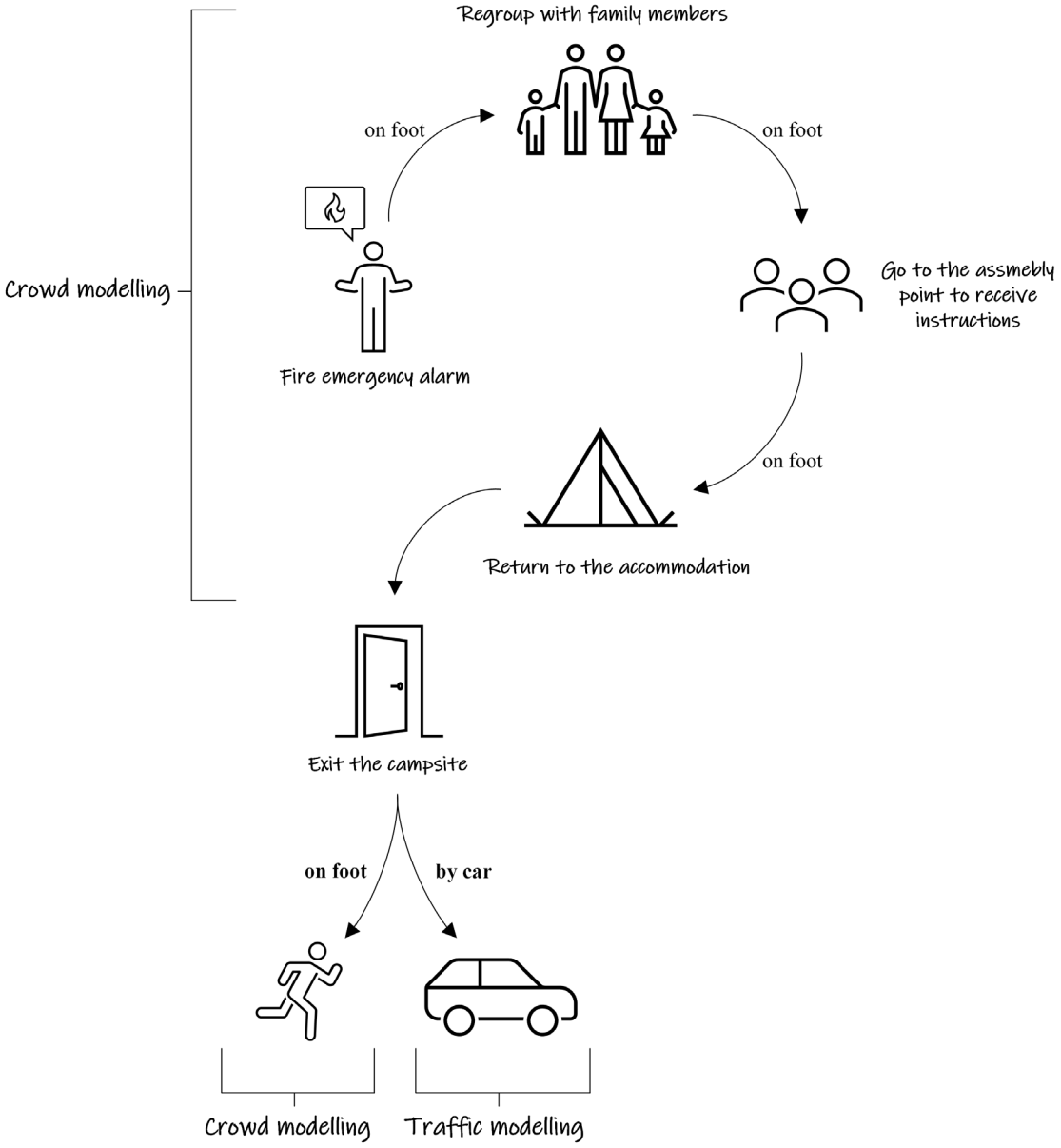

Figure 1 Evacuation event in both campsites.

When the campsite director is alerted to an approaching wildland fire, the fire emergency protocol is activated. Typically, trained staff members or supervisors are responsible for directing people to assembly points where they will receive instructions for emergency evacuation. To facilitate this, voice alert or other systems (i.e., mobile app) may be employed to ensure clear communication.

After being alerted, occupants will gather with their family members and proceed to the designated assembly points. There, they will receive detailed evacuation instructions from the campsite staff and director.

Subsequently, families will return to their accommodations to collect essential belongings and valuables. They should aim to do this as quickly as possible. Once this is done, families will evacuate the campsite either on foot or by vehicle, depending on the campsite's evacuation strategy and the safety of the surrounding areas.
Once occupants have been alerted, they will regroup with family members to reach together the assembly points where the rest of the staff and director will give them the appropriate instructions to evacuate the campsite. The complete staff will evacuate when the last occupant evacuates the campsite.

1.2. Methodology of assessment

Due to the possibly complexity of campsite evacuation routes and the movement of family groups, integrating crowd modelling simulations into the campsite evacuation process is essential. These simulations should include the entire evacuation sequence within the campsite: from the initial alert about the fire emergency through to when occupants return to their accommodations to collect their belongings.

Following this, the scope of the crowd modelling simulations can be expanded depending on the evacuation method. If occupants are evacuating on foot to a designated safety area just outside the campsite, the simulations should continue to track their movement to this safe zone. Conversely, if evacuation involves vehicles, the crowd modelling simulation should conclude once families reach their vehicles.

At that point, traffic modelling becomes necessary to evaluate the flow and impact of vehicles evacuating through a safe area near the campsite. In such scenarios, the outputs from the crowd modelling simulations, specifically the data on how families reach their vehicles, serve as inputs for the traffic model. This approach allows for a comprehensive analysis of both pedestrian and vehicular evacuation processes, ensuring that all aspects of the evacuation are effectively managed.

2. French campsites selection

Two distinctly different French campsites have been selected for the analysis of evacuation strategies in the event of a wildfire: Le Bois de Pins and Le Bois Fleuri (Figure 2). Each campsite presents unique characteristics and challenges, which are detailed in the following sub-sections. Both campsites feature relatively flat terrain with minimal slopes and inclines. They are family-oriented, accommodating many children and minors, often accompanied by adults.

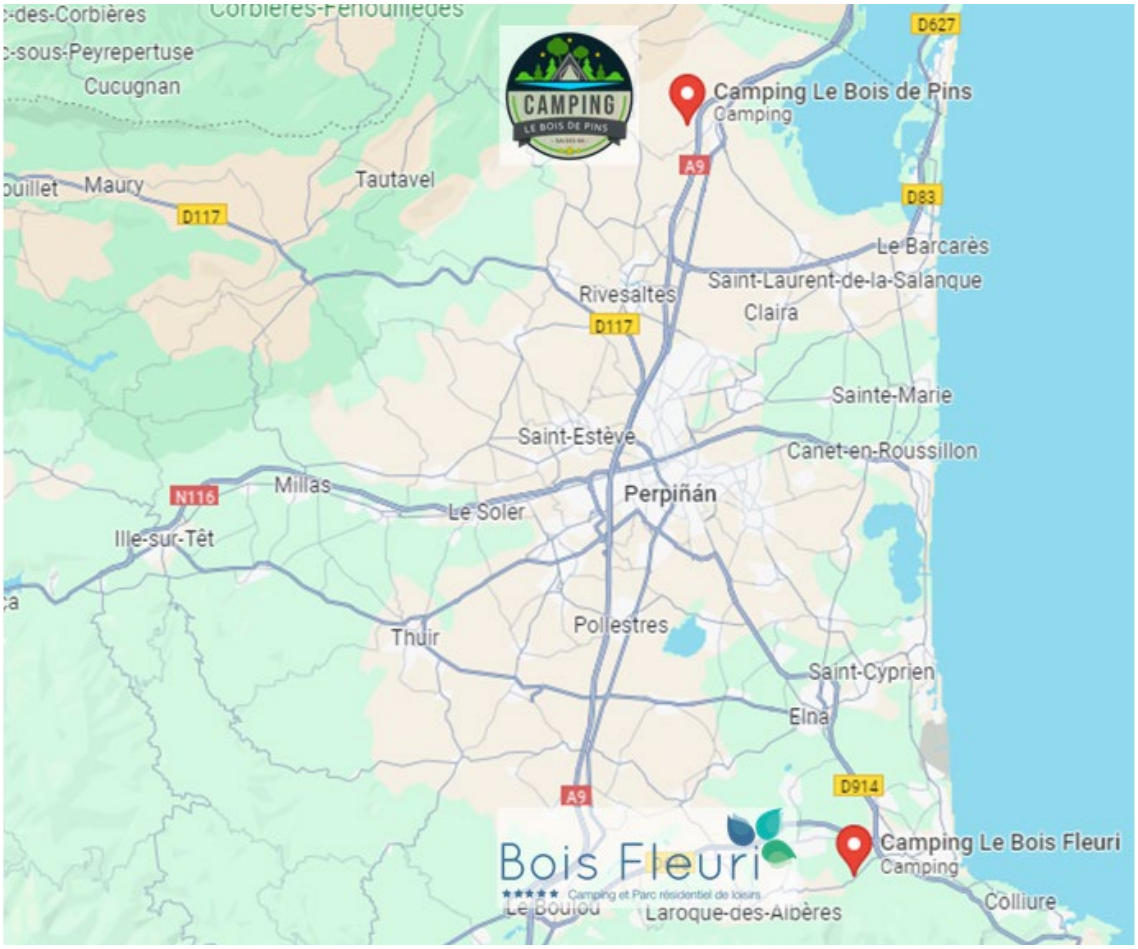

Figure 2 Location of the French campsites proposed for analysis.

This comparative analysis aims to provide a comprehensive understanding of how different campsite configurations and conditions impact the effectiveness of evacuation strategies.

2.1. Le Bois de Pins

Le Bois de Pins is a relatively small campsite (4 ha) with a relatively small number of occupants (less than 600 people), but it features a variety of accommodation types including mobile-homes, tents and caravans (Figure 3). The site is enclosed by wire fences, which define its boundaries and enhance security. There is one primary access road for regular use, supplemented by an additional emergency exit to facilitate evacuations when necessary.

Surrounding Le Bois de Pins is a mix of wooded and agricultural areas. The wooded regions, while offering a scenic and serene atmosphere for campers, also pose a significant wildfire risk. The presence of agricultural land, however, can provide natural firebreaks, potentially slowing the spread of wildfires and offering strategic advantages during an evacuation.

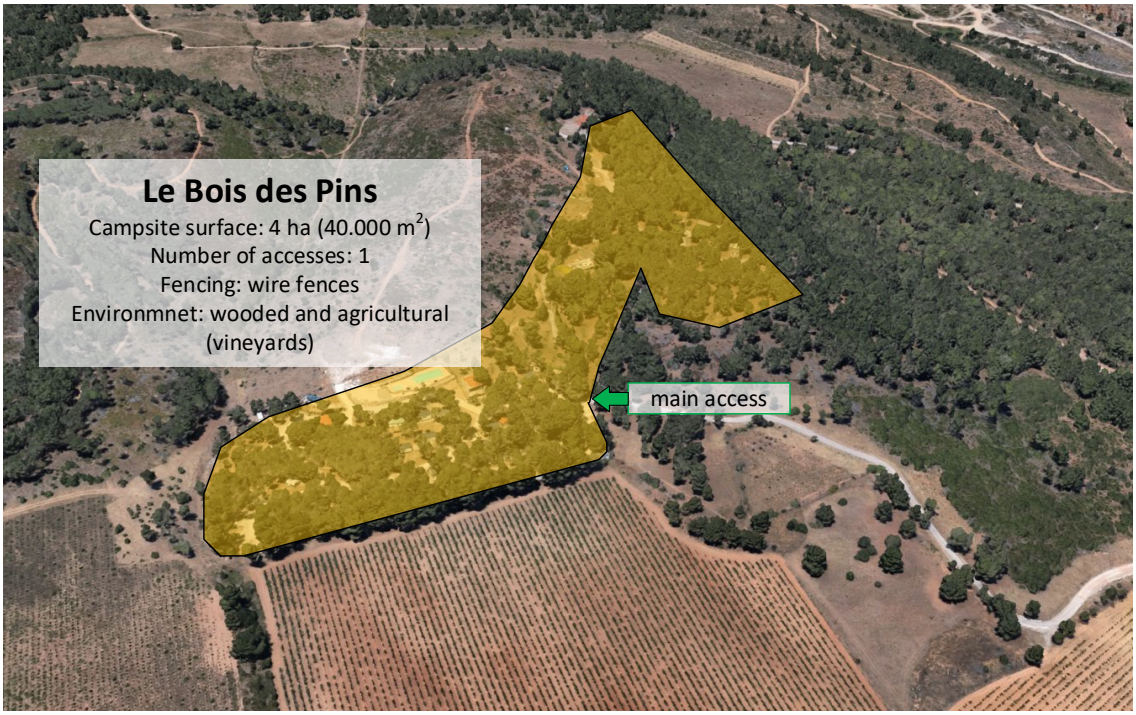

Figure 3 Le Bois de Pins. Google earth© view of the campsite.

A more detailed plan of the available accommodations (100 units) and main services can be seen in Figure 4. The exact number of accommodation units and their capacities are listed in Table 1, with a maximum campsite capacity of 512 people. The staff is assumed to be distributed among the different campsite areas.

Table 1 Le Bois de Pins. Number of available accommodations.

Accommodation	**Capacity**	**Number**	**Occupants**
Caravans/tents	6 people	40 units	240 p
Mobil-homes (4 p)	4 people	44 units	176 p
Mobil-homes (6 p)	6 people	16 units	96 p
Total		**100 units**	**512 p**

In the event of a fire emergency, staff supervisors assigned to the main campsite zones - outlined in Figure 5 - are responsible for issuing the evacuation alert. Emergency messages will also be broadcasted via megaphone to further inform and guide campsite occupants, supporting the efforts of the staff supervisors. The evacuation plan involves guiding all occupants on foot to the designated vineyard area, where they are expected to be met and assisted by fire and emergency services.

Accomodations:

caravans/tents (6 p) mobil-homes (6 p) mobil-homes (4 p)

Others:

miscellaneous services evacuation routes main assembly point secondary assembly point

Figure 4 Le Bois de Pins. Plan of the accommodations and main services.

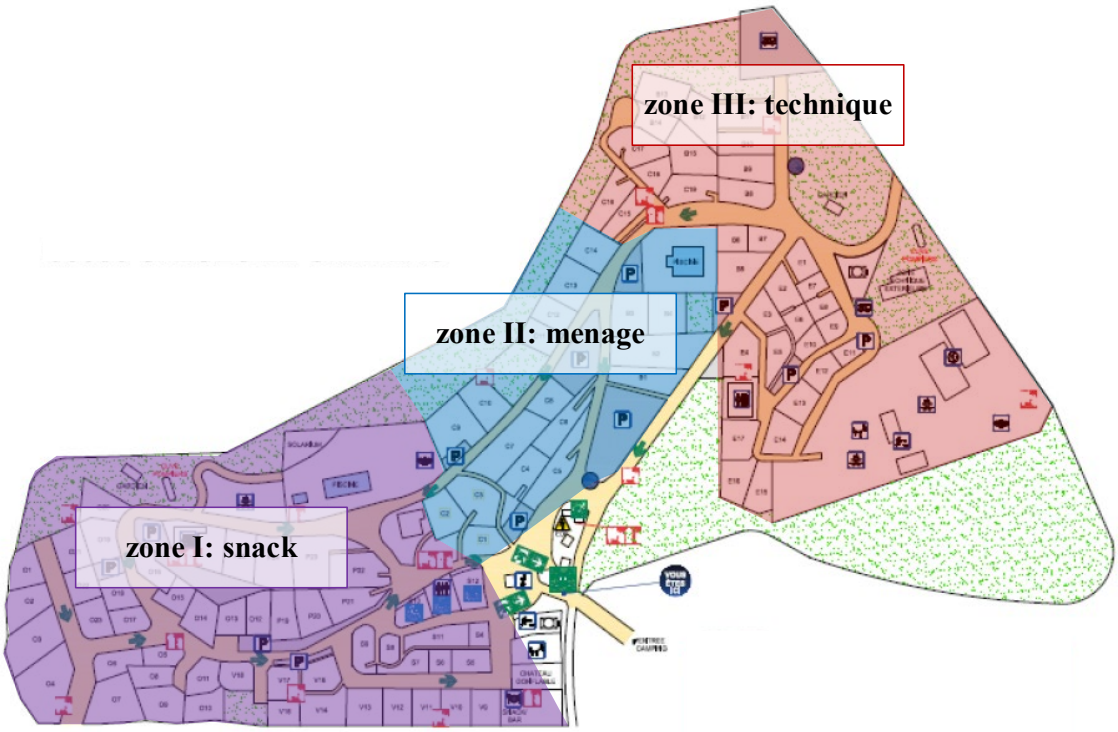

Figure 5 Le Bois de Pins. Main evacuation zones.

2.2. Le Bois Fleuri

Le Bois Fleuri is characterized by its extensive surface area (15 ha) and a relatively high number of occupants (more than 2.000 people), accommodated in mobile homes of different capacities. The campsite is bordered by a wooded area and enclosed by wire fences and a river, which define its boundaries. It has a single primary access road for regular use. The evacuation strategy at Le Bois Fleuri predominantly relies on private vehicles, necessitating a well-coordinated traffic management plan to avoid congestion and ensure a swift evacuation. Due to its extensive layout, occupants may need to traverse long routes, ranging from 700 m to 1 km, to reach the main assembly point.

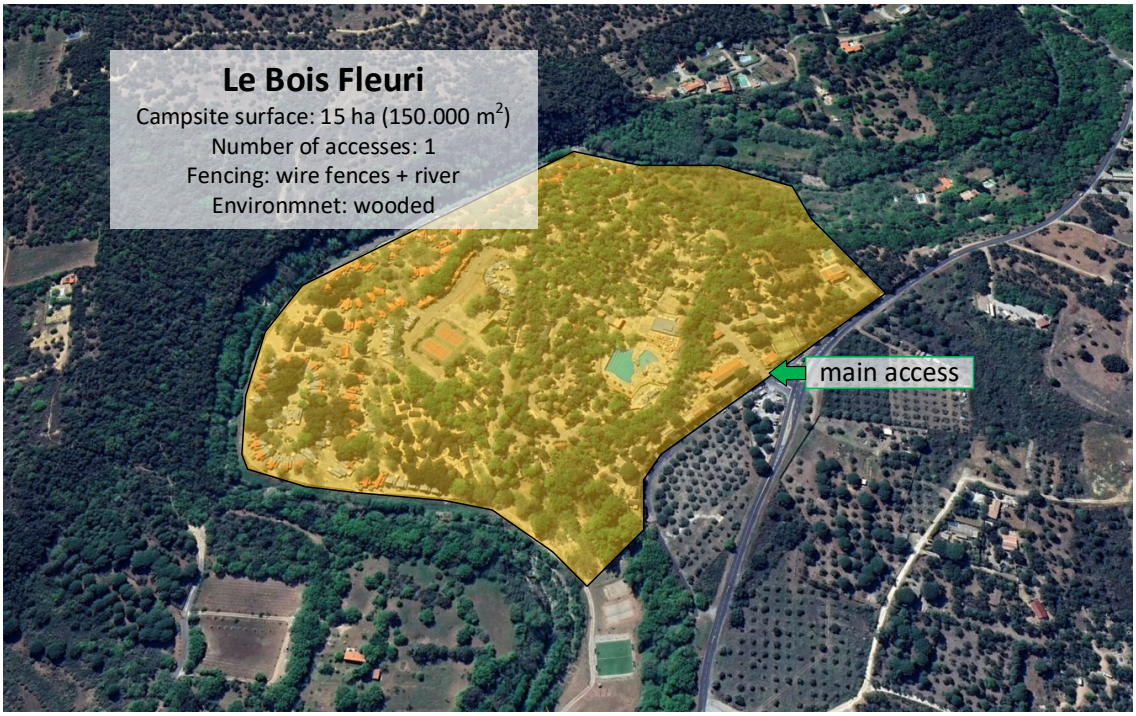

Figure 6 Le Bois Fleuri. Google earth© view of the campsite.

The following table summarizes the number of available accommodations and their capacities by evacuation areas. The campsite has a total of 467 accommodations, with the ability to host up to 2.631 people.

Table 2 Le Bois Fleuri. Number of available accommodations.

Zone	Accommodation	Occupants
Zone ABCD	86 units	498 p
Zone EFPU	66 units	378 p
Zone GHIJ	52 units	297 p
Zone N	124 units	722 p
Zone RS	119 units	622 p
Zone K	20 units	114 p
Total	**467 units**	**2.631 p**

Staff are assumed to be distributed across the various campsite areas. Figure 7 provides information on the campsite evacuation zones and the assembly point. Only the main

exit will be considered in this study, though the evacuation strategy exhibits an alternative exit (not shown here) called “access pompier” that leads to the same assembly point. The main exit is of use when it is accessible, while the alternative exit is for cases where the main exit would not be accessible.

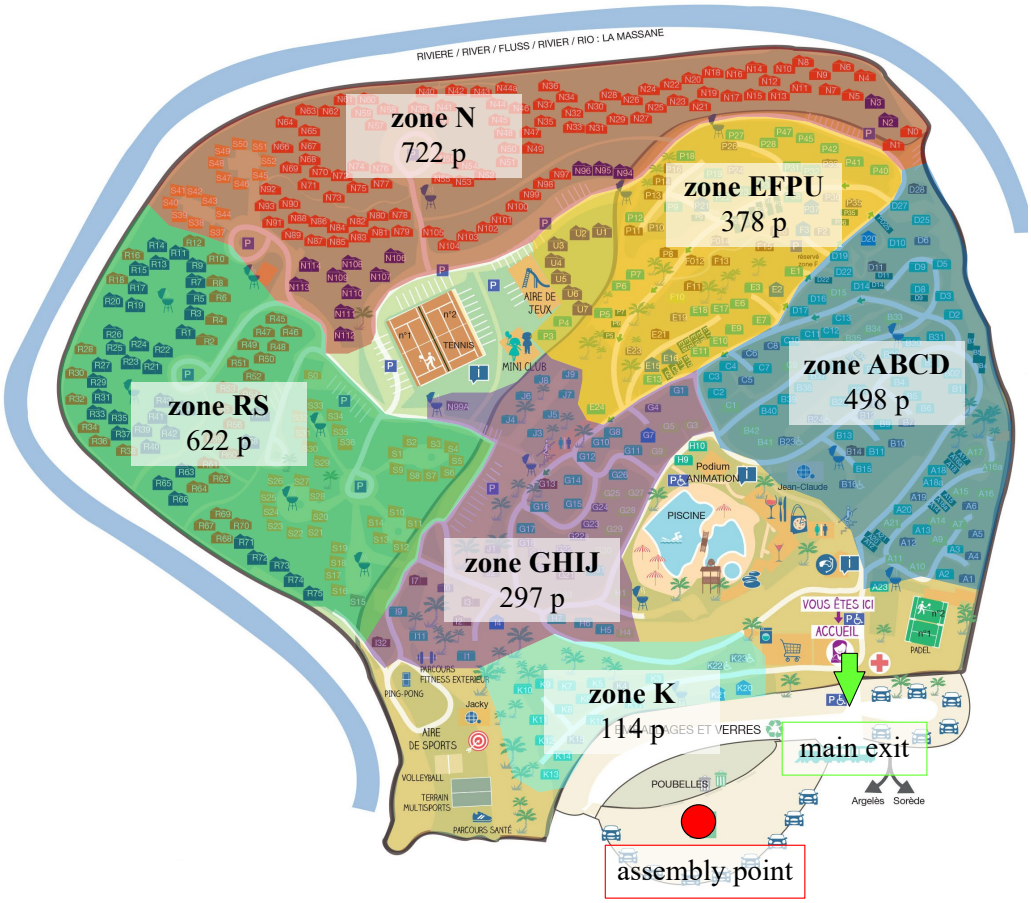

Figure 7 Le Bois Fleuri. Campsite evacuation zones.

3. Pathfinder modelling features

3.1. About Pathfinder

Pathfinder (Thunderhead Engineering 2023) is a microscopic evacuation modelling software developed by Thunderhead Engineering that is widely used in the field of fire safety and emergency planning (Lovreglio et al. 2020). It employs agent-based simulation techniques to model the movement and behaviour of individuals during evacuation scenarios. The software allows for detailed representation of environments, including complex building layouts and varied terrain (by implicitly representing the impact of terrain on walking speeds, since navigation meshes are in 2D), making it suitable for a range of applications from urban buildings to open spaces like campsites. Pathfinder's capabilities include simulating human behaviour, such as decision-making processes, response times, and interaction with other evacuees and obstacles, which are critical for accurate evacuation planning and analysis.

The software includes two options for simulating occupant movement: the Society of Fire Protection Engineering (SFPE) mode and the steering mode. The SFPE mode determines movement speeds based on room occupancy and the flow of people through doors according to their width (Gwynne and Rosenbaum 2016). In contrast, the steering mode allows for the consideration of more complex human behaviours due to the implemented movement algorithms (Reynolds 1999).

In this study, the evacuation simulation is proposed using the steering mode, with occupant behaviour updated every 0.1 seconds (this time interval was decided since it was deemed a reasonable trade-off between computational cost and accuracy). Simulations utilize version 2023.2.1206 of Pathfinder, allowing for a detailed and dynamic analysis of evacuation scenarios.

The following figures illustrates the Pathfinder models for both campsites, highlighting the main routes and evacuation elements represented.

Figure 8 Pathfinder model representing Le Bois de Pins campsite.

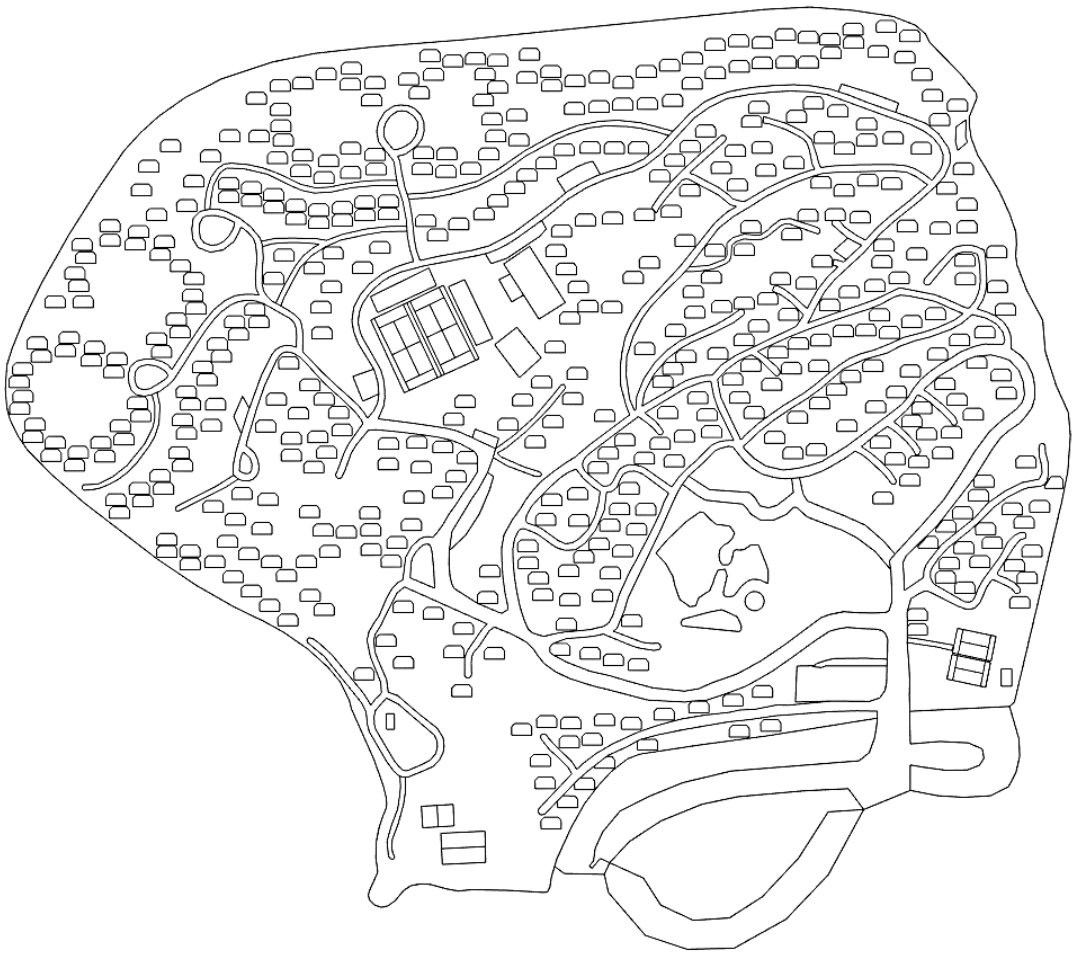

Figure 9 Pathfinder model representing Le Bois Fleuri campsite.

3.2. Occupant profiles

Six distinct profiles are proposed to represent the diverse range of occupants that may be present in the campsites (Boyce et al. 1999, Korhonen and Hostikka 2009, Shields 1993): male, female, child, elderly, persons with reduced mobility (PMR) and wheelchair users. Table 3 details the assumed diameters (since Pathfinder assumes a circular representation of agents) and unimpeded travel speeds of the different occupant's profiles proposed for analysis, which have been represented by using normal distributions.

Table 3 Diameters and travel speeds of the occupant's profiles proposed.

Profile	**Diameter**	**Speed**
Male	0,5 - 0,58 m	1,15 - 1,55 m/s
Female	0,44 - 0,52 m	0,95 - 1,35 m/s
Child	0,39 - 0,45 m	0,6 - 1,2 m/s
Elderly	0,46 - 0,54 m	0,5 - 1,1 m/s
PMR	0,44 - 0,58 m	0,43 - 1,17 m/s
Wheelchair	1,32 m x 0,76 m	0,44 - 1,22 m/s

For Le Bois de Pins, where the evacuation is conducted on foot, a speed reduction factor of 0,25 (Ray and Ebener 2008) is applied for daytime scenarios, and 0,35 for nighttime scenarios, to account for potential terrain irregularities and issues associated with walking in the dark. Conversely, for Le Bois Fleuri, speed reduction factors of 0,35 and 0,45 are applied for daytime and nighttime scenarios, respectively, to consider both terrain irregularities, walking in reduced visibility and the interactions between vehicles and pedestrians on the circulation routes. The remaining occupant characteristics are defined by default settings in Pathfinder.

3.3. Distribution of occupants

Tourists were distributed based on the maximum accommodation capacity, with a significant number of children included, considering that (i) campgrounds are family-oriented tourist destinations and (ii) children typically have reduced travel speed (Najmanová and Ronchi 2023). The distribution of occupants according to accommodation capacity is as follows:

- 2 people: 1 male + 1 female
- 4 people: 1 male + 1 female + 2 child
- 5 people: 1 male + 1 female + 3 child
- 6 people: 1 male + 1 female + 1 elderly + 3 child

The French interministerial circular on accessibility for PMR in public buildings and facilities (Direction Générale de l'urbanisme, de l'habitat et de la construction 2007) does not specify a minimum quota for accommodations at campsites (Ineris 2024). Due to this lack of specific guidance, the percentage of PMR and wheelchair users are based on the based on the Spanish fire safety standard (Ministerio de Fomento 2019), which proposes that 1% of the occupants are wheelchair users and 3% are PMR.

Table 4 details the distribution of different type of profiles in both campsites, considering the maximum occupancy.

Table 4 Distribution of tourist occupants in both campsites.

Profile	**Le Bois de Pins**	**Le Bois Fleuri**
Male	96 p (18,8%)	448 p (17%)
Female	96 p (18,8%)	448 p (17%)
Child	246 p (48%)	1.276 p (48,5%)
Elderly	54 p (10,4%)	353 p (13,5%)
PMR	15 p (3%)	75 p (3%)
Wheelchair	5 p (1%)	25 p (1%)
Total	**512 p (100%)**	**2631 p (100%)**

According to the provided information, one-quarter of the occupants at Le Bois Fleuri campsite participate in daytime outdoor activities organized by the campsite. As a result, the maximum number of tourists present within the campsite during the day is assumed equal to 1.956 people.

According to the data from the Instituto Nacional de Estadística (INE) (Spanish national statistics institute) on campsite occupancy and employment in Spain for August 2022, first and second category campsites have approximately 25 and 10 employees, respectively, who are assumed to be present during daily activities (Instituto Nacional de Estadística 2022). Although specific information about night time security personnel is not available, it is proposed to assume that first-category campsites have 8 employees on duty at night, while second-category campsites have 4 employees during the night time. Table 5 summarizes the maximum number of people at the campsites as a function of the schedule.

Table 5 Maximum number of occupants at both campsites for daytime and night time

Schedule	**Le Bois de Pins**	**Le Bois Fleuri**
Daytime	522 p (512 occupants + 10 staff)	1.981 p (1.956 occupants + 25 staff)
Night time	516 p (512 occupants + 4 security)	2.639 p (2.631 occupants + 8 security)

3.4. Pre-evacuation times

Pre-evacuation time is a crucial factor in emergency evacuation planning. It represents the interval between the activation of the alarm signal and the moment when occupants begin purposive movement towards safety (Proulx 2002). This delay includes several stages: recognizing the alarm, understanding the situation, making decisions, and initiating movement. The duration of this delay can vary based on multiple factors, including the purpose of the area, the occupants' familiarity with the environment, their state of alertness (e.g., sleeping or awake), the type of alarm used, and the effectiveness of management practices.

Fire detection and alarm notification times are not included in the simulation, as these factors should be assessed by the responsible personnel at the campsites. Consequently,

for the purpose of this analysis, both fire detection and alarm notification times are assumed to be zero minutes. This assumption simplifies the model and focuses the analysis on the evacuation process itself, rather than on the initial detection and alert phases

Since specific literature on campsites and tourist areas is lacking, the British standard PD 7974-6 has been utilized (this is often used internationally in evacuation studies) to determine the pre-evacuation times (PD 7974-6, 2019). This standard provides a framework for determining pre-evacuation times based on occupant categories, management levels, building complexity, and alarm systems.

The following table summarizes the features of the campsites required to determine pre-evacuation times for scenarios involving sleeping and unfamiliar occupants.

Table 6 Pre-evacuation distribution for sleeping and unfamiliar occupants

	Value	**Description**
Category	Ciii	Sleeping and unfamiliar
Management level	M2	Trained staff to a relatively high level of fire safety management
Building complexity	B3	Large complex building that could present wayfinding difficulties during evacuation
Alarm system	A2	Pre-alarm system with a manually activated warning sounding throughout occupied area

For awake occupants, reliable Pre-evacuation times are not documented in the literature or in the cited standard. Therefore, a pre-evacuation time ranging from 10 minutes (at the 1st percentile) to 20 minutes (at the 99th percentile) is proposed for analysis. Table 7 provides a summary of the Pre-evacuation times established for both awake and sleeping evacuation scenarios.

Table 7 Pre-evacuation times for both awake and sleeping scenarios in both campsites.

Category	**1st percentile**	**99th percentile**
B1 (awake and unfamiliar)(*)	10 minutes	20 minutes
Ciii (sleeping and unfamiliar)	21 minutes	41 minutes

Pre-evacuation time is typically modelled using a log-normal distribution (Purser and Bensilum 2001). This approach is based on the observation that factors such as social influence and delayed responses can affect pre-evacuation intervals (Nilsson and Johansson 2009), resulting in a non-symmetrical distribution. Unlike the normal distribution, which may not accurately capture these complexities, the log-normal distribution provides a more realistic representation of Pre-evacuation times (Ronchi and La Mendola, 2016). An alternative approach could involve the use of asymmetrically truncated normal distributions; however, this may not be necessary in the present context.

3.5. Group movement

Family members will evacuate in predefined 'movement groups', each led by a designated leader (either male or female). This approach can significantly increase the total evacuation time, as family members must first locate their leader before proceeding to the assembly point. Consequently, the 'movement group' mode generally results in longer evacuation times. In the 'movement group' mode, each family member adheres to their individual pre-evacuation times. This means that every person waits for their designated pre-evacuation interval before starting to move, even if they are with other family members. This requirement to respect individual pre-evacuation times contributes to longer evacuation durations, as it introduces additional delays in the process.

3.6. Waiting times

Once family members have regrouped, they proceed together to the assembly points and wait for 2 to 5 minutes to receive instructions. The waiting time at the assembly points is expected to vary among individuals due to factors such as the language of the instructions, the speed of comprehension, and potential congestion at the meeting point. After receiving instructions, the family members return to their accommodations to retrieve their belongings. They are expected to wait between 3 to 6 minutes, as suggested by Shi et al. 2009, before exiting the campsite either on foot (at Le Bois de Pins) or by car (at Le Bois Fleuri). Both the waiting times at the assembly points and the times spent at the accommodations are modelled using a normal distribution.

3.7. Evacuation modelling scenarios

To conduct a thorough and comprehensive analysis of evacuation events for both campsites, a range of scenarios has been proposed. These scenarios are designed to capture various occupant's conditions states (awake or asleep) and the potential for emergency exits to be blocked (Table 8).

Table 8 Evacuation modelling scenarios proposed for both campsites

Scenario	Campsite	Occupants	Condition	Location	Exits
LBP-A1	Le Bois de Pins	522 p	Awake	Randomly distributed	1 exit
LBP-A2	Le Bois de Pins	522 p	Awake	Randomly distributed	2 exits
LBP-S1	Le Bois de Pins	516 p	Sleeping	Within accommodations	1 exit
LBP-S2	Le Bois de Pins	516 p	Sleeping	Within accommodations	2 exits
LBF-A1	Le Bois Fleuri	1.981 p	Awake	Randomly distributed	1 exit
LBF-S1	Le Bois Fleuri	2.631 p	Sleeping	Within accommodations	1 exit

To account for the impact of behavioural uncertainty on results, 10 repeated simulations are conducted for each scenario (Ronchi et al 2014). Each simulation varies randomly in terms of occupant positions, pre-evacuation times, speeds, and diameters. While more detailed quantitative assessments of the impact of stochastic variables on results are available on the literature (e.g. based on functional analysis or confidence intervals) this approach was deemed sufficient in this case to account for variability and uncertainty in mode inputs (Grandison 2020, Smedberg et al. 2021). .

4. SUMO modelling features

4.1. Overview of the model

"Simulation of Urban MObility" (SUMO) is an open-source, microscopic, multi-modal traffic simulation software (Alvarez López et al 2018). SUMO provides a detailed simulation environment where individual vehicles, each with its own specific route and characteristics, navigate through a predefined road network. This level of detail makes SUMO a powerful tool for analysing and addressing a wide range of traffic management topics.

One of SUMO's standout features is its multi-modal simulation capability. The software supports a variety of transportation modes, including private cars, public transport vehicles, bicycles, and pedestrians. This allows users to create realistic simulations of urban environments where different modes of transportation coexist and interact. For instance, SUMO can model scenarios where buses share roads with cars and cyclists, or where pedestrians navigate through busy intersections.

SUMO's primary feature is its microscopic nature, meaning that every vehicle is modelled explicitly and moves independently through the network. This allows for a high degree of precision in simulating traffic flow and vehicle interactions. Each vehicle in the simulation can have unique properties such as speed, acceleration, and route, reflecting real-world diversity in traffic.

4.2. Building traffic simulations

SUMO relies on two main files to initiate simulations, ensuring a comprehensive and detailed representation of traffic scenarios. The first file, known as the routes file, serves a dual purpose. Primarily, it defines the traffic demand by specifying the routes that vehicles will take within the simulated network. This involves detailing the paths each vehicle will follow from its origin to its destination, capturing the flow of traffic through various segments of the network. The routes file also includes precise departure times for each vehicle, ensuring an accurate temporal distribution of traffic within the simulation. Additionally, the routes file includes extensive details about the characteristics of the vehicles involved. Each vehicle is described with attributes such as its type (i.e., car, bus, truck, bicycle), which influences its behaviour and interaction with the network. The file specifies acceleration and deceleration capabilities, which are critical for modelling realistic vehicle dynamics. Vehicle length is another important parameter, affecting lane-changing behaviour and space occupation on the road. Maximum speed settings for each vehicle type are also included, reflecting the diversity in vehicle performance and regulatory constraints.

The second essential file is the network file (net-file), which represents the network topology. This file provides a detailed and precise illustration of the spatial layout of the simulated environment. It includes information about the roads, specifying attributes such as length, width, number of lanes, and lane connections. Intersections are detailed with their geometries and control mechanisms, such as traffic lights and stop signs. The net-file also defines lane attributes, including lane types (i.e., regular, bus lane, bicycle

lane), speed limits, and allowed turning manoeuvres. Traffic lights are modelled with their signal phases and timing, enabling the simulation of various traffic signal strategies.

4.3. Car-following model

The car-following model is a crucial component in traffic simulation, defining the speed of a vehicle based on the behaviour of the vehicle ahead (Song et al., 2014). This relationship between vehicles is vital as it demonstrates how individual vehicle speeds influence overall traffic flow and can significantly impact critical scenarios such as evacuation times.

The primary car-following model used in SUMO is the Krauß model (Krauß 1998), which is designed to determine the maximum speed a vehicle can travel while ensuring it can stop safely without colliding with the vehicle ahead. This calculated speed is referred to as the safe velocity. The Krauß model is deterministic, meaning that it provides consistent results given the same initial conditions.

The car-following behaviour modelled in SUMO is influenced by a variety of factors. Individual characteristics such as age, gender, risk-taking propensity, and driving skills play a significant role. Additionally, situational factors such as the time of day, road conditions, impairment due to alcohol or fatigue, the purpose of the trip, and the length of the drive also affect how a driver behaves on the road (Ranney, 1999). This level of detail is essential for accurately studying and predicting traffic patterns, assessing the impact of different traffic management strategies, and planning for emergency evacuations.

4.4. Vehicles characteristics

4.4.1.Size and speed

The following table summarizes the main features of the vehicles defined within the traffic modelling simulations, with parameters that are set up by default in the model.

Table 9 Main characteristics of the vehicles modelled within the traffic modelling simulations.

Vehicle	Length x Width x Height	Acceleration	Deceleration	Max. speed
Bicycle	1,6 m x 0,65 m x 1,7 m	1,2 m/s^2	3 m/s^2	50 km/h
Motorcycle	2,2 m x 0,9 m x 1,5 m	6 m/s^2	10 m/s^2	200 km/h
Car	5 m x 1,8 m x 1,5 m	2,6 m/s^2	4,5 m/s^2	200 km/h
Truck	7,1 m x 2,4 m x 2,4 m	1,3 m/s^2	4 m/s^2	130 km/h
Bus	12 m x 2,5 m x 3,4 m	1,2 m/s^2	4 m/s^2	85 km/h
Caravanes(*)	12 m x 1,8 m x 1,5 m	1,3 m/s^2	4,25 m/s^2	165 km/h

(*) Values between those for cars and trucks were used for caravans, as their specifications were not provided in the predefined ones.

For all vehicles, a minimum headway gap of 2,5 meters is maintained as proposed by default in SUMO. This gap ensures that vehicles do not get too close to each other, preventing collisions. If the gap between any two vehicles is reduced below this minimum threshold, a collision is registered. This behaviour is used to detect issues with

the default car-following model, which is designed to never reduce the gap below the minimum value.

Although the attribute maximum speed indicated the maximum speed that a vehicle will travel, the speed-attribute is usually defined for edges but may also differ among the lanes of the same edge. When approaching an edge with a lower speed limit than the current one, a vehicle will slow down so as to stay within the new limit at the time of reaching the new edge. This ensures that vehicles adhere to speed regulations and maintain safe driving practices throughout the simulation.

4.4.2.Intersections

Vehicles approaching an intersection without the right-of-way are required to slow down. If the intersection is occupied by other vehicles with the right-of-way, stopping may be necessary until a safe time window is available. This time window is determined based on the same safety assumptions as the car-following model. Even if a vehicle has the right-of-way, it may need to reduce its speed to accommodate impatient drivers who might cross the intersection unexpectedly. The right-of-way rules at an intersection are defined by the node type attribute and by the traffic lights.

If a vehicle has not yet entered the intersection, it will generally slowdown in response to any vehicles already present in the intersection, unless there is an unobstructed waiting area within the intersection (an internal junction) where it can safely move. When two vehicles are in conflict within the intersection at the same time, a priority order is established based on their entry times, speeds, right-of-way rules, and the state of any traffic lights. This priority order determines which vehicle must yield and which vehicle can proceed without delay.

By default, a vehicle approaching from a minor road will slow down until it is 4,5 m away from the intersection, even if no prioritized vehicles are nearby. Once within this distance, the vehicle may start to accelerate again if a safe gap in traffic is available.

4.5. Road network

The road network of the campsite area has been extracted using OsmWebWizard, a tool that utilizes the open-source geographic dataset from OpenStreetMap (OSM). This tool allows for the automatic creation of traffic demand by specifying the number and types of vehicles involved. This background traffic, which flows through the road network during the simulation, can impact evacuation times by potentially causing congestion, thus its inclusion is a conservative assumption in case of evacuation scenarios.

The traffic demand, including the entrances and destinations, is randomly generated by the OSM tool based on the predefined vehicle types and quantities. This ensures a realistic simulation of traffic conditions, reflecting the possible effects on the evacuation process.

The figure below illustrates the OSM map used for the road network surrounding the Le Bois Fleuri campsite. The traffic assignment zone (TAZ) proposed arbitrarily in this study

is located near the beach, highlighted as a designated safety destination for vehicles exiting the campsite (the actual TAZ for Bois Fleuri is Espace Jean Carrère in Argelès). This zone is intended to manage traffic flow efficiently and ensure a safe evacuation route for visitors.

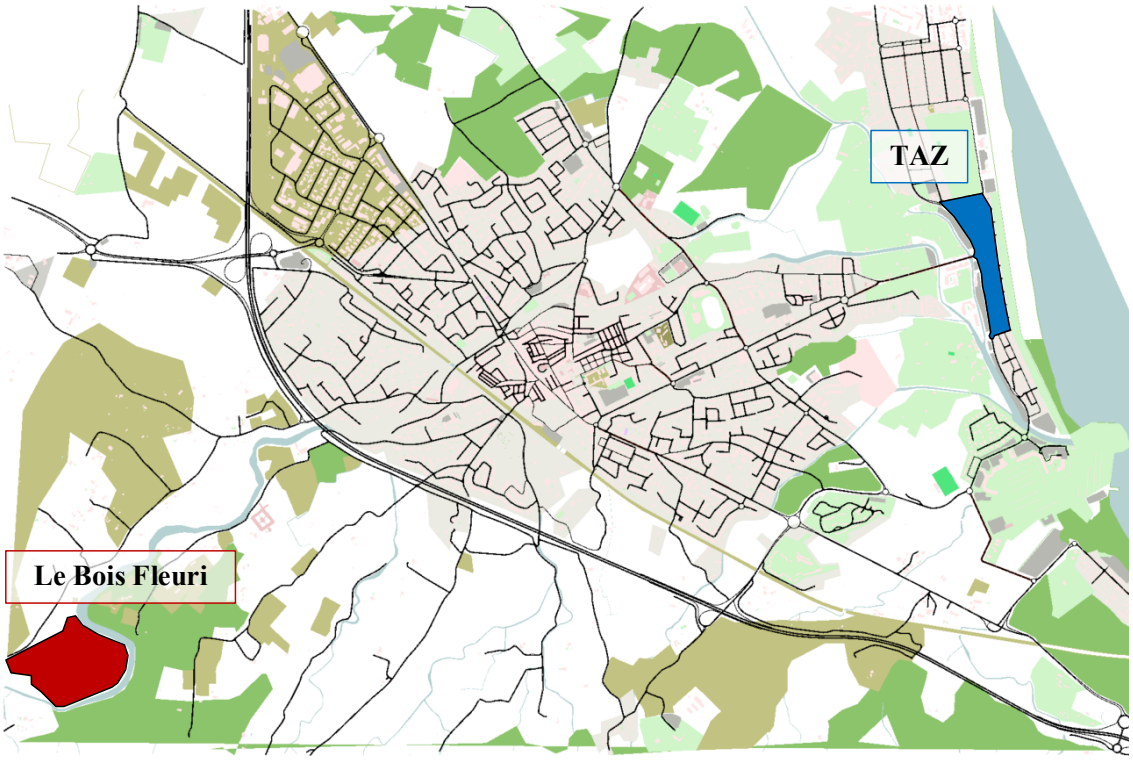

Figure 10 Road network model built in SUMO representing the surroundings of Le Bois Fleuri campsite.

4.6. Traffic modelling scenarios

In addition to crowd movement, traffic vehicle modelling is also a key component of the analysis for Le Bois Fleuri campsite. The following table presents traffic count data for the main routes in the area of interest, between the campsite and the TAZ.

Table 10 Traffic count data of the main routes of the area of interest

Route information	Reference	Annual average	Summer average
D914 (2019)	Data 2024	21.520 vehicles/day	33.601 vehicles/day
D914 (2021)	Data 2024	11.948 vehicles/day	18.256 vehicles/day
A9 (Perpignan-Le Boulou)	Data 2024	36.284 vehicles/day	n.a.
A9 (Perpignan-Le Boulou)	Data 2024a	36.426 vehicles/day	n.a.
A9 (Narbonne-Leucate)	Data 2024a	52.700 vehicles/day	n.a.
D618	Data 2024	13. 000 vehicles/day	19.000 vehicles/day

Due to the challenges in defining reliable data for background traffic during the evacuation event, different traffic modelling scenarios are proposed with varying numbers of vehicles in circulation, ranging from zero to a maximum of 14,514 vehicles (Table 11). All scenarios have been evaluated for awake occupants, while the first three

were specifically assessed for sleeping occupants, during which the number of vehicles is significantly reduced at night.

Table 11 Traffic modelling scenarios proposed for Le Bois Fleuri campsites.

Scenario	Cars	Trucks	Bus	Motorcycles	Bicycles	Total
0	0	0	0	0	0	0 vehicles
1	416	430	431	444	0	1.721 vehicles
2	877	442	879	450	386	3.034 vehicles
3	3.517	442	879	1.804	386	7.028 vehicles
4	5.281	442	1.770	2.703	386	10.582 vehicles
5	7.040	442	2.657	3.604	771	14.514 vehicles

The following figure shows the number of vehicles inserted in the model for the different traffic scenarios proposed during 2 h-duration (120 minutes). This figure, along with the previous table, does not account for the 356 and 465 campsite vehicles that must reach the TAZ point for the awake and sleeping scenarios, respectively.

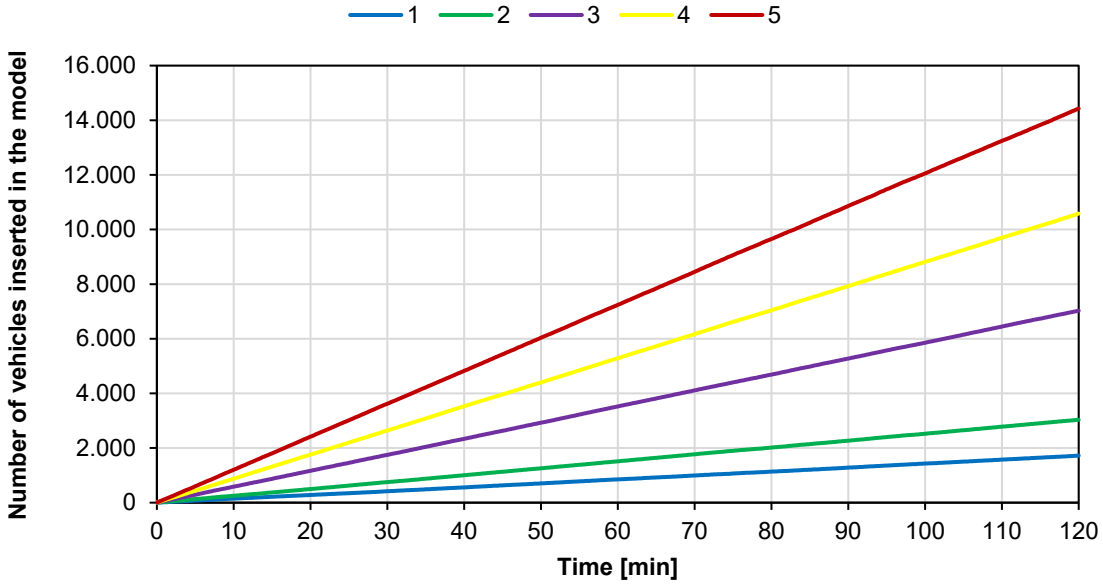

Figure 11 Number of vehicles inserted in the different traffic scenarios of Le Bois Fleuri.

The arbitrary assumptions for traffic counts used here (for all roads between the Le Bois Fleuri campsite and TAZ) fall within the lower range of traffic volumes observed on individual roads in the region (such as the D618 and D914). Additionally, these assumptions do not account for traffic on smaller roads in Argeles-Village and Argeles-Plage. Future work should incorporate more realistic traffic congestion data.

For simplicity, it is assumed that vehicles begin evacuating the campsite 5 minutes after the occupants reach their vehicle location, whether it is in the campsite parking area or at their own plots. Additionally, it is assumed that one-third of the tourists at Le Bois Fleuri use caravans as their primary mode of transportation for exiting the campsite, while the remaining two-thirds use cars.

5. Results and discussion

5.1. Summary of the input and output data

This chapter reveals the main results of the evacuation simulations performed in the two French campsites. Following table summarizes the main features and input data used in the Pathfinder simulations for both campsites.

Table 12 Features and input data used in Pathfinder simulations

Input data	**Le Bois de Pins**	**Le Bois Fleuri**
Surface and topography	40.000 m^2 (relatively flat)	150.000 m^2 (relatively flat)
Number of unit and maximum capacity	100 units (512 p)	467 units (2.631 p)
Number assembly points	1 point in the main exit	
Number of exits	2 exits	1 exit
Evacuation mode	On foot	By car
Profiles: diameter & speed	• Male: 0,5 - 0,58 m & 1,15 - 1,55 m/s • Female: 0,44 - 0,52 m & 0,95 - 1,35 m/s • Child: 0,39 - 0,45 m & 0,6 - 1,2 m/s • Elderly: 0,46 - 0,54 m & 0,5 - 1,1 m/s • PMR: 0,44 - 0,58 m & 0,43 - 1,17 m/s • Wheelchair: 1,32 m x 0,76 m & 0,44 - 1,22 m/s	
Speed reduction factor	• Daytime: 25% • Nighttime: 35%	• Daytime: 35% • Nighttime: 45%
Distribution of profiles according to accommodation capacity	• 2 people: 1 male + 1 female • 4 people: 1 male + 1 female + 2 child • 5 people: 1 male + 1 female + 3 child • 6 people: 1 male + 1 female + 1 elderly + 3 child	
Number of occupants modelled	• Daytime: 522 p • Nighttime: 516 p	• Daytime: 1.981 p • Nighttime: 2.639 p
Pre-evacuation time	• Daytime: between 10 and 20 minutes • Nighttime: between 21 and 41 minutes	
Waiting time	• Assembly point: 2 to 5 minutes • Accommodations: 3 to 6 minutes	

The following table presents the main output data obtained from the Pathfinder simulations of both campsites.

Table 13 Output data obtained from Pathfinder simulations

Output data	**Description**
Evolution of the number of occupants	This data shows how the number of people changes over time within the simulation environment.
Evacuation times and travel distances	These metrics provide information on how long it takes for occupants to evacuate from different locations within the environment and the distance they travel to reach a safe exit.
Cumulative space utilization maps	These maps visually represent how different areas within the environment are used over the duration of the simulation.
Cumulative high-density maps	These maps visually represent the accumulated density within the environment over the duration of the simulation.

For the Le Bois Fleuri campsite, where evacuation is carried out by car, traffic simulations were conducted using SUMO. The main input data for these simulations are presented in the following table:

Table 14 Features and input data used in SUMO simulations

Input data	**Le Bois Fleuri**
Road network	Map and network created from the OSM Web Wizard tool covering from the campsite to Argeles-Plage beach.
Vehicle fleet with number of each category	• Scenario 0: 0 vehicles • Scenario 1: 1.721 vehicles (416 cars; 430 trucks; 431 buses; 444 motorcycles; 0 bicycles) • Scenario 2: 3.034 vehicles (877 cars; 442 trucks; 879 buses; 450 motorcycles; 386 bicycles) • Scenario 3: 7.028 vehicles (3.517 cars; 442 trucks; 879 buses; 1.804 motorcycles; 386 bicycles) • Scenario 4: 10.582 vehicles (5.281 cars; 442 trucks; 1.770 buses; 2.703 motorcycles; 386 bicycles) • Scenario 5: 14.514 vehicles (7.040 cars; 442 trucks; 2.657 buses; 3.604 motorcycles; 771 bicycles)
Characteristics of each vehicle (surface; acceleration; deceleration and max. speed)	• Bicycle: 1,6 m x 0,65 m; 1,2 m^2/s; 3 m/s^2; 50 km/h • Motorcycle: 2,2 m x 0,9 m; 6 m^2/s; 10 m/s^2; 200 km/h • Car: 5 m x 1,8 m; 2,6 m^2/s; 4,5 m^2/s; 200 km/h • Truck: 7,1 m x 2,4 m; 1,3 m^2/s; 4 m^2/s; 130 km/h • Bus: 12 m x 2,5 m; 1,2 m^2/s; 4 m^2/s; 85 km/h • Caravanes: 12 m x 1,8 m; 1,3 m^2/s; 4,25 m^2/s; 165 km/h
Start and end point	From the campsite to Argeles-Plage beach

The following table presents the main output data obtained from the SUMO simulations performed with a different number of vehicles.

Table 15 Output data obtained from SUMO simulations

Output data	**Description**
Evolution of the number of vehicles.	This data shows how the number of vehicles changes over time within the simulation environment.
Maximum arrival times for campsite vehicles	These metrics provide information on the total time required to complete the evacuation form the moment the event begins.
Mean trip duration for campsite vehicles	These metrics provide information on how long it takes for the campsite set of vehicles modelled to achieve their destination.

The results presented reflect the mean values derived from 10 crowd modelling simulations performed in Pathfinder for each scenario and those of traffic modelling performed with SUMO.

5.2. Le Bois de Pins

5.2.1. Evolution of the number of occupants

Following figure shows the evolution of the mean number of occupants as they evacuate the campsites for the different scenarios modelled (the acronyms A and S in the legend represent the ‘awake’ and ‘sleeping’ scenarios, respectively).

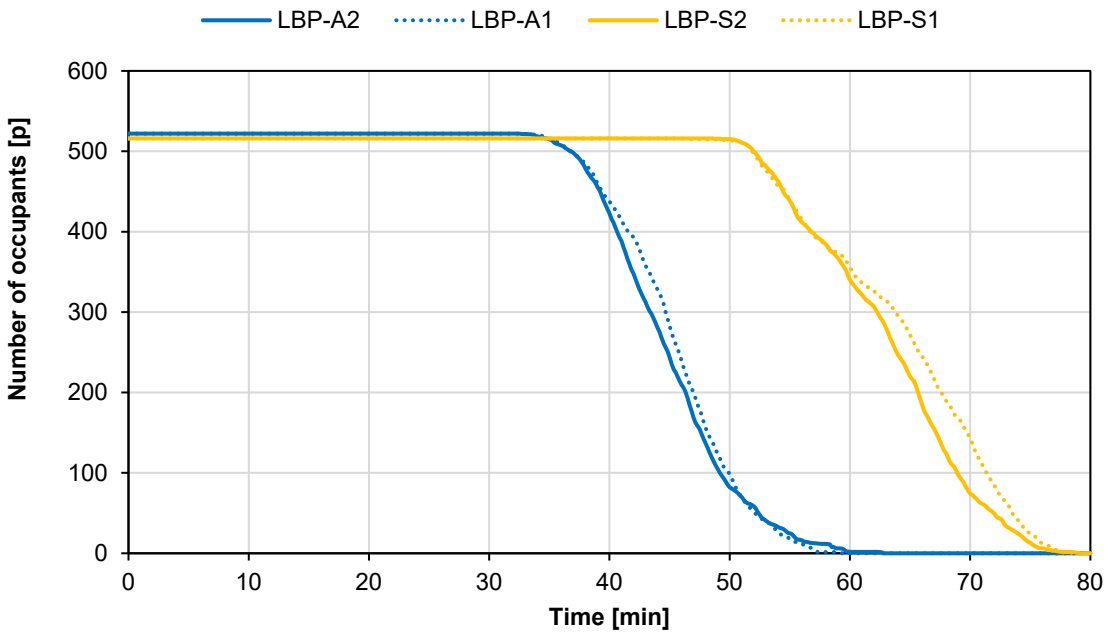

Figure 12 Le Bois de Pins (LBP). Mean evolution of the number of occupants.

As observed, the availability of an additional exit has a negligible impact on the occupant's evolution; nevertheless, if the exits would have been in completely different locations widely separated, its availability could have accelerated the occupant's evacuation event.

The main differences between both scenarios (awake and sleeping occupants) are mainly due to the longer pre-evacuation times, hence revealing that it is a key time component in the whole evacuation event. In a lesser extent, this difference is also due to a reduction in movement speed.

The following figure reveals the mean flow of occupants leaving the campsite, derived from the mean evolution of the number of occupants. For awake occupants, this flow rapidly increases until it reaches its maximum (0,6 p/s), then starts to decline as the number of occupants is reduced by more than 2/3. In contrast, for sleeping occupants, a lower maximum flow rate is achieved (0,4 p/s), primarily due to the wider range of the 1st and 99th percentile pre-evacuation times (from 21 to 41 minutes).

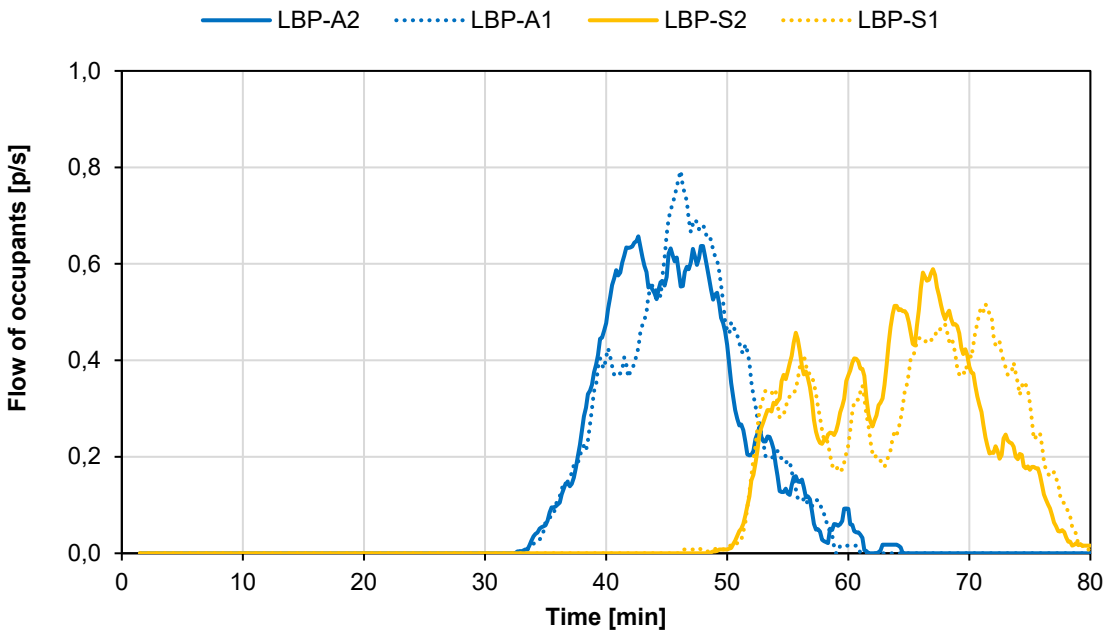

Figure 13 Le Bois de Pins (LBP). Mean flow of occupants leaving the campsite.

5.2.2. Evacuation times and travel distances

Following table shows the main mean times and travel distances of the scenarios modelled. The standard deviation of each value is shown in parentheses.

Table 16 Le Bois de Pins (LBP). Mean evacuation times and travel distances

	Mean travel distances	**Mean active time**	**Mean finish time**	**Maximum evacuation time**
LBP-A1	511 m (± 2 min)	21,2 min (± 0,2 min)	45,5 min (± 0,2 min)	56,6 min (± 1,3 min)
LBP-A2	549 m (± 5 min)	20,6 min (± 0,8 min)	44,9 min (± 0,8 min)	57,9 min (± 2,5 min)
LBP-S1	413 m (± 1 min)	25,1 min (± 0,4 min)	64,3 min (± 0,4 min)	77 min (± 0,9 min)
LBP-S2	447 m (± 1 min)	23,9 min (± 0,3 min)	63,1 min (± 0,3 min)	76,3 min (± 1,5 min)

The maximum evacuation times correspond to the evolution of the number of occupants plotted in Figure 12. As previously discussed, (i) there is a negligible difference between scenarios with different number of exits, and (ii) the maximum evacuation times between scenarios (awake and sleeping occupants), which is of approximately 20 minutes, is due to the delayed pre-evacuation times. Regardless of the number of exits available, it could be stated that the last occupant will need a mean time of 60 and 80 minutes to leave the campsite for awake and sleeping scenarios, respectively.

The travel distances are approximately 100 m larger for awake scenarios as the occupants must regroup before initiating the evacuation event. Then, scenarios with an additional exit are featured with longer travel distances, possibly because family groups could use an exit located far from their accommodations if the main exit is densely

occupied. The maximum evacuation times are very similar between awake and sleeping scenarios, indicating that travel distances are not the most significant factor in the overall evacuation time. The mean finish time indicates the time at which the last occupant left the campsite. It is composed by the waiting and pre-evacuation times, as well as the active time, which indicates the amount of time the occupant was actively seeking a location in the model.

Following graph shows the percentage of the different times composing the mean finish time. The predominant factors, compromising approximately 50%, are the active and pre-evacuation times for both awake and sleeping scenarios. This highlights that awake occupants spend a considerable amount of time regrouping, while sleeping ones require half of their time to initiating the evacuation event.

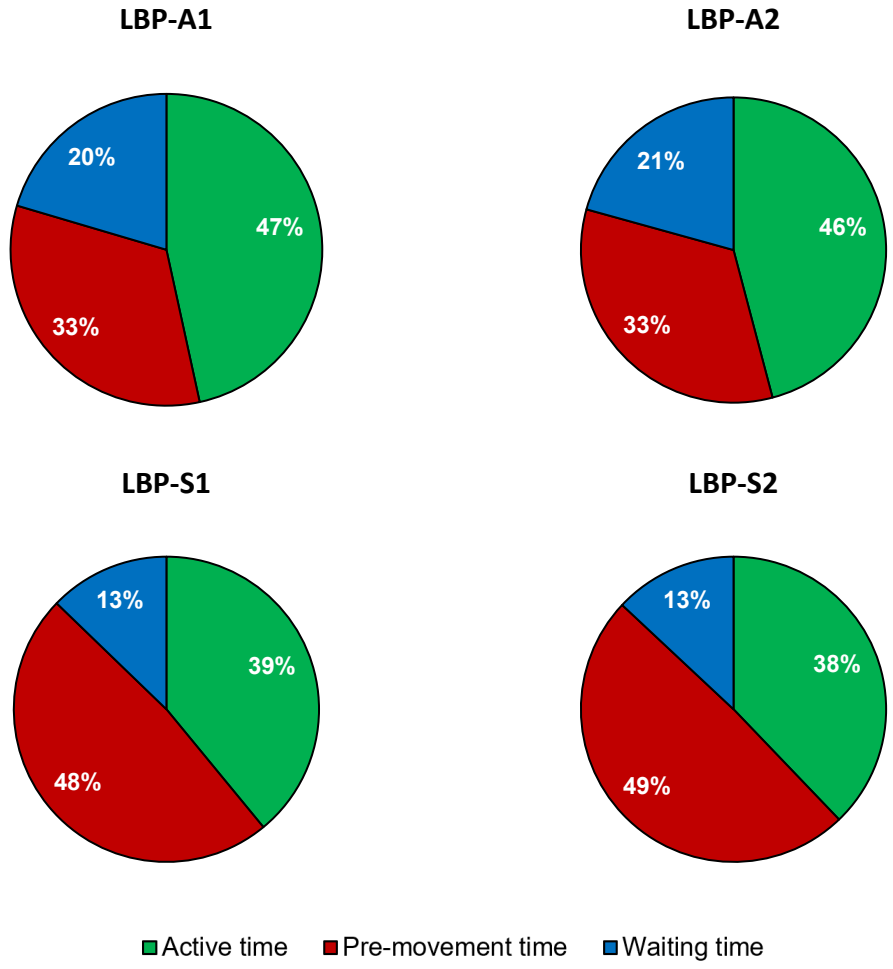

Figure 14 Le Bois de Pins (LBP). Mean times composing the finish time

5.2.3.Cumulative space utilisation maps

Figure 15 and Figure 16 display accumulated space utilization maps, graphically revealing how circulation routes are used by occupants during the simulated time. Although there is no set maximum permissible usage time for circulation spaces, a reference threshold of 10 minutes has been defined for comparison purposes.

The most noticeable differences for awake scenarios are observed in the usage of the additional exit area. Apart from the assembly point, which exceeds the 10 minutes-time as expected, the rest of the circulation routes are used for less than 8 minutes in both awake scenarios. The routes leading to the assembly points are the densest ones.

Although the occupants are directly located within their accommodation and not using various campsite areas (i.e. swimming pool, playground, restaurant, etc.), similar results in terms of accumulated space utilisation are found for sleeping scenarios. There is, however, a slight increase in the space used around the assembly points due to a higher number of occupants gathering there during the same period of time.

5.2.4.Cumulative high-density maps

Figure 17 and Figure 18 show cumulative high-density maps, intended to illustrate the densities registered in various areas of the campsite. Like the space utilisation maps, there is established maximum permissible density for circulations spaces; however, a reference threshold of 4 p/m^2 has been proposed for comparison purposes.

Both awake and sleeping scenarios exceed the 4 p/m² density threshold around the assembly point, with a slightly larger area affected in the sleeping scenarios. Apart from the assembly zone, the rest of the campsite areas do not exceed a density of 3 p/m², indicating that there is no significant difference in density concerning varying pre-evacuation times, available exits, and movement speeds. In addition, the regrouping of family members does not have a significant impact on the achieved density levels.

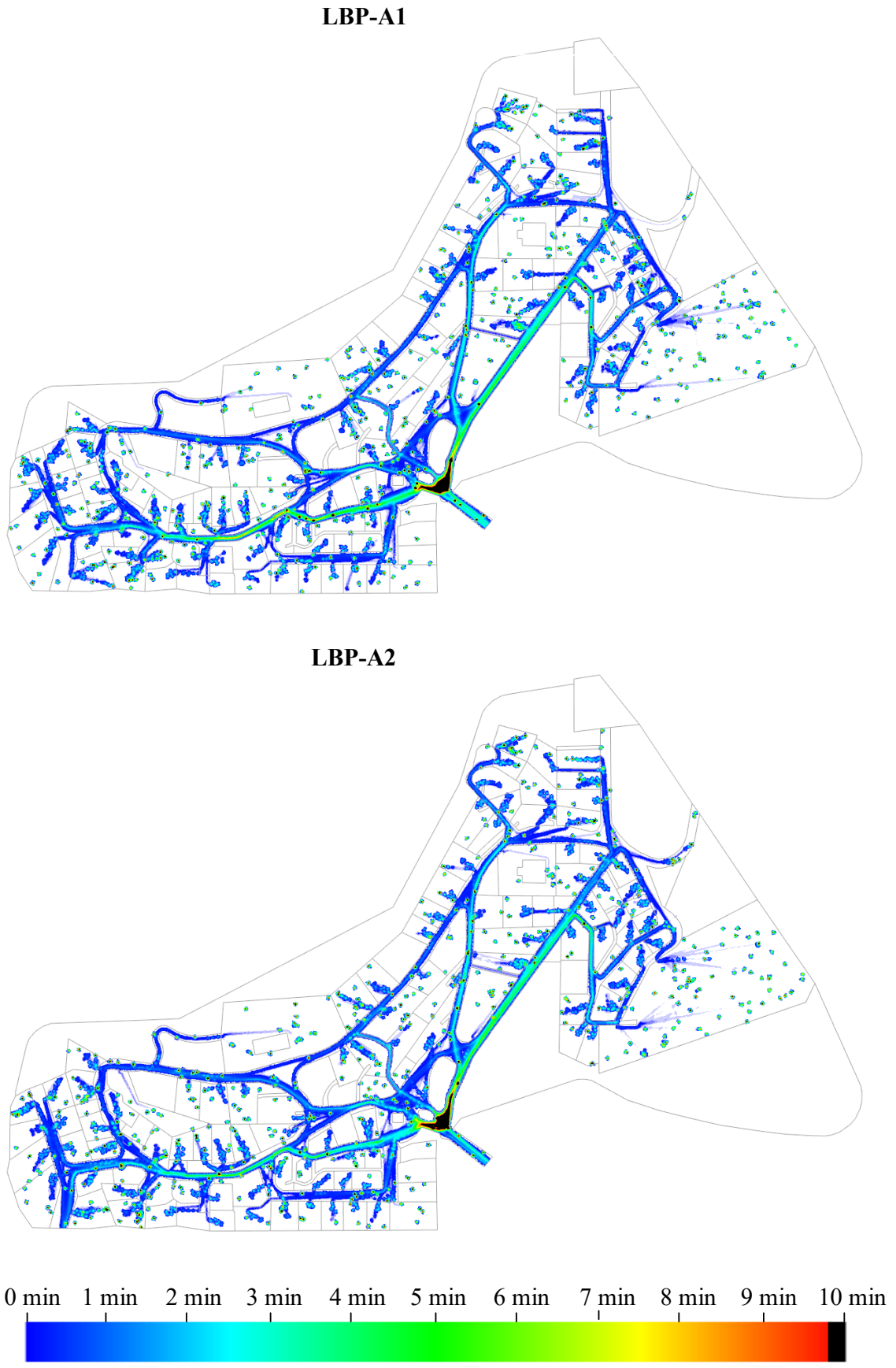

Figure 15 Le Bois de Pins (LBP). Cumulative space utilisation maps of awake scenarios

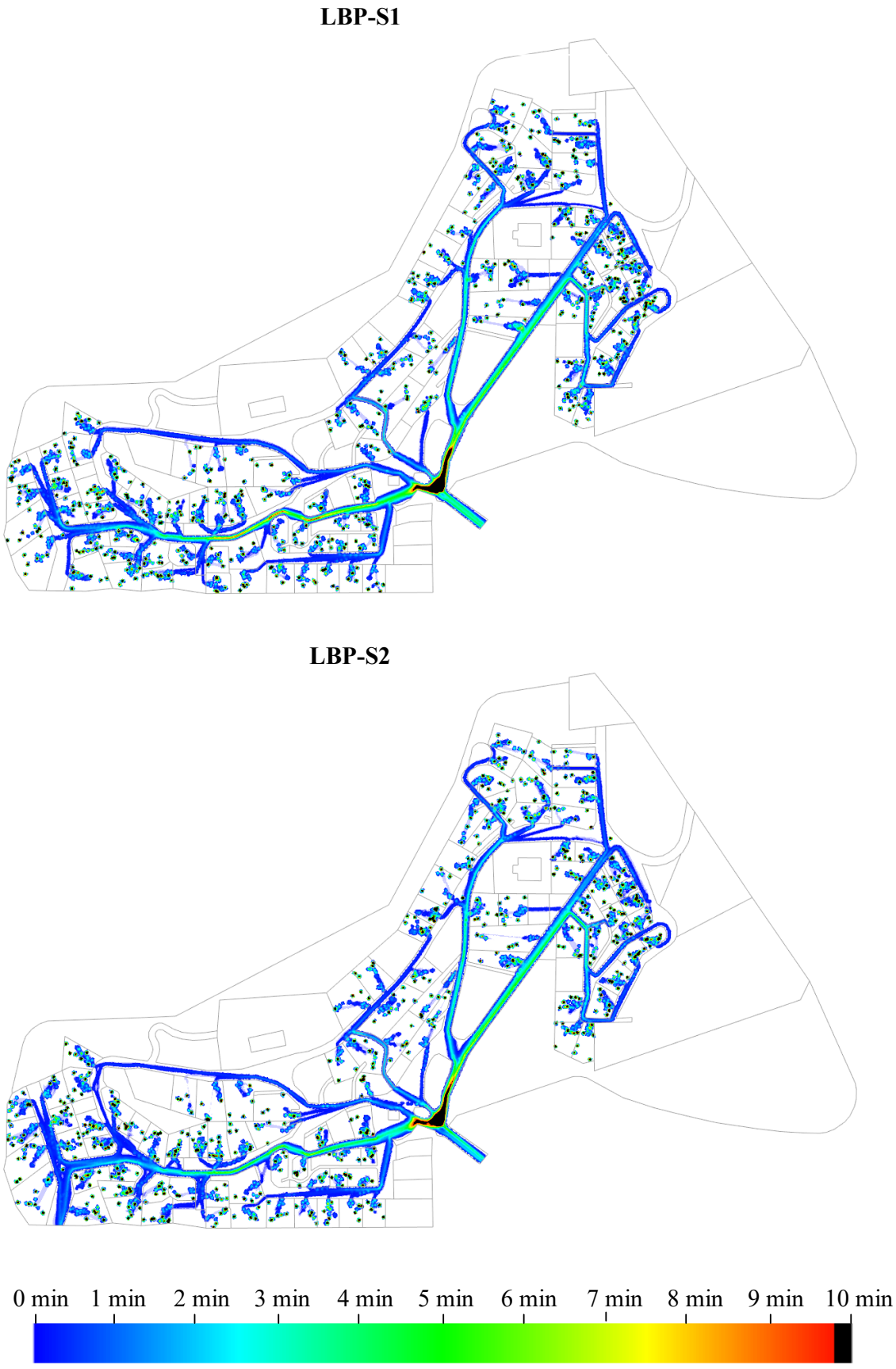

Figure 16 Le Bois de Pins (LBP). Cumulative space utilisation maps of sleeping scenarios

LBP-A1

LBP-A2

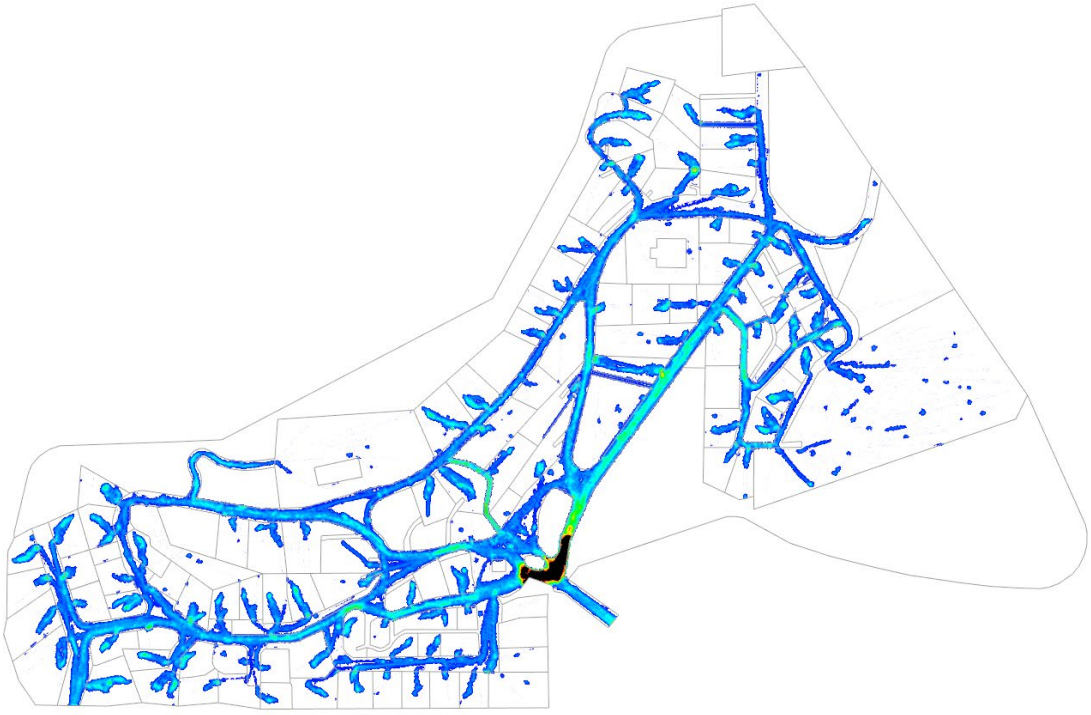

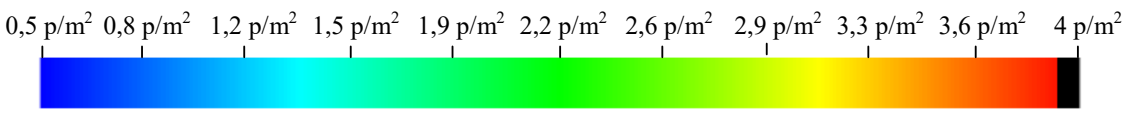

Figure 17 Le Bois de Pins (LBP). Maximum density maps of awake scenarios

LBP-S1

LBP-S2

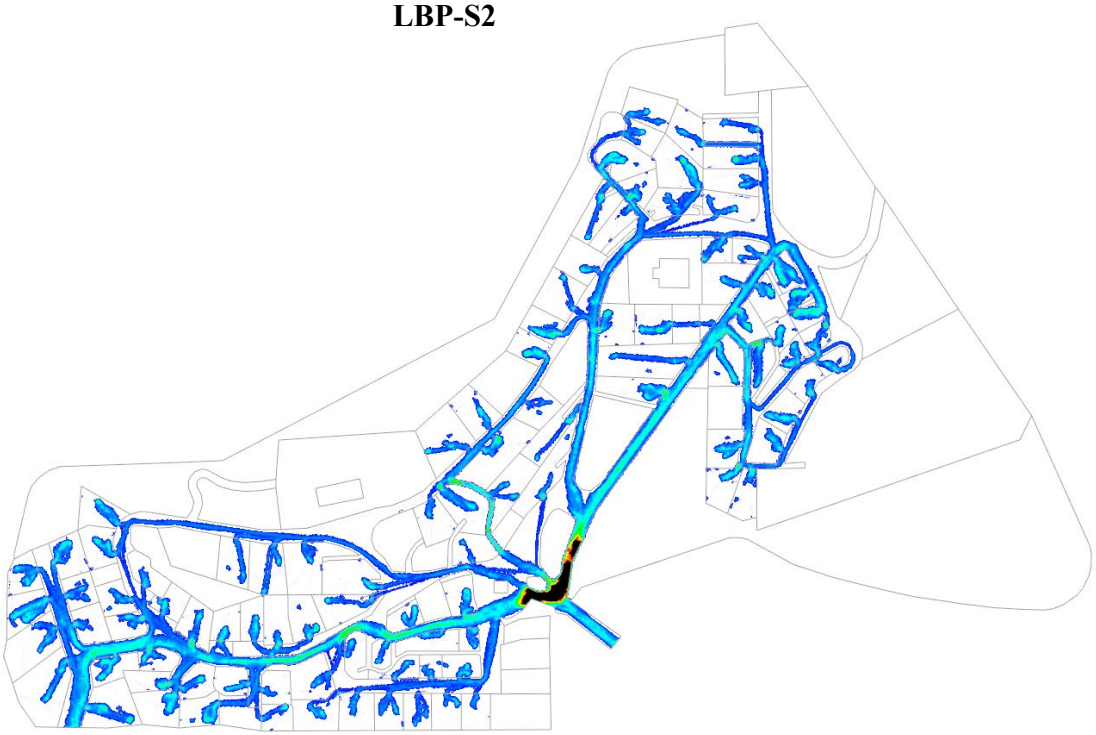

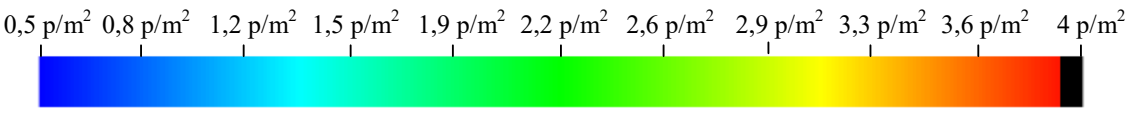

Figure 18 Le Bois de Pins (LBP). Maximum density maps of sleeping scenarios

5.3. Le Bois Fleuri

5.3.1. Evolution of the number of occupants

Figure 19 illustrates the evolution of the mean number of occupants at the Le Bois Fleuri campsite for both scenarios analysed (the acronyms A and S in the legend represent the 'awake' and 'sleeping' scenarios, respectively). When occupants are awake, the average time required for the last tourist to evacuate the campsite is approximately 88 minutes. In contrast, this evacuation time extends to around 118 minutes when the occupants are sleeping. While both curves exhibit a similar trend, the significant difference of approximately 30 minutes can be attributed to (i) the higher number of occupants present in the sleeping scenario and (ii) the longer pre-evacuation time defined for this scenario.

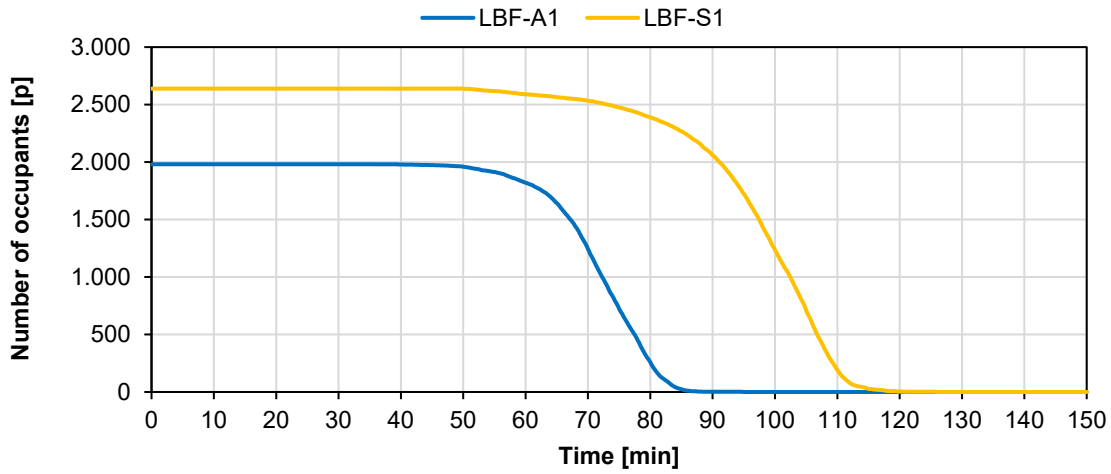

Figure 19 Le Bois Fleuri (LBF). Mean evolution of the number of occupants

Figure 20 shows the mean flow of occupants leaving the campsite. This flow rate increases until it reaches maximum values of 1,8 p/s for awake occupants and 2 p/s for sleeping occupants, after which it begins to decline as the number of remaining occupants decreases by more than 2/3. Despite the similarities in flow evolution between the two scenarios, the observed differences are primarily due to variations in the number of occupants and the pre-evacuation times.

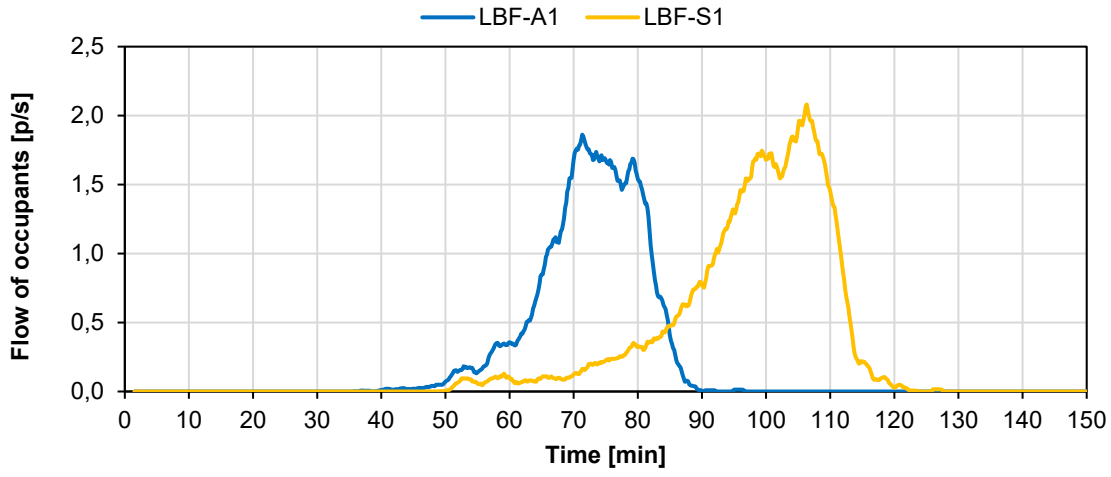

Figure 20 Le Bois Fleuri (LBF). Mean flow of occupants leaving the campsite

5.3.2. Evacuation times and travel distances

Following table shows the main mean times and travel distances of the scenarios modelled for Le Bois Fleuri campsite. The standard deviation of each value is shown in parentheses.

Table 17 Le Bois Fleuri (LBF). Mean evacuation times and travel distances

Scenario	Mean travel distances	Mean active time	Mean finish time	Maximum evacuation time
LBF-A1	858 m (± 7 m)	48,8 min (± 1,2 min)	71,7 min (± 1,2 min)	87,6 min (± 3,1 min)
LBF-S1	758 m (± 5 m)	57,6 m (± 1,6 min)	96,8 min (± 1,6 min)	117,7 min (± 3,9 min)

As with the Le Bois de Pins campsite, travel distances are approximately 100 meters longer for awake scenarios because occupants need to regroup before initiating the evacuation. Specifically, awake occupants cover an average distance of 858 meters, while sleeping occupants cover 758 meters to complete the evacuation.

The difference in mean active time, which reflects the time occupants spend actively searching for a location or waiting in the model, is approximately 10 minutes between scenarios. Considering that sleeping occupants do not need to regroup with their families - thereby significantly reducing their active time - it suggests that in certain areas near the assembly point, the routes become densely populated, which in turn impedes the occupant's movement and contributes to longer evacuation times. This occurs due to an increase in the number of people heading directly toward the sole assembly point, rising from 1.981 in awake scenarios to 2.631 in sleeping scenarios, without making use of other areas of the campsite to search for their relatives.

Additionally, the mean finish time, which indicates the time at which the last occupant leaves the campsite, differs by approximately 25 minutes between scenarios. This difference primarily arises from a 15-minute increase in the pre-evacuation time (rising from an average of 15 minutes to 30 minutes for both awake and sleeping occupants) and an additional 10 minutes due to the congestion in densely populated areas near the assembly point.

The following graph illustrates the percentage distribution of various time components that contribute to the mean finish time. In this context, active time is the predominant factor affecting the evacuation duration, likely due to the extensive evacuation routes of the campsite. In sleeping scenarios, the increased percentage is attributed to longer pre-evacuation times, as individuals wait before beginning their evacuation process.

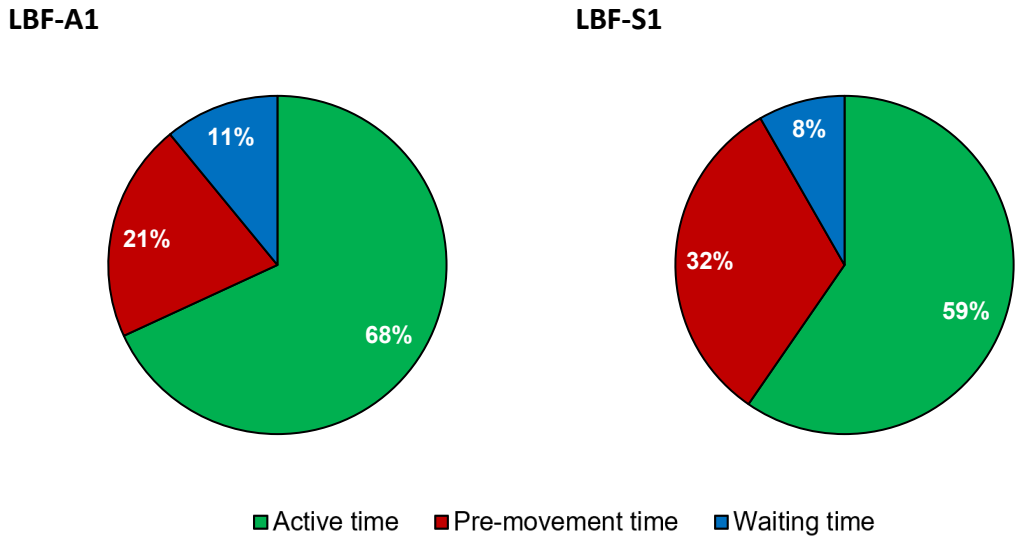

Figure 21 Le Bois Fleuri (LBF). Mean times composing the finish time

5.3.3. Cumulative space utilisation maps

Figure 22 below shows maps of accumulated space utilization, visually illustrating how circulation routes are utilized by occupants throughout the simulation period. While there is no fixed maximum allowable time for using circulation spaces, a reference threshold of 20 minutes has been established for comparison.

The most notable differences between awake and sleeping scenarios are observed in the usage of the main route leading to the assembly point. In the sleeping scenarios, this route is used more frequently compared to the awake scenarios. This increased usage is due to a higher number of occupants heading to the same assembly point during the same period.

In contrast, in the awake scenarios, occupants must first regroup by families, which can delay their movement to the assembly point and, at the very least, lead to greater dispersion among those heading there. In both scenarios, the time taken to reach the assembly point and the main entry route exceeds 20 minutes.

Another significant difference is that a larger area of the campsite is utilized in the awake scenarios, as the occupants are randomly distributed at the start of the simulation. This random distribution affects how different areas of the campsite are used throughout the evacuation process.

LBF-A1

LBF-S1

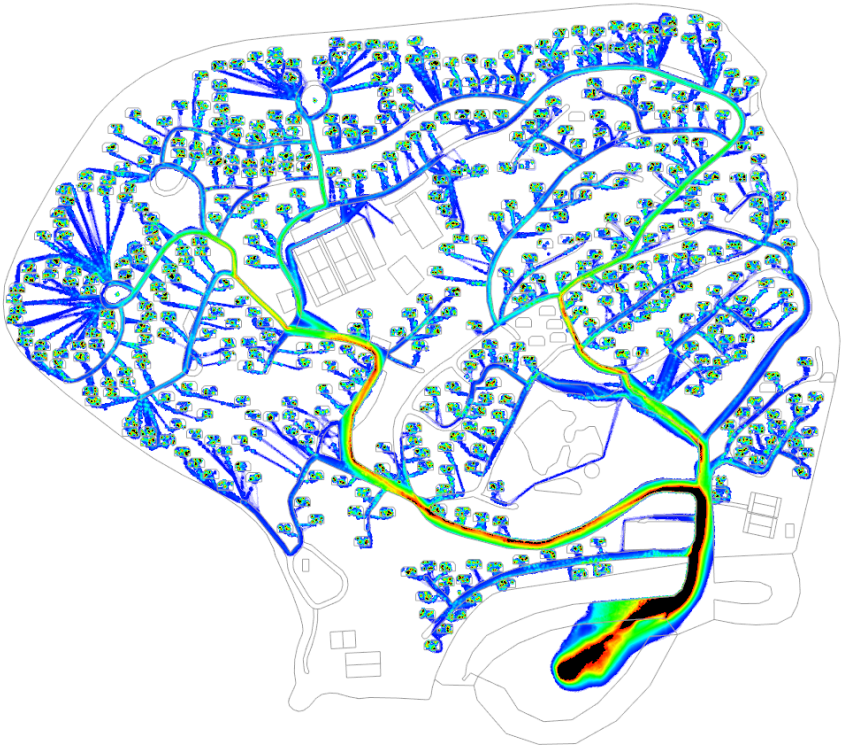

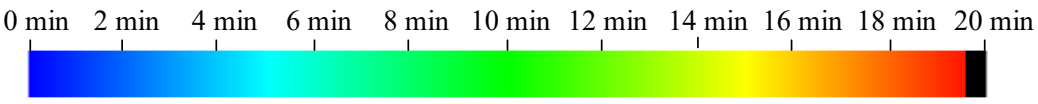

Figure 22 Le Bois Fleuri (LBF). Cumulative space utilisation maps

5.3.4.Cumulative high-density maps

Figure 23 presents cumulative high-density maps designed to depict the densities recorded in different areas of the campsite. Similar to the space utilization maps, a maximum permissible density has been set for circulation areas. For comparative purposes, a reference threshold of 4 p/m² has been suggested.

Both awake and sleeping scenarios exceed the 4 p/m² density threshold at the assembly point. Additionally, in the sleeping scenarios, this density threshold is surpassed along the entry routes leading to the assembly point, as well as in certain routes where the width is reduced.

These results, in conjunction with those from Le Bois de Pins, reveal that the greater dispersion of occupants in awake scenarios and the fact that they follow different routes to regroup by families facilitate a smoother flow of people on the more crowded routes, such as the main entry one and the assembly point. This improved distribution helps mitigate crowding and congestion, allowing for more efficient movement in these critical areas.

LBF-A1

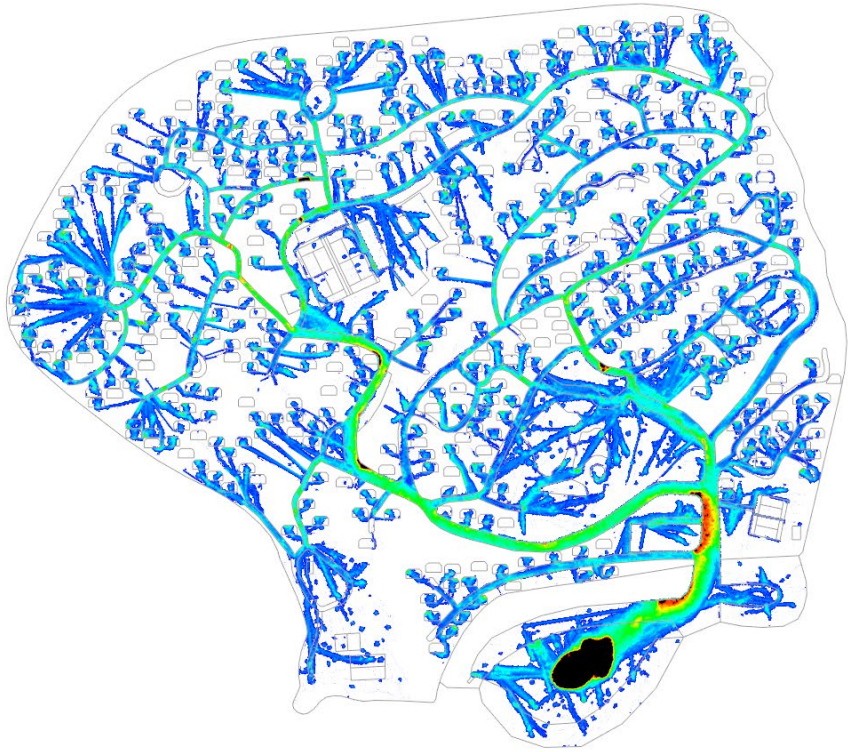

LBF-S1

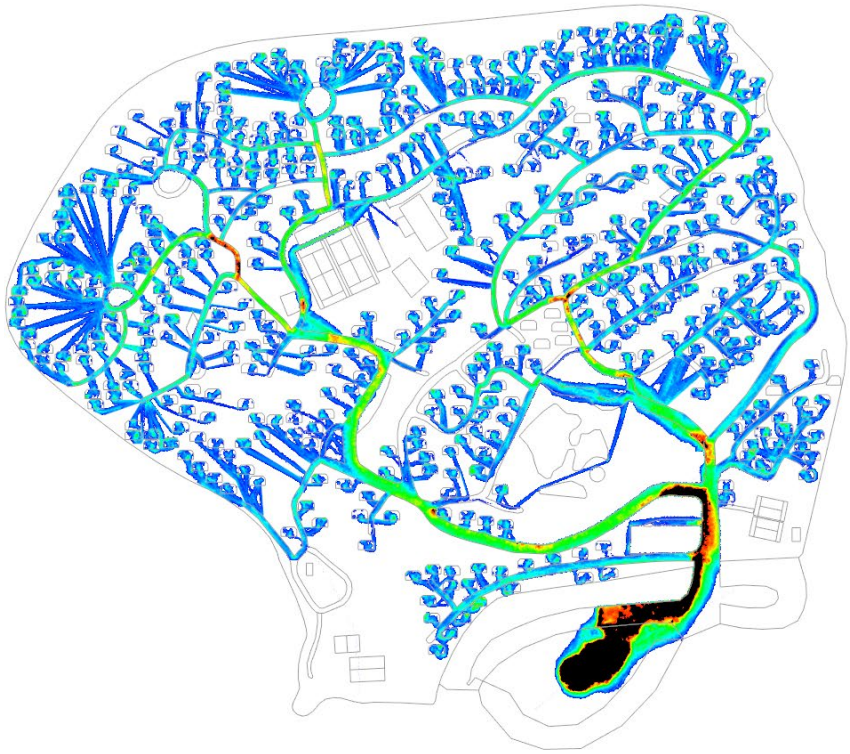

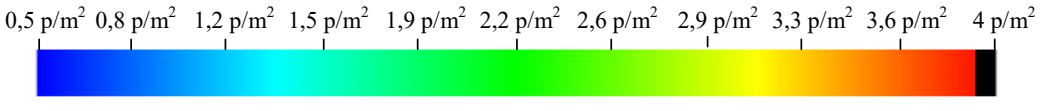

Figure 23 Le Bois Fleuri (LBF). Maximum high-density maps.

5.3.5. Evolution of the number of vehicles

Figure 24 reveals the flow of vehicles running in the model for awake and sleeping scenarios.

Awake scenario

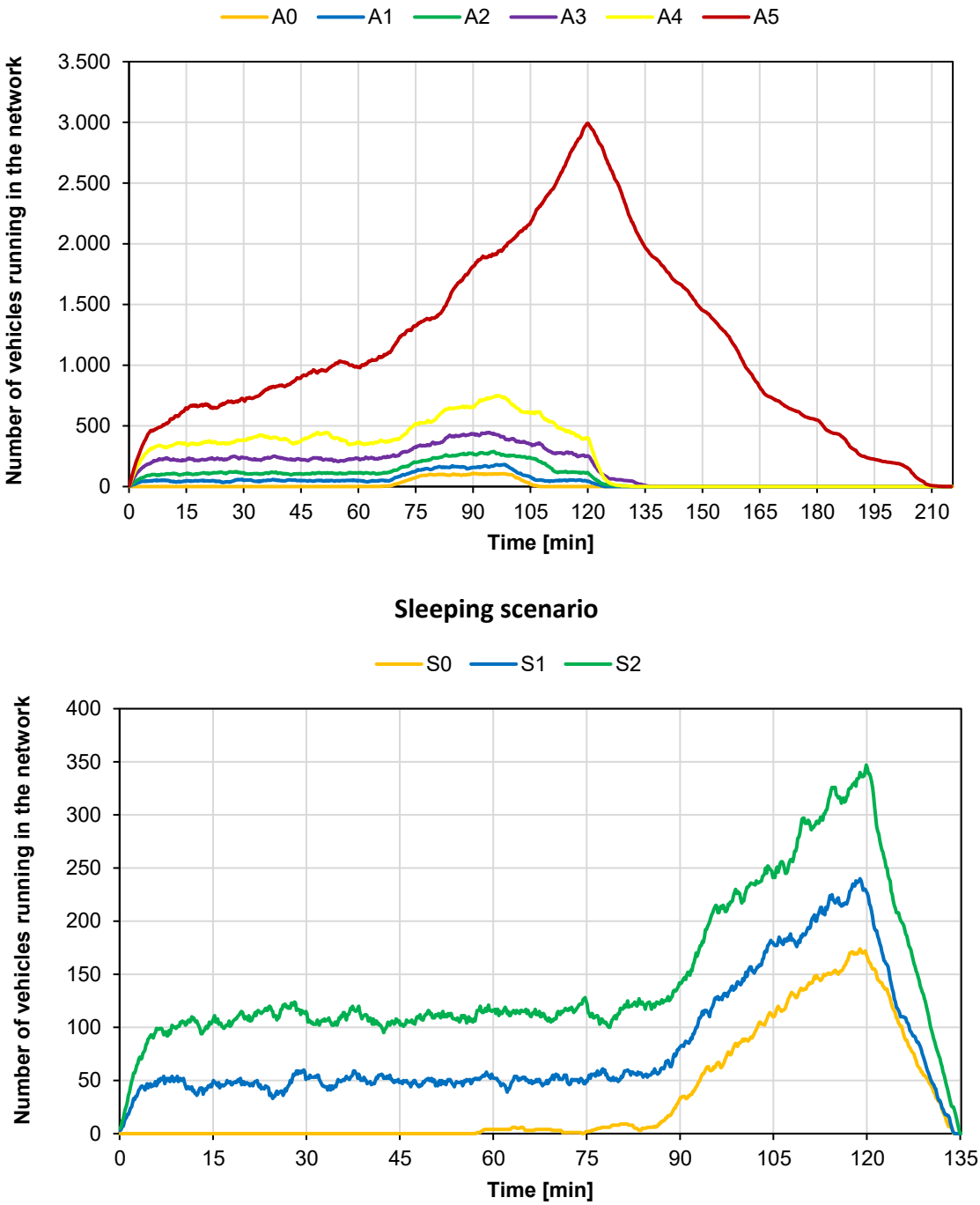

Figure 24 Le Bois Fleuri (LBF). Number of vehicles running in the network for awake (up) and sleeping (down) scenarios

In the awake scenario, the number of vehicles for scenarios A0 to A4 remains relatively constant until the campsite vehicles enter the model, causing a slight increase in the overall vehicle flow. However, shortly after the last vehicle has entered, there is a

notable decrease in the number of vehicles in these scenarios. This suggests that campsite vehicles can reach their TAZ destinations relatively fast, with minimal traffic disruptions, when the background vehicle count is approximately 10,500 or lower.

In contrast, for the A5 scenario, which features a higher background vehicle count of 14,500, the vehicle flow continues to increase throughout the simulation, with the effect becoming more pronounced after the campsite vehicles enter the model. The network is found to be completely clear 90 minutes after the last vehicle has entered, highlighting a critical congestion issue where vehicles experience significant difficulty reaching their final destinations. This scenario underscores the challenges posed by higher vehicle volumes and the impact on overall traffic flow and congestion.

In the sleeping scenario, the three traffic simulations exhibit similar trends, with variations attributed to differences in the number of vehicles within the network. As with the awake scenarios, the vehicle flow remains relatively steady until the campsite vehicles enter the model, at which point the flow of vehicles increases noticeably. It is also observed that all vehicles reach their destinations within 15 minutes of the last vehicle's entry into the model. This rapid clearance underscores that vehicles are able to navigate the network with minimal congestion, ensuring a smooth and efficient flow on the roads.

5.3.6. Maximum arrival time for campsite vehicles

Figure 25 illustrates the time at which the last campsite vehicle arrives at the Traffic Analysis Zone (TAZ). The primary difference between awake and sleeping scenarios is due to the increased pre-evacuation time.

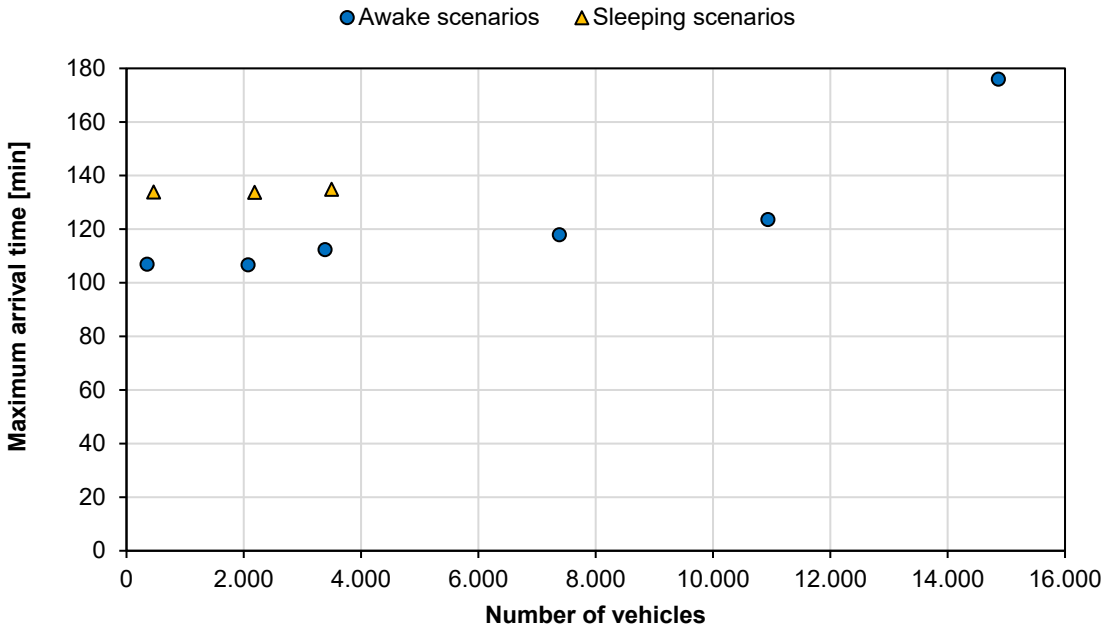

Figure 25 Le Bois Fleuri (LBF). Maximum arrival times for campsite vehicles to TAZ

Regardless of whether occupants are awake or asleep, it is noted that with fewer than 4,000 vehicles, the maximum arrival time remains consistent, indicating that there is no congestion and vehicles move smoothly through the network. The maximum arrival time

is approximately 110 minutes for the awake scenario and about 134 minutes for the sleeping scenario.

On the other hand, when the number of vehicles exceeds 7,000, the maximum arrival time begins to increase. In particular, for the A5 scenario, which features approximately 14,500 background vehicles entering the model, there is a 70-minute increase in the maximum arrival time compared to the scenario with only campsite vehicles. This is due to growing congestion on the routes, which leads to delays and a more gradual flow of traffic as the network becomes increasingly congested.

5.3.7. Mean trip duration for campsite vehicles

Figure 26 shows the average trip duration of campsite vehicles for both scenarios. For scenarios with fewer than 4,000 vehicles (both awake and sleeping), the average time for a campsite vehicle to reach the TAZ is approximately 10 to 11 minutes. Given that the mean finish time within the campsite is about 72 minutes for the awake scenarios and 97 minutes for the sleeping scenarios, the driving time from the campsite to the TAZ constitutes approximately 13% of the total evacuation time (includes both the movement of people within the campsite and the vehicle trips to the TAZ) for awake scenarios and 10% for sleeping scenarios.

As the number of background vehicles increases, the average trip duration also grows. This is due to increased congestion on the routes, which impedes vehicle movement and leads to noticeable delays. More densely occupied routes cause significant traffic bottlenecks, further extending travel times and impacting overall evacuation efficiency.

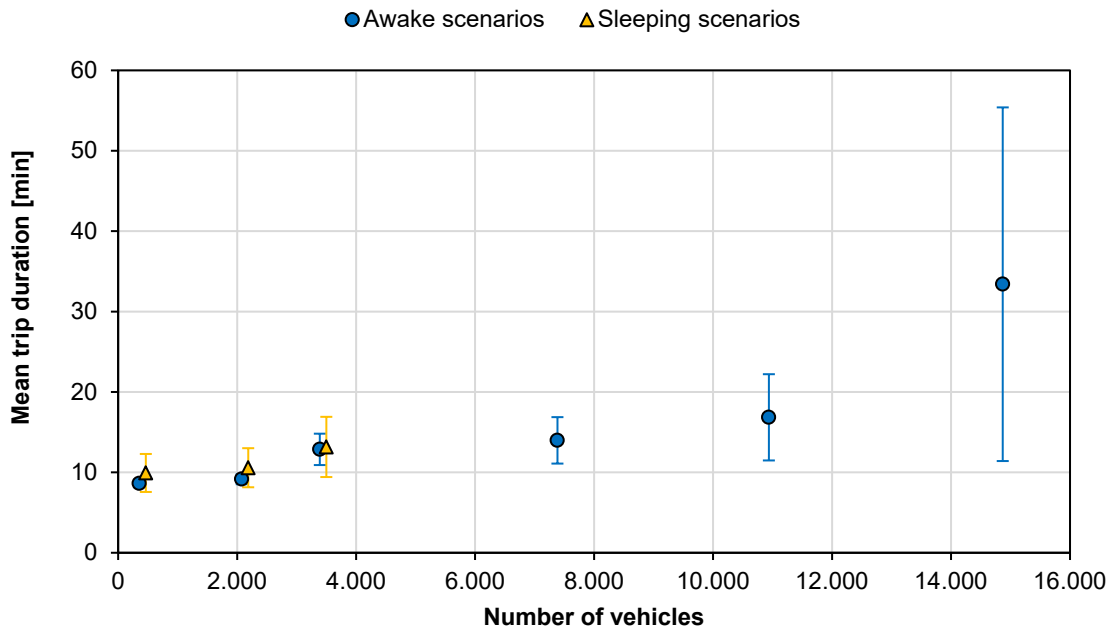

Figure 26 Le Bois Fleuri (LBF). Mean trip duration for campsite vehicles

6. Conclusions

An evacuation study has been carried out at two French campsites with differing characteristics, such as occupancy, size, evacuation methods, etc. Using the Pathfinder tool, various evacuation scenarios were simulated for each campsite, focusing mainly on the occupant's state (awake or asleep) and the number of available exits. The following summarises the key findings from the evacuation events at both campsites:

- The availability of an additional exit has minimal impact on the evacuation process for a relatively low-populated campsite, such as Le Bois de Pins, where the maximum number of occupants is less than 600.

- Travel distances in awake scenarios are approximately 100 meters longer than in sleeping scenarios because occupants must first regroup before initiating the evacuation. However, this additional distance is not the primary factor influencing the overall evacuation time.

- For both scenarios (awake and sleeping), pre-evacuation time is a crucial factor in the overall evacuation duration. To a lesser extent, the differences are also influenced by reduced movement speeds during the night time.

- The primary factors affecting mean finish times in both awake and sleeping scenarios are active time and pre-evacuation time. In awake scenarios, occupants spend considerable time covering longer distances to regroup with family members before starting the evacuation. Conversely, while sleeping occupants are typically closer to their starting points and do not need extensive regrouping, they still require a significant amount of time to initiate the evacuation event.

- In both scenarios, the assembly point and the entrance route leading to it are the most congested areas of the campsites. However, higher density values are observed in the sleeping scenarios compared to the awake scenarios. These indicate that the greater dispersion of occupants in awake scenarios, combined with their need to follow different routes to regroup with family members, facilitates a smoother flow of people through the more crowded routes, such as the main entry route and the assembly point. This improved distribution helps reduce crowding and congestion, leading to more efficient movement in these critical areas.

In addition, for the campsite evacuated by car after the completion, the following conclusions have been drawn from various traffic modelling scenarios, with the primary variable being the number of vehicles:

- In traffic modelling scenarios with 10.500 or fewer vehicles, the flow of vehicles within the network remains relatively steady until campsite vehicles are introduced, causing a slight increase in overall vehicle flow. This indicates that

campsite vehicles can reach their TAZ destinations relatively quickly, with minimal traffic disruptions.

- In scenarios with a higher volume of background vehicles, the vehicle flow continues to increase throughout the simulation, with the impact becoming more noticeable after the campsite vehicles are introduced. This scenario highlights the challenges associated with higher vehicle volumes and their effect on overall traffic flow and congestion

- For scenarios with fewer than 10.500 vehicles (both awake and sleeping), the mean trip duration for campsite vehicles to reach the TAZ is less than 15 minutes. In these cases, the driving time from the campsite to the TAZ accounts for approximately 13% of the total evacuation time in awake scenarios and 10% in sleeping scenarios.

Based on the analysis of the results, the following recommendations are proposed to reduce the overall evacuation time:

- If a safe area can be reached, evacuation on foot is generally preferable to evacuation by private vehicles. To facilitate this, campsite owners should establish designated fire safety areas capable of accommodating all occupants (as seen at the Le Bois de Pins campsite), rather than relying on vehicle evacuations to a TAZ.

- Implementing multiple exits simultaneously used, positioned in widely separated locations would expedite the evacuation process by providing more direct routes and decreasing congestion in densely populated areas near the assembly points. Additionally, it is essential to ensure that the signage for evacuation routes is highly visible and illuminated, allowing it to be used effectively even in reduced visibility conditions and at night. This will help increase movement speed and prevent disorientation.

- Having multiple assembly points would alleviate the high densities observed along evacuation routes and reduce overall travel distances.

- Alternative means of emergency alert may be put in place (such as mobile apps) to avoid attending the assembly point or reducing the pre-evacuation times, which has been determined as one of the key parameters governing the overall evacuation times. Additionally, it is crucial to have a functioning siren, with its operational status regularly checked throughout the wildfire season.

- Complementary use for evacuation of the public transportation (bus, touristic trains) would largely help improve the preparedness.

7. Acknowledgements

The authors wish to thank Dr Enrico Ronchi and his colleagues at Lund University for providing useful feedback on the work related to the crowd-movement and traffic modelling. The authors also thank all campsite's stakeholders to deliver the required data needed to complete the analysis.

References

Aliperti, G., Cruz, A.M. (2019). Investigating tourists' risk information processing. Annals of Tourism Research, 79, 102803.

Alvarez Lopez, P., Behrisch, M., Bieker-Walz, L., Erdmann, J., Flötteröd, Y.P., Hilbrich, R., Lücken, L., Rummel, J., Wagner, P., Wießner, E. (2018) Microscopic Traffic Simulation using SUMO. In: 2019 IEEE Intelligent Transportation Systems Conference (ITSC), Seiten 2575-2582. doi: 10.1109/ITSC.2018.8569938.

Arce, R. S. C., Onuki, M., Esteban, M., Shibayama, T. (2017). Risk awareness and intended tsunami evacuation behaviour of international tourists in Kamakura City, Japan. International Journal of Disaster Risk Reduction, 23, 178–192.

Benichou, N., Adelzadeh, M., Singh, J., Gomaa, I., Elsagan, N., Kinateder, M., Ma, C., Gaur, A., Bwala, A., Sultan, M. (2021). National Guide for Wildland-urban interface fires: Guidance on hazard and exposure assessment, property protection, community resilience and emergency planning to minimize the impact of wildland-urban interface fires. National Research Council of Canada.

Boyce, K., Shields, T., Silcock, G. (1999) Toward the characterization of building occupancies for fire safety engineering: capabilities of disabled people moving horizontally and on an incline, Fire Technology 35, 51-67. doi: 10.1023/A:1015339216366.

Bubola, E., & Kitsantonis, N. (2023). Greek Hotels Fear a Burning Future: 'Even the Animals Are Moving Away'. International New York Times.

Data gouvernemental République Française (2024). Données SIG de Comptages Routiers sur la voirie départementale des P.O en 2022.

Data gouvernemental République Française (2024a). Trafic moyen journalier annuel sur le réseau routier national.

Direction générale de l'urbanisme, de l'habitat et de la construction (2007) Circulaire interministérielle nº 2007-53 DGUHC du 30 novembre 2007 relative à l'accessibilité des établissements recevant du public, des installations ouvertes au public et des bâtiments d'habitation. nor: MLVU0766613C.

Grandison, A. (2020) Determining Confidence Intervals, and Convergence, for Parameters in Stochastic Evacuation Models, Fire Technology 56, 2137-2177. doi: 10.1007/s10694-020-00968-0.

Gupta, G. (2023). The Maui fires are more deadly than Hawaii's 1960 tsunami. The New York Times (Digital Edition).

Gwynne, S.M.V, Rosenbaum, E.R. (2016). Employing the Hydraulic Model in Assessing Emergency Movement, SFPE Handbook of Fire Protection Engineering (5th Ed.), Chapter 59, doi: 10.1007/978-1-4939-2565-0.

Ineris (2024). SSTIE - La réglementation de la Santé et de la Sécurité au Travail dans les Industries Extractives.

Instituto Nacional de Estadística (INE). Encuestas de ocupación en alojamientos turísticos extra hoteleros. Agosto 2022. Datos provisionales.

Korhonen, T., Hostikka, S. (2009) Fire Dynamics Simulator with Evacuation: FDS + Evac Technical Reference and User's Guide, VTT Technical Research Center of Finland, pp. 19 (Working paper No. 119).

Krauß, S. (1998). Microscopic modeling of traffic flow: Investigation of collision free vehicle dynamics.

Labhiri, A., Vaiciulyte, S., Kuligowski, E., Ronchi, E. (2024). Evacuation decisions of tourists in wildfire scenarios, International Journal of Disaster Risk Reduction 113, 104836. doi: 10.1016/j.ijdrr.2024.104836.

Lovreglio, R., Ronchi, E., Kinsey, M.J. (2020) An online survey of pedestrian evacuation model usage and users, Fire Technology 56, 1133-1153. doi: 10.1007/s10694-019-00923-8.

Ministerio de Fomento (2019) Real Decreto 732/2019, de 20 de diciembre por el que se modifica el Documento Básico de Seguridad en Caso de Incendio (DB-SI).

Nilsson, D., Johansson, A. (2009) Social influence during the initial phase of a fire evacuation - Analysis of evacuation experiments in a cinema theatre, Fire Safety Journal, Volume 1 (1), 71-79. doi: 10.1016/j.firesaf.2008.03.008.

Najmanová, H., Ronchi, E. (2023) Experimental data about the evacuation of preschool children from nursery schools, Part II: Movement characteristics and behaviour, Fire Safety Journal, Volume 139. doi: 10.1016/j.firesaf.2023.103797.

PD 7974-6 (2019) Application of fire safety engineering principles to the design of buildings. Part 6: Human factors: Life safety strategies - Occupant evacuation, behaviour and condition (Sub-system 6).

Proulx, G. (2002) Movement of People: The evacuation timing, SFPE Handbook of Fire Protection Engineering (3rd Ed.), Chapter 3-13.

Purser, D.A., Bensilum, M. (2001) Quantification of behaviour for engineering design standards and escape time calculations, Safet Science, Volume 2 (2), 157-182. doi: 10.1016/S0925-7535(00)00066-7.

Ranney, T.A. (1999) Psychological factors that influence car-following and car-following model development. Transportation Research Part F: Traffic Psychology and Behaviour, 2(4), 213-219. doi: 10.1016/S1369-8478(00)00010-3.

Ray, N., Ebener, S. (2008) AccessMod 3.0: computing geographic coverage and accessibility to health care services using anisotropic movement of patients, International Journal of Health Geographics 7 (63).

Reynolds, C.W. (1999) Steering Behaviors For Autonomous Characters, In Proceedings of Game Developers Conference, 763-782.

Ronchi, E., La Mendola, S. (2016) Evacuation modelling for underground physics research facilities. Lund University, Department of Fire Safety Engineering.

Ronchi, E., Rein, G., Gwynne, S., Wadhwani, R., Intini, P., Bergstedt, A. (2017). e-Sanctuary: Open Multi-Physics Framework for Modelling Wildfire Urban Evacuation. Fire Protection Research Foundation.

Ronchi, E., Reneke, P.A., Peacock, R.D. (2014) A Method for the Analysis of Behavioural Uncertainty in Evacuation Modelling, Fire Technology 50, 1545-1571. doi: 10.1007/s10694-013-0352-7.

Ronchi, E. (2023) Evacuation modelling for wildland-urban interface fires in touristic areas. Report 3264, Department of Fire Safety Engineering, Lund University (Sweden).

Shields, T.J. (1993) Fire and disabled people in buildings. Building Research Establishment Report BR231, ISBN 0851255469.

Shi, L., Xie, Q., Cheng, X., Chen, L. (2009) Developing a database for emergency evacuation model, Building and Environment 44 (8) 1724-1729. doi: 10.1016/j.buildenv.2008.11.008.

Smedberg, E., Kinsey, M., Ronchi, E. (2021) Multifactor Variance Assessment for Determining the Number of Repeat Simulation Runs in Evacuation Modelling, Fire Technology 57, 2615-2641. doi: 10.1007/s10694-021-01134-w.

Song, J., Wu, Y., Xu, Z., & Lin, X. (2014). Research on car-following model based on SUMO. The 7th IEEE/International Conference on Advanced Infocomm Technology, 47-55. doi: 10.1109/ICAIT.2014.7019528.

Thunderhead Engineering (2023) Patfhinder Technical Reference Manual version 2023-2.